Role of the ubiquitin-like modifier FAT10 in protein degradation and immunity

Dissertation

zur Erlangung des akademischen Grades
des Doktors der Naturwissenschaften
(Dr. rer. nat.)
an der Universität Konstanz
Fachbereich Biologie

vorgelegt von

Birte Katharina Henriette Kalveram

Tag der mündlichen Prüfung: 06.04.09
1. Referent: Prof. Dr. Marcus Groettrup, Universität Konstanz
2. Referent: Prof. Dr. Martin Scheffner, Universität Konstanz

Contents

Acknowledgements

First of all, I would like to thank Prof. Dr. Marcus Groettrup for giving me the opportunity to do this work and for teaching me a lot during these past few years.

Many thanks also go to...

Dr. Gunter Schmidtke for his biochemistry toolbox and for teaching me the “appropriate” way to ask questions.

My fellow (PhD) students on the FAT10 project, expecially Sebastian Lukasiak, Anja Holtz and Christiane Peltzer, for many stimulating discussions and many bars of chocolate.

Dr. Matthias Langhorst for taking the time to teach me confocal microscopy, Dr. (in spe) Jaqueline Möbius for teaching me how to do an ICS and Dr. Eva Schlosser for showing me how to make BMDCs.

All of my colleagues in the Groettrup lab (whose names could not be cited due to space constraints) for always lending a hand when I needed it and for generally making this an enjoyable place to work in.

Dr. Henner Brinkmann for helping me take my first steps in the exciting world of scientific research.

Dr. Marian Schwartz for showing me how much fun biology could be.

1000 Dank auch den “Lustigen Biologen”, insbesondere Drs. Isa Pochic und Katrin Styp von Rekowski sowie Drs. (in spe) Eva Billerbeck, Helgard Fischer, Sonja Fraas, Nina Jagmann, Silke Litzinger und Sonja Weinitschke für die unzähligen gemeinsamen Stunden und die vielen Blicke über den Tellerrand hinaus.

Last but not least gilt mein Dank meinen Eltern für ihre Liebe, ihre Unterstützung – und die frühkindliche Prägung auf die wissenschaftliche Denkweise.

Summary / Zusammenfassung

English

FAT10 is a ubiquitin-like protein which is encoded in the major histocompatibility complex class I locus and is synergistically inducible with the proinflammatory cytokines IFN-γ and TNF-α in cells of nearly every tissue origin. It consists of two ubiquitin-like domains, which are connected by a short linker, and bears a free diglycine-motif at its C-terminus through which it can become covalently conjugated to so far unidentified target proteins. Overexpression of the wild-type protein – but not a diglycine-deficient mutant – leads to the induction of caspase-dependent apoptosis in murine as well as human cell lines. Both FAT10 and its conjugates are rapidly degraded by the proteasome at a similar rate, and the N-terminal fusion of FAT10 to long-lived proteins such as GFP or DHFR reduces their half-life as potently as their fusion with ubiquitin. The proteasomal degradation of FAT10, which occurs independently of ubiquitylation, can further be accelerated by non-covalent interaction with the UBL-UBA domain protein NEDD8 ultimate buster 1-long (NUB1L).

The primary purpose of this thesis was to gain a more detailed insight into the mechanistics of FAT10-mediated protein degradation. Furthermore, a monoclonal antibody directed against human FAT10 was raised and FAT10 could be shown to be required for the proper down-regulation of the antiviral $CD8^+$ T cell response.

NUB1L, which was identified through a yeast two-hybrid screen as a non-covalent binding partner of FAT10, could previously be shown to accelerate the proteasomal degradation of FAT10 when the two proteins were co-expressed. This thesis dissects the molecular determinants of the aforementioned acceleration and uncovers a dual role of NUB1L as a proteasomal receptor for FAT10 as well as a facilitator of its degradation. Although FAT10 is capable of direct interaction with the 26S proteasome, NUB1L can function as a soluble FAT10-receptor by

binding to the proteasome with its UBL domain and to FAT10 with its UBA domains. Interestingly, the interaction of FAT10 with NUB1L is, at least *in vivo*, strictly dependent on the presence of all three of its UBA domains. The facilitation of FAT10 degradation, on the other hand, is strictly dependent on the ability of NUB1L to interact with the 26S proteasome through its UBL domain and shows no requirement for any of its three UBA domains. Furthermore, degradation of the N-terminal UBL domain of FAT10 – which can interact with the 26S proteasome, but not with NUB1L – can still be accelerated by co-expression of NUB1L.

Through experiments using an *in vitro* system consisting of purified 26S proteasome and recombinantly expressed substrates, this thesis demonstrates the 26S proteasome to be able to degrade the model substrate FAT10-dihydrofolate reductase (DHFR) – although only in the presence of NUB1L. Furthermore, the study of FAT10-DHFR degradation in NUB1L knock-down cells revealed this absolute requirement for NUB1L to also apply to *in vivo* situations, suggesting that – at least in the case of this model substrate – mere binding of FAT10 to the proteasome is not sufficient to ensure the degradation of its target proteins.

Another non-covalent interaction partner of FAT10, histone deacetylase 6 (HDAC6), was also identified through a yeast two-hybrid screen. HDAC6, which is a primarily cytoplasmatic protein, is involved in the deactylation of α-tubulin, HSP90 and cortactin. In addition to its two deacetylase domains, it also encompasses a dynein-binding domain as well as a ubiquitn-binding zinc finger (BUZ domain) and tethers polyubiquitylated proteins to the dynein-motor during their microtubule-dependent transport to the aggresome. The herein presented results uncover a role for HDAC6 not only in the transport of polyubiquitylated cargo, but also in the transport of the ubiquitin-like modifier FAT10 and its conjugates. Under conditions of misfolded protein stress FAT10 interacts with HDAC6 and localizes to the aggresome in a microtubule-dependent manner. The binding of FAT10 is mediated by two different domains of HDAC6, the BUZ domain and surprisingly also the first catalytic domain, but it is not dependent on the catalytic activity of HDAC6. Furthermore, this thesis showed FAT10-containing as well as ubiquitin-containing aggresomes to be reduced in both size and number in HDAC6 deficient fibroblasts, which suggests that, although HDAC6 plays an important role in aggresomal targeting, it is not essential for the transport of proteasomal substrates to the aggresome.

In conclusion, these results suggest FAT10 to mediate the rapid and inducible destruction of its target proteins through association with two different adaptor proteins. With help of the UBL-UBA domain protein NUB1L, FAT10 is able to promote the degradation of its conjugates by the 26S proteasome. Under conditions of proteasome impairment, however, FAT10 interacts with the linker protein HDAC6 and instead mediates the sequestration of its substrates in the aggresome.

Deutsch

FAT10 ist ein Ubiquitin-ähnliches Protein, welches im Haupt-Gewebe-Kompatibilitäts (MHC) Lokus der Klasse I kodiert liegt. Mit den proinflammatorischen Zytokinen TNF-α und IFN-γ ist es in Zellen fast jeder Herkunft induzierbar. FAT10 besteht aus zwei durch einen kurzen Linker verbundenen Ubiquitin-ähnlichen Domänen und besitzt an seinem C-terminus ein Di-Glycin-Motiv, über welches es an seine Zielproteine kovalent konjugiert werden kann. Überexpression des wild-typ Proteins – aber nicht einer Mutante ohne Di-Glycin-Motiv – führt zur Induktion von Caspase-abhängiger Apoptose in murinen und humanen Zelllinien. Sowohl FAT10 als auch seine Konjugate werden vom Proteasom mit der gleichen Geschwindigkeit abgebaut; und die N-terminale Fusion von FAT10 an langlebige Proteine wie GFP oder DHFR reduziert deren Halbwertszeit ebenso potent wie eine Fusion mit Ubiquitin. Der proteasomale Abbau von FAT10 – welcher unabhängig von Ubiquitin erfolgt – kann zusätzlich beschleunigt werden durch nicht-kovalente Interaktion von FAT10 mit dem UBL-UBA Protein NEDD8 Ultimate Buster 1-Long (NUB1L).

Ziel dieser Doktorarbeit war es, einen tieferen Einblick in den Prozess des FAT10-vermittelten Proteinabbaus zu erlangen. Des weiteren wurde ein monoklonaler Antikörper gegen humanes FAT10 hergestellt und es konnte gezeigt werden, dass FAT10 für die korrekte Herrunterregulation der $CD8^+$ T Zell-vermittelten antiviralen Immunantwort benötigt wird.

Bereits im Vorfeld konnte gezeigt werden, dass NUB1L, welches über einen Yeast Two-Hybrid Screen als nicht-kovalenter Interaktionspartner von FAT10 identifiziert wurde, durch seine Co-Expression zusammen mit FAT10 dessen Abbau beschleunigen konnte. Die vorliegende Arbeit untersucht die molekularen Faktoren dieser Beschleunigung und deckt eine doppelte Rolle für NUB1L sowohl

als proteasomaler Rezeptor für FAT10 als auch als sogenannter “Facilitator” seines Abbaus auf. Obwohl FAT10 in der Lage ist, direkt mit dem 26S Proteasom zu interagieren, kann NUB1L als löslicher FAT10-Rezeptor fungieren indem es über seine UBL Domäne an das Proteasom und über seine drei UBA Domänen an FAT10 bindet. Interessanterweise ist die Interaktion zwischen NUB1L und FAT10 – zumindest *in vivo* – abhängig vom Vorhandensein aller drei UBA Domänen. Im Gegensatz dazu beruht Beschleunigung des FAT10-Abbaus alleine auf der Fähigkeit von NUB11L, über seine UBL Domäne an das 26S Proteasom zu binden. Des weiteren kann der Abbau der N-terminalen UBL Domäne von FAT10 – welche mit dem 26S Proteasom, aber nicht mit NUB1L interagieren kann – immer noch durch die Co-Expression von NUB1L beschleunigt werden.

Mit Hilfe von Experimenten in einem *in vitro* System, welches aus aufgereinigtem 26S Proteasom sowie rekombinant exprimierten Substraten bestand, zeigt diese Arbeit, dass das 26S Proteasom durchaus in der Lage ist das Modell-Substrat FAT10-DHFR *in vitro* abzubauen – allerdings nur in der Gegenwart von NUB1L. Versuche in NUB1L knock-down Zellen lassen den Schluss zu, dass diese absolute Abhängigkeit des FAT10-gesteuerten Abbaus von NUB1L auch auf die Situation *in vivo* zutrifft. Dies ist ein Hinweis darauf, dass – zumindest im Falle des hier untersuchten Modell-Substrats – die Bindung von FAT10 an das Proteasom alleine nicht ausreicht, um einen effizienten Abbau seiner Zielproteine zu ermöglichen.

Wiederum durch einen Yeast Two-Hybrid Screen wurde Histon Deacetylase 6 (HDAC6) als weiterer, nicht-kovalenter Interaktionspartner von FAT10 identifiziert. HDAC6 ist ein Protein mit größtenteils cytoplasmatischer Lokalisierung, welches für die Deacetylierung von α-Tubulin, HSP90 und Cortactin verantwortlich ist. Zusätzlich zu seinen beiden katalytischen Domänen besitzt es eine Dynein-Bindedomäne sowie einen Ubiquitin-bindenden Zink-Finger (BUZ Domäne). Mit Hilfe dieser beiden Domänen fungiert es als Verbindung zwischen dem Dynein-Motor sowie polyubiquitylierten Proteinen und ermöglicht auf diese Weise deren Transport entlang von Mikrotubuli zum Aggresom. Diese Arbeit zeigt, dass HDAC6 nicht nur für den Transport von polyubiquitylierten Proteinen, sondern auch für den Transport von FAT10 und seinen Konjugaten zuständig ist. Unter Bedingungen in denen das Proteasom nur eingeschränkt funktioniert bindet HDAC6 an FAT10 und vermittelt seinen Transport zum Aggresom. Die Interaktion mit FAT10 wird durch zwei verschiedene Domänen von HDAC6 vermittelt, nämlich die BUZ Domäne und – überraschenderweise – die erste katalytische Domäne, obwohl die Interaktion der beiden Proteine

nicht von der katalytischen Aktivität von HDAC6 abhängig ist. Des weiteren zeigt diese Arbeit, dass sowohl die Anzahl als auch die Größe von FAT10- und Polyubiquitin-haltigen Aggresomen in HDAC6-defizienten Zellen stark reduziert sind. Dies deutet darauf hin, dass HDAC6 eine wichtige Rolle im Transport von proteasomalen Substraten zum Aggresom spielt, obgleich es hierfür nicht essentiell ist.

Zusammengenommen weisen diese Ergebnisse darauf hin, dass FAT10 den schnellen und induzierbaren Abbau seiner Zielprotein durch nicht-kovalente Interaktion mit zwei verschiedenen Adapterproteinen vermittelt. Mit Hilfe des UBL-UBA Proteins NUB1L ist FAT10 in der Lage, seine Zielproteine dem Abbau durch das 26S Proteasom zuzuführen. Ist das Proteasom jedoch beeinträchtigt, vermittelt FAT10 stattdessen über seine Bindung an HDAC6 die Isolierung seiner Zielproteine im Aggresom.

Introduction

Protein Degradation

Nearly all proteins in our body are not stable constituents but are rather subject to dynamic turnover through degradation and neosynthesis. Protein degradation is a highly complex and tightly regulated process and is essential for a broad range of cellular functions. These include processes spanning from the response to nutrient starvation over quality control to activation and silencing of transcription, regulation of the cell cycle, signal transduction, apoptosis and antigen presentation. Cellular proteolysis in eukaryotic cells is mediated by two distinct systems, the proteasome and the lysosome. The proteasome is a large, barrel-shaped protease which is responsible for the degradation of about 80% of all intracellular proteins, the majority of which are short-lived. Access to the proteolytic core of the proteasome is regulated by covalent modification of the targeted proteins with a ubiquitin “tag”. The lysosome, in contrast, is a membrane-enclosed organelle which contains various proteolytic enzymes with a functional optimum at an acidic pH. Exogenous proteins can be targeted to the lysosome either by receptor-mediated endocytosis or by pino- or phagocytosis, which can be summarized as heterophagy. In addition, the lysosome is also involved in the bulk degradation of cellular proteins as well as the degradation of organelles in a process termed autophagy.

The Ubiquitin-Proteasome-System

The Proteasome

The 20S Proteasome

The proteasome, a large, cylindrical multi-enzyme complex, is the central element of the ubiquitin-proteasome system (UPS). It can be subdivided into two dissociable assemblies; the core complex, also known as the 20S proteasome, and one or two regulatory particles which cap the ends of the core particle. Four hetero-heptameric rings are axially stacked to form the 20S proteasome, where subunits α1-α7 make up the outer and subunits β1-β7 the inner two rings (Fig. 1). Enzymatic activity is restricted to the central lumen of the cylinder, which effectively prevents unspecific access to the active sites and thus aberrant degradation. Through N-terminal extensions, the α-subunits further occlude the central pore, which can only be opened by association with a regulatory complex (Groll et al., 2000). Only three of the β-subunits in each ring (β1, β2 and β5) display catalytic activity, and their active sites point toward the inside of the proteolytic chamber. All of these subunits are threonine-proteases, but each of them displays different proteolytic preferences, which have been classified according to the residue N-terminal of the cleaved peptide-bond: acidic (caspase-like, β1), basic (trypsin-like, β2), and hydrophobic (chymotrypsin-like, β5) (Groll and Clausen, 2003). The cylindrical shape of the 20S proteasome promotes a processive degradation of its substrates by preventing the dissociation of partially processed polypeptides, and thus releases short peptides ranging from three to 25 residues. These peptides can now be further processed into single amino acids by cytoplasmatic aminopeptidases, or they can be – if they meet the requirements – loaded onto MHC class I molecules and subsequently be presented to circulating lymphocytes (Coux et al., 1996; Baumeister et al., 1998).

In higher vertebrates, the release of interferon (IFN)-γ leads to the induction of three additional, non-essential subunits: β1i (LMP2), β2i (MECL-1) and β5i (LMP7), which are incorporated into the proteasome during neosynthesis. Proteasomes which contain these inducible subunits are termed “immunoproteasomes” and display an altered cleavage pattern which could be shown to generate more peptides suitable for presentation (Groettrup et al., 2001a,b; Goldberg et al., 2002). In addition to these three inducible subunits, one other differentially

expressed subunit, called β5t, has been found. Its expression is restricted exclusively to cortical thymic epithelial cells, which are responsible for the positive selection of developing thymocytes (Murata et al., 2007).

The 26S Proteasome

The 26S proteasome is a 2.4 MDa supercomplex which consists of the 20S core and two 19S regulatory subunits which cap both ends of the core particle (Fig. 1). The latter are responsible for mediating functions associated with substrate recognition and insertion, contain intrinsic unfoldase activity, which is ATP-dependent (Liu et al., 2002), and serve as a docking platform for substoichiometric components of the proteasome. The 19S regulatory complex, which is also known as PA700, can be further subdivided into the proximal "base", which directly abuts to the α-rings, and the distal "lid". The "base" consists of six AAA-family ATPases (Rpt1-Rpt6) and four non-ATPase subunits (Rpn1, 2, 10 and 13). The ATPases form a hexameric ring which mediates ATP-dependent opening of the pores formed by the α-subunit rings and unfolding of substrate proteins (Glickman et al., 1999). The remainder of the approximately 20 PA700 subunits make up the "lid"; and while some of them could be shown to display deubiquitylating activity – among them Rpn11/S13 – most of their functions remain unknown (Smith et al., 2006).

The majority of proteins is targeted for proteasomal degradation through covalent attachment of a small protein called ubiquitin. This ubiquitin-tag is then recognized by the 26S proteasome, which leads to the subsequent unfolding and degradation of the target protein. Five components of the 19S regulator have been implicated in ubiquitin-recognition, although this list is in all likelihood far from complete. These ubiquitin-receptors employ two different modes of operation: the subunits S5a/Rpn10 (Deveraux et al., 1994), S6'/Rpt5 (Lam et al., 2002) and ADRM1/Rpn13 (Husnjak et al., 2008; Schreiner et al., 2008) are able to bind to ubiquitin directly, whereas S1/Rpn2 and S2/Rpn1 recognize substrates indirectly by binding to linker proteins such as hHR23/Rad23 and hPLIC/Dsk2 (Elsasser et al., 2002; Saeki et al., 2002b; Seeger et al., 2003). Interestingly, Rpn13 is also responsible for tethering the deubiquitylating enzyme UCH37 to the proteasome through a second domain (Yao et al., 2006).

Apart from the 19S regulator, the 20S proteasome can pair with several alternative regulatory particles to form a number of structurally different proteasome-

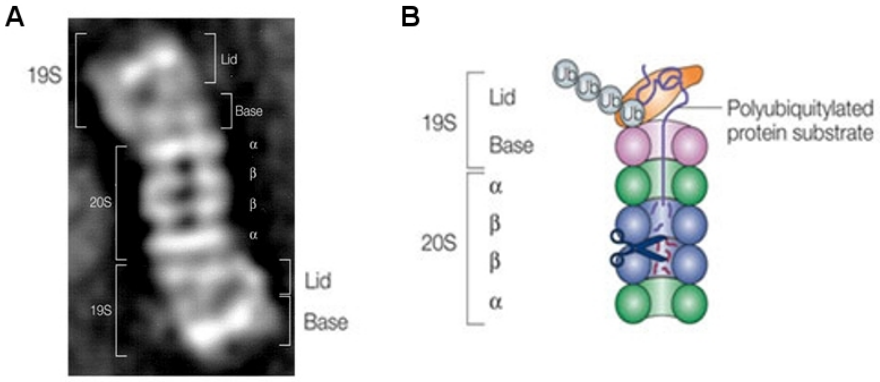

Figure 1: The 26S proteasome. The proteasome is a large, multicatalytic protease that degrades polyubiquitylated proteins to produce small peptides. It is composed of two subcomplexes – a 20S core particle (CP) that carries the catalytic activity, and a 19S regulatory particle (RP). The 20S CP is a barrel-shaped structure that is composed of four stacked rings, two identical outer α-rings and two identical inner β-rings. The eukaryotic α- and β-rings are each composed of seven distinct subunits, which gives the 20S complex the general structure of α1–7β1–7β1–7α1–7. The catalytic sites are localized to some of the β-subunits. One or both ends of the 20S barrel can be capped by a 19S RP. Following substrate degradation, short peptides that have been derived from the substrate are released, as is reusable ubiquitin. Part **(A)** of the figure shows an electron-microscopy image of a 26S proteasome from Saccharomyces cerevisiae, and part **(B)** shows a schematic representation of the structure and function of the 26S proteasome. Ub, ubiquitin. (Modified from Ciechanover, 2005).

regulatory complexes (Schmidt et al., 2005). These alternative regulators, which include PA28$\alpha\beta$ (also known as the 11S regulator), PA28γ as well as PA200, do not contain ATPases and stimulate proteasome activity solely by removing the occlusions at the outer pores of the 20S core particle. As a consequence, they are unable to unfold complex substrates and can only enhance the hydrolysis of short peptides. In addition, they are devoid of any ubiquitin-binding activity (Rechsteiner and Hill, 2005). Interestingly, the PA28α and PA28β genes are encoded in the major histocompatibility class I locus adjacent to the inducible 20S subunits LMP2 and LMP7, and expression of PA28$\alpha\beta$ is also upregulated in response to cytokines such as IFN-γ. Furthermore, the 20S core particle can associate with two different regulators at either end, creating a hybrid-proteasome with catalytic properties which differ from those displayed by proteasomes containing only one type of regulator. Indeed, proteasomes capped with both the 19S and 11S regulator are able to generate a unique pool of peptides with an increased affinity for MHC class I molecules (Rechsteiner et al., 2000). Alternatively, proteasomal activity can not only be stimulated, but also attenuated by a different class of inhibitory regulators such as PI31, which competes with PA28$\alpha\beta$ for proteasome binding (Rechsteiner and Hill, 2005).

The 26S proteasome plays a pivotal role in many cellular processes and its substrates come from a variety of sources and are targeted for a number of different reasons. These reasons can be grouped into two categories: recycling and regulation. The former is perhaps the more obvious: proteins which are defective or no longer needed are disassembled into single amino acids which can then be used for neosynthesis. The latter utilizes degradation as a fast, efficient and irreversible means to the inactivation of regulatory proteins such as cell-cycle regulators or components of signaling cascades. Of course, these two functions are not entirely unrelated, as even those proteins which are primarily targeted for degradation to ensure their inactivation are ultimately reduced to their building blocks and subsequently recycled. Conversely, even peptides derived from defective proteins which were targeted in the course of waste disposal might end up being presented on MHC class I molecules (Yewdell et al., 1996; Schubert et al., 2000).

One prominent example for the regulatory function of the proteasome is the targeted distruction of cyclins and Cdk inhibitors – which, through their periodic degradation and neosynthesis, ultimately drive the cell-cycle (Nigg, 1995; Obaya and Sedivy, 2002). Another is that of the tumor suppressor p53, which, when stabilized by stress stimuli such as DNA-damage, is responsible for the transcriptional activation of a broad array of proteins involved in cell-cycle control, apoptosis and senescence (Lavin and Gueven, 2006). A third example is that of the enzyme ornithine-decarboxylase (ODC), which catalyzes the first and rate-limiting step in the synthesis of cellular polyamines. Interestingly, ODC also doubles as the most prominent example of ubiquitin-independent proteasomal degradation (Kahana et al., 2005).

The non-functional proteins which are targeted for proteasomal degradation as a means of waste-disposal originate from several sources: Aging, previously fully functional proteins can become become damaged, primarily through oxidation, over the course of their lifetime (Grune et al., 1997). Alternatively, proteins can be targeted to the proteasome right after synthesis due to failure to pass the stringent cellular quality control mechanisms. As many as 30% of all newly synthesized proteins are ubiquitylated and degraded by the proteasome. Most of these proteins, which are called defective ribosomal products (DRiPs), result from errors in the process of protein synthesis, such as misincorporation of amino acids, premature termination or deletion of residues. Post-translational mistakes which can occur during folding, oligomer assembly or intracellular sorting can also lead to the generation of DRiPs. Importantly, even though they are targeted for degradation through the action of quality control mechanisms, DRiPs

are the major source of antigenic peptides for MHC class I restricted presentation (Yewdell et al., 1996, 2001).

Ubiquitin and Ubiquitin-Like Proteins

Ubiquitin

Ubiquitin is a small, highly conserved protein of 76 amino acids and of compact, globular structure. It exerts its function mainly through covalent attachment to other proteins and is coded for by a number of different genes, which are scattered throughout the genome. In all cases, ubiquitin is expressed as a proprotein with a C-terminal extension and needs to be proteolytically processed before yielding functional, monomeric ubiquitin (Jentsch et al., 1991). The conjugation of ubiquitin to its target proteins, which is termed ubiquitination, ubiquitinylation or ubiquitylation, is dependent on the presence of two consecutive glycine residues at its very C-terminus and requires the sequential action of three enzymes. In a first step, the C-terminal glycine residue of ubiquitin is activated in an ATP-dependent step by a specific ubiquitin activating enzyme, or E1. This step consists of an intermediate formation of ubiquitin adenylate, with the release of pyrophosphate (PPi), followed by the binding of ubiquitin to a cysteine residue of the E1 enzyme in a thiolester linkage, with the release of AMP. In a second step, ubiquitin is transferred to the active site cysteine residue of a ubiquitin-conjugation enzyme, or E2. The third enzyme in this cascade, the ubiquitin-protein ligase, or E3, catalyzes the isopeptide linkage of the ubiquitin C-terminus to an ε-amino group in of one of the substrate protein's lysine residues (Hershko and Ciechanover, 1998 and Fig. 2).

In most cases, modification of the substrate protein is not limited to the attachment of a single ubiquitin moiety. Instead, the newly attached ubiquitin now serves as the acceptor for a new round of ubiquitylation, which eventually results in the formation of ubiquitin chains. In some cases, the action of an additional enzyme – a multiubiquitin-chain assembly factor, termed E4 – is required for extension of the polyubiquitin chain (Hoppe, 2005). Ubiquitin possesses seven lysine residues, all of which are potentially involved in chain formation. However, only linkages through K48, K63 and sometimes also K29 are readily observed in nature (Haglund and Dikic, 2005). Ubiquitin was first identified as the tag which targets proteins for ATP-dependent degradation (Ciechanover et al., 1978), which

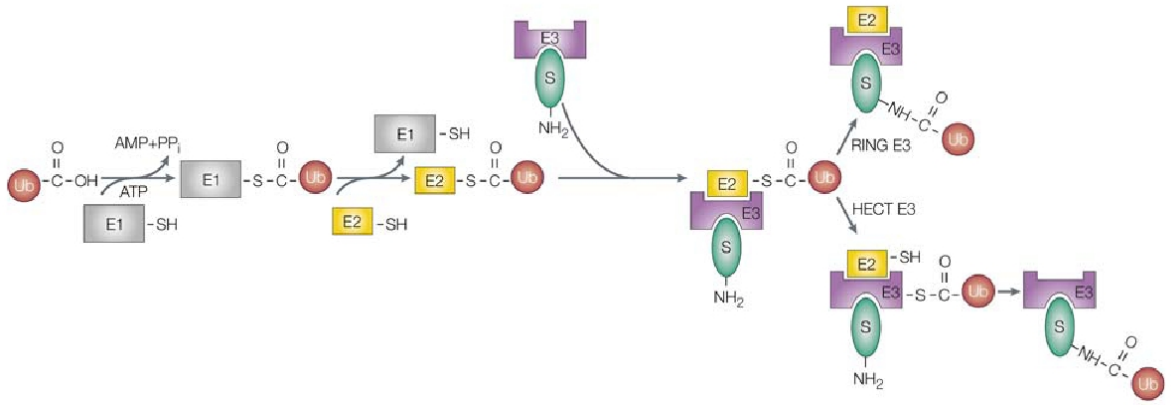

Figure 2: The ubiquitylation pathway. Free ubiquitin (Ub) is activated in an ATP-dependent manner with the formation of a thiol-ester-linkage between E1 and the carboxyl terminus of ubiquitin. Ubiquitin is then transferred to one of a number of different E2s. E2s associate with E3s, which may have substrate already bound. For HECT domain E3s, ubiquitin is next transferred to the active-site cysteine of the HECT domain followed by transfer to substrate(s) (as shown) or to a substrate-bound polyubiquitin-chain. For RING E3s, current evidence indicates that ubiquitin is transferred directly from the E2 to the substrate. (Modified from Fang and Weissman, 2004).

turned out to indeed be the most prevalent function of ubiquitin conjugation. Proteasomal targeting of proteins is mediated by the attachment of a chain of four or more K48-linked ubiquitin moieties (Thrower et al., 2000). In a limited number of cases, the attachment of a K29-linked chain also leads to proteasomal degradation (Johnson et al., 1995), however, most other variations of ubiquitin attachment are means to a different end. K63-linked ubiquitin displays a distinct chain topology and is involved in signal transduction (Krappmann and Scheidereit, 2005) and DNA repair (Friedberg et al., 2005). In some instances, modification of the target protein with a single ubiquitin moiety (monoubiquitylation), or with several separate ubiquitins at different lysines (multiubiquitylation) is sufficient to modify a protein's activity or to create a new binding site. As such, monoubiquitylation has been implicated in endocytosis, vesicular sorting, histone regulation and the budding of retroviruses (Hicke, 2001; Di Fiore et al., 2003).

Substrate specificity of the ubiquitin system is conferred by a multitude of E3 enzymes, which are responsible for recognizing their specific target protein. In genomics studies, several hundered putative E3 candidate genes have been identified. E3 ubiquitin-protein ligases are defined as enzymes which bind, through direct interaction or with the help of additional adaptor proteins, specific protein substrates and facilitate the transfer of ubiquitin from a thiolester intermediate of their cognate E2 enzyme to an isopeptide linkage with the target protein. The

majority of ubiquitin-protein ligases fall into one of two subcategories, the HECT-domain E3s or the RING-finger E3s (Fang and Weissman, 2004).

The HECT (Homologous to E6-AP C-terminus)-domain family was the first family of ubiquitin-ligases to be identified. The first member of this family, E6-AP, was discovered as a cellular protein which was required for the ubiquitylation and subsequent degradation of the p53 tumor suppressor by the human pappilomavirus E6 oncoprotein (Scheffner et al., 1994). HECT-domain E3s first transfer ubiquitin from the bound E2 onto their active site cysteine in the C-terminal HECT-domain before they pass it on to their substrate protein.

The RING (Really Interesting New Gene)-domain family is the largest family of ubiquitin-ligases. The RING-finger is defined by eight conserved cysteines and histidines which together coordinate two zinc ions (Borden and Freemont, 1996). The first member of this family which was identified is the ubiquitin-ligase E3α, which is responsible for ubiquitylating substrates of the N-end rule pathway. RING-domain E3s do not transfer the activated ubiquitin onto themselves, but rather facilitate its transfer from the tightly bound E2 directly onto the substrate protein. This family of E3s consists of both single subunit enzymes, which contain all the necessary domains in one protein, for example Cbl, as well as large multimeric complexes such as the SCF-complex, or the anaphase-promoting-complex, in which the RING domain exists as a separate subunit (Joazeiro and Weissman, 2000).

The other two subfamilies are relatively small and both contain variants of the RING-domain. The PHD-finger was first identified as a component of viral ubiquitin-ligases, but has subsequently also been found in mammalian proteins (Coscoy and Ganem, 2003). The U-box, in turn, is a modified RING-domain with no coordinated zinc ions. The ubiquitin-ligase CHIP for example, which functions as an E3 for HSP90 interacting proteins, is a member of this last family (Jiang et al., 2001).

In contrast to the large number or E3 enzymes, the mammalian genome encodes for only about 30 different E2 ubiquitin-conjugating enzymes (von Arnim, 2001). As a consequence, each E2 enzyme is responsible for serving a number of different E3s. All known E2 enzymes belong to the same family, which is characterized by the presence of a catalytic domain called the UBC-domain. Some E2s possess additional C-terminal or N-terminal extensions, which are responsible for mediating subcellular localization or recognition of E3 enzymes. With a few exceptions

– among them BRUCE, a 528 kDa inhibitor of apoptosis (Hauser et al., 1998) – most E2s are of rather small size (Jentsch et al., 1990).

Two different E1 enzymes are able to activate ubiquitin in the first step of the ubiquitin conjugation process. These ubiquitin-activating enzymes, which are called UBE1 and UBA6, serve distinct, but overlapping pools of E2s. Although both E1s are broadly expressed in all tissue types, deletion of either one of them is lethal, indicating that there is little redundancy in the system. Interestingly, UBE1 – which was long thought to be the only ubiquitin-conjugating enzyme in existence – is expressed at a much higher level in most tissues and accounts for up to 85% of all ubiquitin conjugates observed (Groettrup et al., 2008).

A further layer of complexity is added to the ubiquitin-system through the actions of a group of deubiquitylating enzymes, or DUBs, the majority of which fall into one of two subgroups: The family of ubiquitin C-terminal hydrolases (UCHs) or the family of ubiquitin-specific processing proteases (UBPs). DUBs carry out a variety of processing or editing functions. Some of them are responsible for the processing of linear ubiquitin-fusions and are required for the generation of active ubiquitin from newly synthesized precursor proteins. Others are responsible for the removal of polyubiquitin-chains from proteins targeted for proteasomal degradation, ensuring that these are not degraded along with their substrates but instead recycled. Once the ubiquitin chains are liberated, a second group of DUBs then disassembles them into ubiquitin monomers. Yet another group is involved in the modulation of various ubiquitin signals. They can, for example, rescue proteins from degradation by removing their ubiquitin-tags before they come into contact with the proteasome, or attenuate signal transduction cascades by removing the activating K63-linked chains (Amerik and Hochstrasser, 2004).

Both the enzymes involved in ubiquitin-processing as well as the effector proteins which act downstream of the ubiquitin signal need to interact with ubiquitin, and this recognition is mediated by a plethora of different ubiquitin-binding domains. These include – but may not be limited to – sixteen different domains: UBA, UIM, MIU, DUIM, CUE, GAT, NZF, A20 ZnF, BUZ, UBZ, Ubc, UEV, UBM, GLUE, Jab1/MPN and PFU. Interestingly, although several of these domains display absolutely no sequence similarity and seem to have evolved independently of each other, most of them bind to ubiquitin through a conserved surface encompassing residues Leu8, Ile44 and Val70, which is called the “hydrophobic patch”. A notable exception to this rule is the BUZ domain, a zinc-finger which instead interacts with ubiquitin through its free C-terminal diglycine-motif, and is for

example contained in the deubiquitylating enzyme isopeptidase T or the tubulin deacetylase HDAC6. Most ubiquitin-binding domains display a preference for either monoubiquitin, different polyubiquitin chain topologies or ubiquitin-like domains, although the exact molecular determinants of this ability to discriminate remain unknown (Hurley et al., 2006).

Ubiquitin-Like Proteins

All eukaryotic cells contain several additional proteins which are related to ubiquitin in either sequence or structure. Like ubiquitin, these proteins are involved in a vast number of fundamental cellular processes. Collectively known as ubiquitin-like proteins, they can be subdivided into the families of ubiquitin-like modifiers and ubiquitin-domain proteins (Fig. 3). Members of the first group function – as their name suggests – as modifiers, and are covalently attached to other proteins in a manner analogous to ubiquitin conjugation. Members of the second group are larger proteins and contain a ubiquitin-like domain as an integral part of their sequence, but are otherwise functinally diverse (Jentsch and Pyrowolakis, 2000).

Ubiquitin-Like Modifiers

With the exception of ATG8, ATG12 and URM1, all ubiquitin-like modifiers (UbLs) display a high level of sequence homology to ubiquitin and, regardless of their sequence, they all share essentially the same three-dimensional structure. In addition, those UbLs which are capable of covalent attachment to another protein invariably share a conserved glycine residue at their C-terminus, and the carboxyl group of this glycine is the site of attachment to their substrates. Like ubiquitin, most of them are generated as precursors with C-terminal extensions of variing length and need to be activated through endoproteolytic processing. This step is mediated by UbL-specific proteases (ULPs), which function in a manner analogous to DUBs and are also capable of hydrolizing the isopeptide bond between their specific UbL and its target proteins. Exceptions to this rule are ATG12, URM1 and FAT10, which already contain a free glycine at their C-terminus and have no requirement for processing.

Ubiquitin-like modifiers are also conjugated to their target proteins by way of a multi-enzyme cascade, in a manner analogous to that of ubiquitin conjugation,

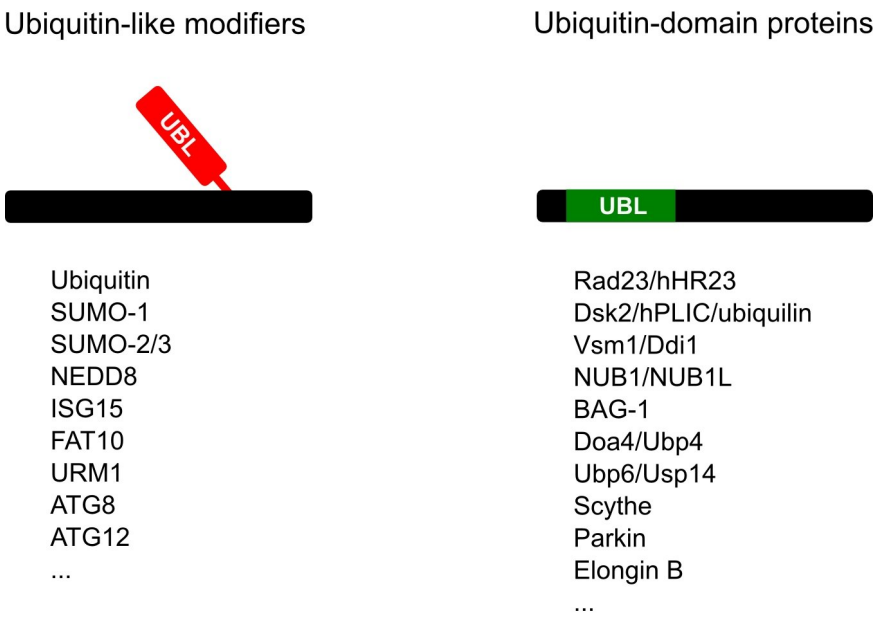

Figure 3: Two families of ubiquitin-like proteins. Ubiquitin-like modifiers (UbLs, red) are conjugated to their target proteins in a manner analogous to that of ubiquitin. Ubiquitin-domain proteins (UBDs) contain an integral ubiquitin-like domain (green), but do not form conjugates. (Modified from Jentsch and Pyrowolakis, 2000).

which ultimately results in the formation of an isopeptide linkage between the C-terminal glycine of the UbL and a lysine residue of the target protein. Many of the enzymes involved in the conjugation of UbLs have recently been discovered, and although the pathways appear to be for the most part distinct, there appears to be a certain amount of enzyme sharing between different modifiers. ATG8 and ATG12, the two UbLs involved in autophagosome formation, for example share a single E1, ATG7, but each of them has their own E2. Conversely, two different E1s specific for different UbLs can share the same E2; UBEL1, the E1 for ISG15, and UBE1, the E1 for ubiquitin, both can both transfer their respective modifier to the E2 UbcH8. Apart from FAT10, none of the other UbLs are directly involved in the targeting of proteins for proteasomal degradation. Instead, through their attachment, they are for example able to alter the function or subcellular localization of their target protein (Welchman et al., 2005; Kerscher et al., 2006).

SUMO (Small ubiquitin-like modifier), which is perhaps the most well-studied member of this group, exists in the form of three isoforms, SUMO-1, SUMO-2 and SUMO-3, of which the latter two are virtually identical in sequence and are functionally distinct from SUMO-1. Interestingly, SUMO-2/3 are the only

two modifiers apart from ubiquitin which could be shown to form polyUbL-chains (Tatham et al., 2001). In many cases, the attachment of SUMO leads to a change in the subcellular localization of its target proteins, for example in the case of RanGAP1, which is involved in nuclear import/export and is targeted to the nuclear pore complex by modification with SUMO-1 (Matunis et al., 1996). In the case of the promyelotic leukemia (PML) protein, SUMOylation is required for its function as a scaffold promoting the formation of PML nuclear bodies, which are subnuclear structures implicated in transcriptional regulation and DNA repair (Zhong et al., 2000). Interestingly, PML can also be polySUMOylated, and this leads to the recruitment of the SUMO-interaction (SIM) domain containing ubiquitin-ligase RNF4/SNURF. Recruitment of RNF4 then facilitates the polyubiquitylation of PML which ultimately results in the destruction of PML via proteasomal degradation (Tatham et al., 2008; Lallemand-Breitenbach et al., 2008). Furthermore, several proteins can be modified by either SUMO or ubiquitin at the same lysine residue. The attachment of either SUMO or ubiquitin is mutually exclusive, and for a number of proteins – among them the DNA-replication processivity factor PCNA (Hoege et al., 2002), or the tumor suppresor p53 (Rodriguez et al., 1999) – it could be shown that SUMOylation can prevent ubiquitylation at the same residue. Interestingly, many of SUMO's target proteins contain a consensus SUMOylation site, which can be directly recognized by the E2, thereby obliterating the need for an E3 (Johnson, 2004).

NEDD8 (Neuronal precursor cell-expressed developmentally down-regulated 8) was originally characterized as a protein able to regulate the activity of ubiquitin-ligases. NEDDylation of cullins, which are scaffoliding subunits of multi-component RING E3s, enables the interaction of the E3 with its cognate E2 (Pan et al., 2004). Another example of a target of NEDDylation is the tumor suppressor p53, which in addition to being subject to both ubiquitylation and SUMOylation, can also be modified by NEDD8. Like ubiquitylation, attachment of NEDD8 can inhibit p53 activity and is mediated by the same E3 ligase, Mdm2 (Xirodimas et al., 2004).

ISG15 (Interferon-stimulated gene 15) consists of two UBL domains in a tandem array and is the only ubiquitin-like modifier which can be secreted into the extracellular space (Knight and Cordova, 1991). Several components of the ISG-conjugation and deconjugation machinery, such as its E1 UBE1L (Yuan and Krug, 2001), its E2 UbcH8 (Kim et al., 2004) and the deconjugating enzyme UBP43 (Malakhov et al., 2002), as well as ISG15 itself are inducible with IFN-α and IFN-β. Free ISG15 displays immunemodulatory functions and has been shown

to stimulate the IFN-γ production by $CD3^+$ cells (Recht et al., 1991) and activate the proliferation of $CD56^+$ natural killer cells (D'Cunha et al., 1996). Furthermore, in accordance with its function as a putative antiviral effector, several viruses actively block the conjugation of ISG15 to its target proteins (Yuan and Krug, 2001; Guerra et al., 2008). Several key factors involved in signal transduction, among them phospholipase Cγ1, the kinases JAK1 and ERK1, as well as the transcription factor STAT1, have been reported to be substrates of ISG15 (Malakhov et al., 2003), however, the biological significance of their modification remains unknown.

FAT10

FAT10 (HLA-F locus associated transcript 10) is a ubiquitin-like modifier of 165 amino acids in length and encompasses two ubiquitin-like domains in a head-to-tail formation, which are connected by a short linker. Owing to its resemblance to a tandem fusion of two ubiquitins, it was originally also called "diubiquitin" or "ubiquitin D". Its N-terminal and C-terminal ubiquitin-like domains are more closely related to ubiquitin than to each other and show 29% and 36% sequence identity to ubiquitin, respectively. Four of the lysine residues involved in polyubiquitin-chain formation – corresponding to K27, K33 and most notably K48 and K63 – are conserved in both ubiquitin-like domains of FAT10. In addition, it does not carry a C-terminal extension, but rather ends with a free diglycine-motif (Fig. 4). The *fat10* gene lies encoded in the MHC class I HLA-F locus on chromosome 6, adjacent to the genes for the interferon-inducible subunits LMP2 and LMP7 of the proteasome and was thus originally suspected to have a function in antigen processing and presentation (Fan et al., 1996; Bates et al., 1997).

FAT10 is constitutively expressed in dendritic cells and mature B cells (Bates et al., 1997), and FAT10 mRNA was readily detectable in spleen and thymus both by Northern blot, *in situ* hybridization (Liu et al., 1999) as well as qRT-PCR (Lukasiak et al., 2008). However, expression of FAT10 is not restricted to cells of the immune system, but can be synergistically induced with the proinflammatory cytokines TNF-α and IFN-γ in cells of almost every tissue origin. Induction of the FAT10 mRNA did not rely on *de novo* protein synthesis and was partially dependent on proteasomal activity, as treatment with proteasome inhibitors prevented induction of FAT10 with TNF-α, but not IFN-γ (Raasi et al., 1999). In addition, the *fat10* promotor was shown to contain a p53-binding site and transcription of the *fat10* gene appeared to be negatively regulated by p53 (Zhang et al., 2006a).

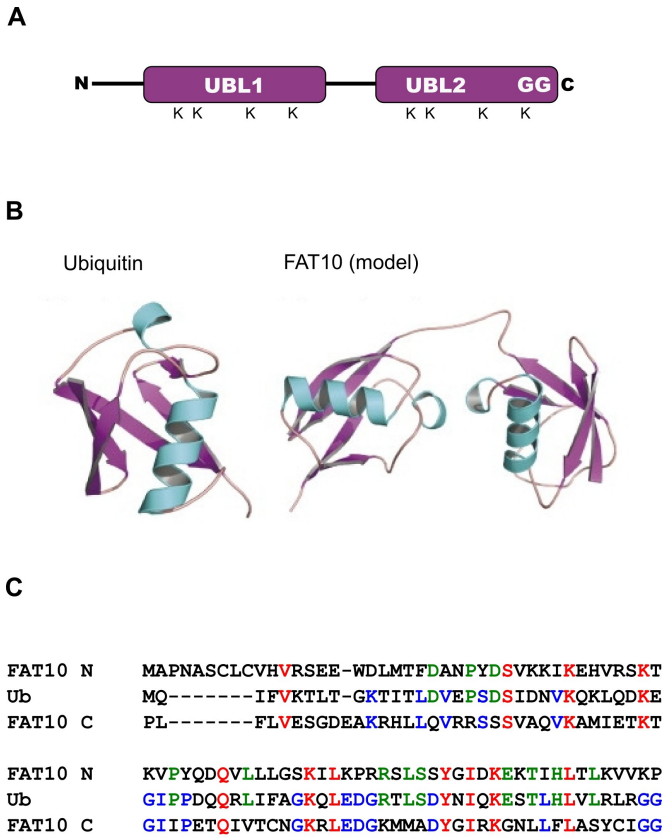

Figure 4: Comparison of sequence as well as predicted tertiary structure of FAT10 with ubiquitin. (A) FAT10 encompasses two ubiquitin-like domains (UBLs) which are 29% and 36% identical to ubiquitin. The C-terminal diglycine-motif is conserved in the second domain of FAT10. In addition, four of the lysines involved in polyubiquitin-chain formation – corresponding to K27, K33, K48 and K63 – are conserved. **(B)** Ribbon diagrams of the ubiquitin structure and the predicted structure of FAT10. (Modified from Groettrup et al., 2008). **(C)** Sequence alignment of the N- and C-terminal parts of FAT10 with ubiquitin.

Although the identity of its target proteins remains elusive, FAT10 could be shown to form covalent conjugates through its C-terminal glycine (Raasi et al., 2001), and the E1 enzyme responsible for its activation was recently discovered (Chiu et al., 2007). Interestingly, FAT10 shares its activating enzyme, UBA6, with ubiquitin, although both modifiers appear to be passed on to different E2 enzymes.

FAT10 shares one additional important property with ubiquitin, as both modifiers can promote the proteasomal degradation of their substrates with equal potency, an ability intrinsic to no other member of the ubiquitin superfamily. Interestingly, although ubiquitin is a remarkably stable protein, both FAT10 as well as its conjugates are rapidly degraded. This finding, together with the apparent lack of a FAT10-specific protease suggests that, rather than being recycled, FAT10 is degraded along with its substrates (Hipp et al., 2005), and experiments with a

diglycine-deficient mutant of FAT10 revealed that conjugation to a substrate was not required for its degradation (Hipp, 2004). In addition, the degradation of FAT10 could be further accelerated through coexpression of a non-covalent interaction partner, the UBL-UBA domain protein NUB1L (Hipp et al., 2004). Despite the striking similarities between ubiquitin- and FAT10-mediated degradation, FATylation of a protein appears to be sufficient to promote its degradation, as two experimental approaches demonstrated no further requirement for ubiquitylation. A mutant version of FAT10, which due to a lack of lysines is unable to serve as a substrate of ubiquitin conjugation, was still able to promote the degradation of a model substrate. Likewise, a cell line carrying a thermolabile mutant of the major ubiquitin-activating enzyme showed no accumulation of an artificial FAT10-conjugate (Hipp et al., 2005).

Evidence for a role of FAT10 in immunity has remained sparse. In fact, the only two connections to the immune response derive from the study of FAT10 gene-targeted mice, which display a hypersensitivity to LPS as their major phenotype to date (Canaan et al., 2006), and the finding that FAT10 might be able to inhibit hepatitis B virus expression in a hepatoblastoma cell line (Xiong et al., 2003). A recent number of publications have, however, implicated FAT10 in cancer, although it is still a matter of debate whether it functions as a tumor suppressor or rather an oncogene.

One study found FAT10 to be highly upregulated in hepatocellular carcinoma as well as other cancers of the gastrointestinal tract and female reproductive system (Lee et al., 2003). Another identified FAT10 as a potential marker for liver preneoplasia, as it was highly overexpressed in a model of Mallory-Denk body containing chronic liver diseases, which are thought to progress to hepatocellular carcinoma (Oliva et al., 2008). Both suggested an active role of FAT10 in tumorigenesis based on its interaction with the spindle assembly checkpoint protein MAD2 (Liu et al., 1999). Through non-covalent interaction, FAT10 is thought to displace MAD2 from the kinetochore during prometaphase, which leads to faulty chromosomal segregation and ultimately results in the formation of cells containing abnormal chromosome numbers (Ren et al., 2006). This hypothesis is further corroborated by the finding that the expression of FAT10 is cell-cyle regulated at transcript level and is kept low in G2/M phase, presumably to prevent FAT10 from interfering with chromosomal segregation (Lim et al., 2006).

Strong evidence for the function of FAT10 as a tumor suppressor, on the other hand, comes from the finding that expression of FAT10 is able to induce caspase-

dependent apoptosis in a variety of models. Studies in a mouse fibroblast line demonstrated that overexpression of FAT10 resulted in massive caspase-dependent cell death within 24 to 48 hours, and that this induction of apoptosis was dependent on the conjugation of FAT10 to so far unidentified target proteins (Raasi et al., 2001). A different study found FAT10 to be highly upregulated in the HIV-1 induced dysregulated apoptosis of renal tubular epithelial cells and was able to show that expression of FAT10 promoted apoptosis in a culture of those cells (Ross et al., 2006). In addition, two groups described their inability to generate stable transfectants of FAT10 as a result of profound cell death caused by the overexpression of FAT10 (Liu et al., 1999; Raasi et al., 1999). Furthermore, NIH3T3 transformation assays revealed FAT10 to have no transforming capability and the same study also demonstrated that the upregulation of FAT10 in liver and colon cancer cells could be attributed to the synergistic action of IFN-γ and TNF-α due to an ongoing immune response (Lukasiak et al., 2008).

Ubiquitin Domain Proteins

Ubiquitin domain proteins (UBDs) are a structurally and functionally heterogeneous group and are characterized by the presence of an integral ubiquitin-like (UBL) domain. This domain lacks the C-terminal diglycine-motif found in ubiquitin and most ubiquitin-like modifiers and can neither be conjugated to other proteins nor is it a signal for degradation. Instead, it functions as a mediator of protein-protein interactions through recognition by ubiquitin-binding domains. In most cases, the UBL domain is situated near or at the N-terminus of the UBD while the C-terminus contains one or more additional, unrelated domains pertaining to the function of the protein. (Jentsch and Pyrowolakis, 2000). Interestingly, many ubiquitin-domain proteins are able to interact with the 19S proteasomal regulator, which appears to be a common mechanism of tethering proteins with different functions to the 26S proteasome (Schauber et al., 1998). Among them are deubiquitylating enzymes, such as Ubp4/Doa4 (Papa et al., 1999) and Usp14/Ubp6, which binds to the S1 and S2 subunits of the 19S regulator (Leggett et al., 2002) and is also able to delay proteasomal degradation through a second, noncatalytic mechanism (Hanna et al., 2006). E3s can also associate directly with the proteasome; for example the ubiquitin-ligase parkin (Shimura et al., 2000), which binds to the S5a subunit via its UBL domain (Sakata et al., 2003). Other proteins simply serve as adaptors, such as BAG-1 (Bcl2-associated athanogene-1), which is responsible for tethering both HSP70 as well as the HSP70-interacting E3 ligase CHIP to the proteasome (Lüders et al., 2000; Alberti et al., 2002).

A distinct subgroup consists of ubiquitin domain proteins which are characterized by the possession of one or more ubiquitin-associated (UBA) domains and are thought to function as soluble ubiquitin receptors and facilitators of proteasomal degradation. Members of this family of UBL-UBA domain proteins include hHR23/Rad23 (Chen and Madura, 2002), hPLIC/ubiquilin/Dsk2 (Funakoshi et al., 2002), NUB1 (Kito et al., 2001), and Ddi1/Vsm1 (Bertolaet et al., 2001), which is the only member of this family containing a putative aspartyl protease domain (Sirkis et al., 2006). Although there are conflicting data, a growing body of evidence now supports a model in which UBL-UBA proteins function as proteasome-substrate carriers by binding to the proteasome through their UBL domain and to polyubiquitylated cargo through their UBA domain(s).

Most of the evidence comes from the study of Rad23, which was originally discovered as a component of nuclear excision repair, and Dsk2. Both proteins could be shown to interact via their UBL domain with the S5a (Hiyama et al., 1999; Walters et al., 2002) and S2 (Elsasser et al., 2002) subunits of the proteasome and with polyubiquitylated cargo through their UBA domains (Chen et al., 2001; Zhang et al., 2008a). Through genetic studies, which were mostly performed in yeast, it could be shown that deletion of either of these proteins resulted in the accumulation of high molecular weight ubiquitin conjugates and impaired degradation of a limited number of proteasomal substrates (Chen and Madura, 2002; Funakoshi et al., 2002; Rao and Sastry, 2002). It would be expected that the overexpression of UBL-UBA proteins, in turn, stimulates the degradation of these substrates, which could indeed be observed in some cases (Funakoshi et al., 2002; Verma et al., 2004b). However, it appears that the system is highly sensitive to pertubations in the level of UBL-UBA proteins, as their overexpression often leads to the stabilization, rather than accelerated degradation, of proteasomal substrates (Kleijnen et al., 2000; Ortolan et al., 2000). This effect can probably be attributed to the sequestration of polyubiquin chains by an excess of soluble UBA domain containing proteins, which effectively prevents their association with all sorts of ubiquitin-interacting proteins including not only proteasomal subunits (Raasi and Pickart, 2003), but also for example enzymes involved in polyubiquitin-chain assembly (Ortolan et al., 2000), or deubiquitylation (Hartmann-Petersen et al., 2003). As most manipulations concerning a single proteasome receptor have only mild effects on the bulk turnover of polyubiquitylated proteins, there appears to be a high level of redundancy in the delivery of polyubiquitylated substrates to the proteasome. Accordingly, only the combined deletion of the three proteasome receptors Rpn10, Rad23 and Dsk2 results in a severe (Saeki et al., 2002a) or lethal (Wilkinson et al., 2001) phenotype in yeast.

Interestingly, a recent study has uncovered a dual role of these ubiquitin-receptors in both substrate delivery and the stimulation of proteasomal activity (Verma et al., 2004a). Although Rad23 was sufficient to physically link a polyubiquitylated substrate to the proteasome, the presence of the VWA domain of Rpn10 – but not its UIM domain – was required to facilitate its degradation. As this requirement for facilitation was only observed for one of the substrates under investigation, it appears that despite of all redunancy, different substrates are preferrentially targeted to the proteasome via different mechanisms.

NUB1

NUB1 was originally identified as a protein able to interact with and down-regulate cellular NEDD8 levels via proteasomal degradation (Kito et al., 2001; Kamitani et al., 2001) and was thus christened "NEDD8 ultimate buster 1". It is a member of the family of UBL-UBA domain proteins and exists in the form of two splicing variants, a short version of 601 amino acids in length (NUB1), which contains two UBA domains, and a long version (termed NUB1long or NUB1L) containing an insertion of 14 amino acids, which generates a third UBA domain sandwiched inbetween the two existing ones (Tanaka et al., 2003). NUB1 has a somewhat unique status among the UBL-UBA proteins, as it is the only member of this family which contains UBA domains that are unable to associate with either polyubiquitin-chains or monoubiquitin (Raasi et al., 2005). The binding of NEDD8 was mapped to the second UBA domain (UBA2) as well as a short sequence near the C-terminus of NUB1, which includes the C-terminal half of a PEST domain. In addition, NUB1 was also reported to interact with the ubiquitin-precursor UbC1, however, the functional significance of this finding remains unknown (Tanaka et al., 2004). In addition, it is able to associate with the proteasomal subunit S5a/Rpn10 (Kamitani et al., 2001), and this interaction has surprisingly been reported to be mediated not through its UBL domain but rather through a short C-terminal region between amino acids 536 and 584 (Tanji et al., 2005). NUB1 is inducible with IFN-β as well as IFN-γ and its subcellular localization is mainly nuclear, owing to the presense of a nuclear localization signal (NLS) between residues 414 and 431 (Kito et al., 2001). Even though it is cytokine-inducible, NUB1/NUB1L appears to be universally expressed in all tissue types, although the two isoforms differ in their level of mRNA expression (Tanaka et al., 2003).

NUB1 has recently been implicated in two different types of neurodegenerative diseases, although the evidence is, admittedly, only circumstantial. NUB1 has been found to interact with AIPL1 (Aryl hydrocarbon receptor-interacting protein-like 1), a protein which is expressed solely in the rod photoreceptors of the adult human retina and is mutated in patients with Leber congenital amaurosis (LCA), a severe, early-onset form of retinal degeneration (Akey et al., 2002). AIPL1 functions as part of a chaperone heterocomplex containing both HSP70 and HSP90 (de Quintana et al., 2008) and is able to promote the translocation of NUB1 from the nucleus to the cytoplasm as well suppress the formation of NUB1 containing cytoplasmatic inclusions (van der Spuy and Cheetham, 2004). Interestingly, mutations in both the chaperone (de Quintana et al., 2008) as well as the NUB1 (Kanaya et al., 2004) binding sites have been found in patients with Leber congenital amaurosis. The second link to neurodegeneration derives from the interaction of NUB1 with synphilin-1, which is a major component of inclusion bodies found in the brains of patients with neurodegenerative α-synucleinopathies, such as Parkinson's disease. It could be shown that NUB1 is able to suppress the formation of synphilin-1 containing inclusion bodies, presumably by proteasomal degradation of synphilin-1 (Tanji et al., 2006). The same study also demonstrated the presence of NUB1 in synphilin-1 positive Lewy bodies of Parkinson's disease, while a follow-up study revealed NUB1 to only be present in inclusions found in patients with α-synucleinopathies, but not in inclusions observed in patients with other neurodegenerative diseases (Tanji et al., 2007).

Through a yeast two-hybrid screen with the ubiquitin-like modifier FAT10 as a bait, NUB1L was recently identified as a non-covalent binding partner of FAT10, which could be verified both *in vivo* as well as *in vitro*. In addition, NUB1L was shown to specifically interact with FAT10 and failed to bind either ubiquitin or SUMO. Strikingly, this study was unable to reproduce the interaction with NEDD8, neither *in vivo* nor *in vitro*, although under the same conditions, FAT10 displayed robust interaction with NUB1L. Furthermore, even a 10-fold excess of NEDD8 was unable to compete with FAT10 for NUB1L binding. Overexpression of NUB1L had no influence on the subcellular localization of FAT10. It did, however, lead to a marked increase in the rate of FAT10 degradation, which is consistent with its role as a putative proteasomal FAT10-receptor. (Hipp et al., 2004).

The Autophagy-Lysosome System

Autophagy is an intracellular degradation system which delivers cytoplasmatic compontents to the lysosome. There are three distinct types of autophagy – microautophagy, chaperone-mediated autophagy and macroautophagy – and the name "autophagy" usually refers to the process of macroautophagy unless otherwise specified (Mizushima and Klionsky, 2007). Microautophagy involves the budding of small cytosol-containing vessels directly into the lysosomal lumen. During chaperone-mediated autophagy, proteins carrying a signal-peptide for lysosomal sorting are directly transported into the lysosome by the transporter LAMP-2a, which is assisted by cytosolic and lysosomal chaperones of the HSC70 family (Massey et al., 2006). Macroautophagy is mediated by a unique organelle termed the autophagosome. During its process, a crescent-shaped isolation membrane forms *de novo* and encloses cytoplasmatic components – sometimes including whole organelles – in a double-membraned vesicle, which subsequently fuses with a lysosome for the degradation of its cargo and inner membrane (Ohsumi, 2001 and Fig. 5).

Nutrient starvation – and the lack of amino acids in particular – is the most typical trigger of autophagy, although a number of other factors inclucing, but not limited to, insulin, growth factors or TRAIL are also able to negatively or positively affect autophagy (Mizushima, 2007). Many of the signals modulating autophagy converge at mTOR (mammalian target of rapamycin), which is a master regulator of nutrient signaling and potent inhibitor of autophagy. Inhibition of mTOR ultimately results in autophagosome formation, which is mediated through the concerted action of approximately 20 autophagy-related (ATG) proteins and involves the action of two ubiquitin-like conjugation systems. In a first step, the ubiquitin-like modifiers ATG8 – which requires prior processing by ATG4 to remove its C-terminal extension – and ATG12 are activated through their common E1 enzyme ATG7. ATG8, which in mammals is known as LC3 (light chain 3), then becomes conjugated to the lipid phosphatidyl-ethanolamine in the forming isolation membrane through its E2 enzyme ATG3. Following completion of the autophagosome, ATG8 gets recycled from the outer autophagosomal membrane by deconjugation from the phospholipid, however, it remains attached to the inner membrane and this portion is degraded upon fusion with the lysosome. Owing to its prominent localization to the inside of the autophagosomal membrane, ATG8 has been suggested to function as an anchor for autophagy substrates. ATG12 in turn becomes conjugated to ATG5 through the action of its E2 enzyme ATG10.

The ATG12-ATG5 complex then associates with ATG16 and is thought to create a scaffold for the formation of the isolation membrane (Xie and Klionsky, 2007).

As autophagy functions by engulfing a portion of the cytoplasm, it was generally thought to be a non-selective degradation system. However, this view has recently been challenged by a number of reports which describe the specific targeting of certain substrates to the autophagosome.

Misfolded Protein Stress, Aggresomes and the Connection between Autophagy and the UPS

The existence of misfolded proteins in cells is an inevitable consequence of partial unfolding during thermal or oxidative stress and of alterations in primary structure caused by mutation, translational misincorporation or premature termination. Due to the exposure of hydrophobic regions, misfolded proteins are prone to aggregation, and – if not immediately cleared – ultimately accumulate in insoluble cytoplasmatic or nuclear inclusions (Kopito, 2000). The accumulation of protein aggregates has been tightly linked to neuronal degeneration or organ failure in a number of diseases such as Alzheimer's, Parkinson's or Huntington's disease and alcohol or drug induced liver damage (Gregersen et al., 2006). Although the exact reasons behind the cytotoxicity of protein aggregates remain unknown, a number of likely mechanisms have been proposed: First of all, the accumulation of aggregates refractory to unfolding could lead to impairment of the ubiquitin-proteasome system simply by "clogging" the proteasome, as the unfolding of its substrates is a prerequisite for their degradation (Bence et al., 2001; Bennett et al., 2005). Alternatively, aggregates could lead to the disruption of microtubule-dependent axonal transport (Gunawardena et al., 2003), or they could directly interact with transcription factors or membrane receptors, which might result in an aberrant activation of signal transduction pathways (Yan et al., 2000).

In any case, whatever the reason for the cytotoxicity of misfolded proteins, cells have evolved a number of ways to counter the formation of protein aggregates. First in line are the molecular chaperones, which transiently associate with unfolded or partially folded intermediates and shelter hydrophobic surfaces from forming inappropriate intra- or intermolecular contacts. Chaperones are constitutively active in the quality control of nascent polypepdides, but can also be

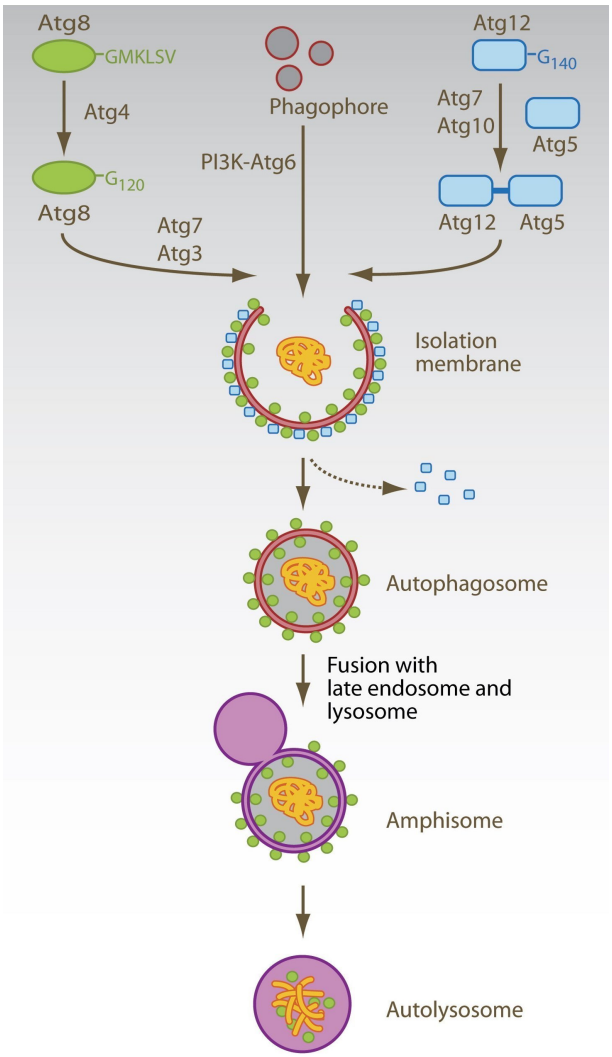

Figure 5: Molecular machinery of autophagy. Two ubiquitin-like systems are required for formation of the isolation membrane and couple ATG8 (LC3) and ATG12 to phosphatidylethanolamine (PE) and ATG5, respectively. The five C-terminal amino acids of ATG8 are cleaved of by ATG4 to reveal glycine 120 (G120), which is required to link the protein after activation by ATG7 and ligation by ATG3 to PE in the autophagosomal membrane (green circles). Similarly, glycine 140 (G140) is used by ATG7 and ATG10 to couple ATG12 to ATG5. This complex then localizes to the outer membrane of the forming autophagosome (blue squares). Upon autophagosome completion, the ATG12-ATG5 complex recycles from the outer membrane, and only ATG8 remains associated with the completed autophagosome. Autophagosomes then fuse with late endosomes and lysosomes for degradation of their cargo and their intravesicular membranes. (Modified from Schmid and Münz, 2007).

strongly induced under conditions which lead to the massive generation of misfolded proteins, such as heat-shock or oxidative stress (Hendrick and Hartl, 1995; Bukau et al., 2006).

Proteins which do not pass quality control mechanisms or fail to successfully complete chaperone-mediated refolding are eventually targeted for proteasomal degradation through the attachment of a polyubiquitin-chain. This mechanism has been well established for proteins degraded via the ER-associated degradation pathway (ERAD), but is also thought to apply to misfolded proteins originating from the cytoplasm or nucleus (Meusser et al., 2005). The ubiquitin-ligase CHIP, for example, represents an interesting connnection between the chaperone machinery and the ubiquitin-proteasome system. It is able to simultaneously associate with both the proteasome as well as chaperones of the HSC70 family and is responsible for the polyubiquitinylation of those chaperone substrates which fail to aquire proper folding (McDonough and Patterson, 2003). Removal of misfolded proteins by the proteasome, however, is complicated by the fact that substrate unfolding is a prerequisite for proteasomal degradation. Thus, for misfolded proteins to be cleared by the proteasome, they need to be present in soluble, monomeric form. As soon as they aggregate into insoluble polymers, the proteasome is no longer able to mediate their destruction, resulting in a vicious circle as insoluble protein aggregates in turn are potent inhibitors of proteasomal degradation (Bence et al., 2001).

Fortunately, cells have evolved a way out of this predicament through the sequestration of misfolded proteins in a subcellular structure called the aggresome. The aggresome is a pericentriolar body which forms mainly under conditions of misfolded protein stress and is encaged by a tight mesh of vimentin filaments, presumably to prevent its contents from dissociating. In addition, it contains a large amount of proteins associated with protein refolding or removal, such as heat-shock proteins or proteasomes (Kopito, 2000; Garcia-Mata et al., 2002). Primarily in the form of microaggregates, misfolded proteins are actively delivered to the aggresome via dynein-dependent transport along the microtubule network (Johnston et al., 2002). Although the majority of misfolded proteins is polyubiquitylated prior to their delivery to the aggresome, a small number of proteins can apparently be targeted without the involvement of ubiquitin, as overexpression of inherently unstable proteins such as GFP-250 (Garcia-Mata et al., 1999) as well as mutant SOD (Johnston et al., 2000) or ATP7B (Johnston et al., 1998) leads to the formation of aggresomes which do not stain positively for polyubiquitin.

The transport of misfolded proteins to the aggresome serves a dual purpose. As an immediate response to the danger posed by toxic protein aggregates, it collects them in a centralized "landfill" where they can no longer do the cell any harm. Later on, the centralized location of these aggregates simplifies their complete removal, as they can be more easily be picked up and disposed of via autophagy (Iwata et al., 2005; Pandey et al., 2007b). Interestingly, the cytoplasmatic inclusions which are a hallmark of many conformational diseases, such as Lewy bodies of Parkinson's disease (Olanow et al., 2004), or Mallory-Denk bodies of chronic liver disease (French et al., 2001), display a striking resemblance to aggresomes.

Autophagy and the aggresome are not only components of an emergency waste disposal mechanism, but are also also involved in a number of other fundamental processes such as cell death or immunity. Both aggresomes as well as autophagy have been implicated in pathogen defense through the innate immune response, in addition, autophagy has emerged as a source of intracellular peptides for MHC class II presentation (Schmid and Münz, 2007). DALIs, in turn, which are aggresome-like structures specific to activated dendritic cells, have been shown to function as storage compartments of proteins targeted for presentation via the class I pathway (Pierre, 2005). Furthermore, autophagy is able to both positively and negatively regulate apoptosis through interaction with the anti-apoptotic proteins BCL-2 and BCL-X_L, as well as through additional, so far unidentified mechanisms (Thorburn, 2008).

Two proteins are responsible for making the connection between the ubiquitin-proteasome system and autophagy. These are the cytoplasmatic deacetylase HDAC6 and p62, which is also known as sequestosome 1 (SQSTM1). Both function as adaptor proteins and are able to recognize polyubiquitylated substrates through a ubiquitin-binding domain in their C-terminus. p62 contains a UBA domain in its C-terminus, which is responsible for mediating the recognition of polyubiquitin, as well as a PB1 domain near its N-terminus. Interestingly, PB1 domains display significant homology to UBL domains and the PB1 domain of p62 is indeed able to tether the protein to the S5a subunit of the 26S proteasome (Seibenhener et al., 2004). This domain also mediates dimerization of p62 as well as its association with a number of additional proteins (Wilson et al., 2003). In addition to being able to attach to the proteasome, p62 is also able to localize to the aggresome through association with ATG8/LC3 (Pankiv et al., 2007; Shvets et al., 2008). Furthermore, p62 has been shown to be capable of sequestering polyubiquitin in aggresomes (Shin, 1998), and was found to be a component of Lewy

bodies, Mallory-Denk bodies, the neurofibrillary tangles of Alzheimer's disease and huntingtin aggregates (Zatloukal et al., 2002; Kuusisto et al., 2001; Nagaoka et al., 2004), although the domain responsible for mediating its localization to aggresomes has yet to be identified. Thus, p62 appears to function as a shuttling factor which can alternate between the delivery of polyubiquitylated proteins to either the proteasome or the aggresome or even directly into the autophagosomal vesicle. Indeed, p62 could be shown to target tau for proteasomal degradation (Babu et al., 2005), while it was also able to direct mutated huntingtin to the autophagosome (Bjørkøy et al., 2005).

HDAC6

HDAC6 (histone deacetylase 6) is a cytoplasmatic class II deacetylase (Verdel and Khochbin, 1999; Yang and Grégoire, 2005) and is responsible for the deactylation of α-tubulin (Hubbert et al., 2002; Matsuyama et al., 2002; Zhang et al., 2003b), HSP90 (Bali et al., 2005) and cortactin (Zhang et al., 2007), although it could be shown to also deacetylate histones *in vitro* (Haggarty et al., 2003). HDAC6 is the only member of the histone deacetylase family which encompasses two catalytic domains and presumably does not rely on dimerization to exert its catalytic function (Zhang et al., 2006b). In addition to its two catalytic domains, HDAC6 possesses a SE14 repeat domain, which acts as a cytoplasmatic retention signal (Bertos et al., 2004), a dynein binding domain (Kawaguchi et al., 2003) and a C-terminal BUZ domain, which is able to interact with polyubiquitin chains as well as monomeric ubiquitin (Seigneurin-Berny et al., 2001; Hook et al., 2002).

Under conditions of misfolded protein stress HDAC6 is able to associate simultaneously with the dynein motor complex through its dynein binding domain as well as with polyubiquitylated proteins through its BUZ domain. Through these interactions, it is able mediate the relocalization of polyubiquitylated cargo to the aggresome via retrograde transport along the microtubule network (Kawaguchi et al., 2003). HDAC6 associates with the chaperone-like AAA ATPase p97/Cdc48 (Seigneurin-Berny et al., 2001), which is also able to associate with the proteasome and assists in the degradation of misfolded proteins (Römisch, 2006; Rumpf and Jentsch, 2006). p97/Cdc48 is able to control the fate of misfolded polyubiquitylated proteins by dissociating them from HDAC6 and redirecting them to proteasomal degradation (Boyault et al., 2006). Furthermore, HDAC6 is responsible for transporting proteins modfied with K63-linked polyubiquitin chains directly to the aggresome and for subsequent autophagic degradation even under conditions

where the proteasome is functioning normally (Olzmann et al., 2007; Olzmann and Chin, 2008). Moreover, HDAC6 has been found to be a component of Lewy bodies as well as of aggresomes induced by proteasome inhibition or ER stress (Kawaguchi et al., 2003), is required for the clearance of mutated huntingtin via autophagy (Iwata et al., 2005) and could be shown to mediate the rescue of neurodegeneration by compensatory autophagy (Pandey et al., 2007b,a). In addition to its role in the transport of polyubiquitylated proteins to the aggresome, HDAC6 is also involved in its autophagic clearance by transporting autophagosomal membranes as well as lysosomes to the pericentriolar region, although the domain which is responsible for the binding of these structures remains unidentified (Iwata et al., 2005). Interestingly, although catalytic activity of HDAC6 is neither required for the assiociation with dynein nor for the binding of polyubiquitylated cargo, most studies reveal the actual transport of cargo to be dependent on its enzymatic function. Although the reasons for this requirement are unknown, this effect could be attributed to the modulation of tubulin stability or kinesin-1 association through its acetylation status (Palazzo et al., 2003; Reed et al., 2006).

In addition to its role in the transport of polyubiquitylated proteins, HDAC6 is also involved in controlling the cellular response to protein aggregates. A recent report has demonstrated HDAC6 to act as a sensor for the accumulation of polyubiquitylated proteins and to mediate the induction of major cellular chaperones by triggering the release of heat-shock factor 1 (HSF1) from a repressive HDAC6/HSF1/HSP90 complex (Boyault et al., 2007). Interestingly, this function of HDAC6 is independent of its catalytic activity, although HSP90 has been identified as a substrate of HDAC6-mediated deacetylation. Furthermore, HDAC6 has been found to be a critical component of stress granules, which are dynamic cytoplasmatic structures involved in reversible translational repression as a response to environmental stress (Kwon et al., 2007).

Through deactylation of HSP90, HDAC6 is able to modulate its chaperone activity (Bali et al., 2005) and ultimately control activation of the glucocorticoid receptor (Kovacs et al., 2005; Murphy et al., 2005) and growth factor-induced actin remodeling as well as endocytosis (Gao et al., 2007). Probably through a combination of HSP90 mediated actin remodeling and deacetylation of cortactin as well as α-tubulin, HDAC6 is involved in the control of cell motility (Tran et al., 2007; Zhang et al., 2007), lymphocyte chemotaxis (Cabrero et al., 2006) and formation of the immune synapse (Serrador et al., 2004), although it might further contribute to these processes via deacetylase-independent scaffolding functions

(Cabrero et al., 2006). Interestingly, HDAC6 overexpression could be shown to prevent HIV-1 envelope-dependent cell fusion and infection through the deacetylation of α-tubulin (Valenzuela-Fernandez et al., 2005). Furthermore, HDAC6 seems to be involved in osteoclast maturation through interaction with the RhoA-effector mDia2 (Destaing et al., 2005), however, it is interesting to note that HDAC6-deficient mice have only minor differences in bone density (Zhang et al., 2008b). In addition, they display increased levels of α-tubulin and HSP90 acetylation, although lymphoid development as well as microtubule organization and stability remain remarkably unaffected.

Recently, HDAC6 has emerged as a target of the pharmaceutical industry, although whether the observed tumor-selective activity of HDAC6 inhibitors indeed results from its involvement in the clearance of misfolded proteins – as suggested by their synergism with proteasome inhibitors (Hideshima et al., 2005) – remains unclear. Especially as HDAC6 has also been implicated in tumor cell invasion and metastasis through interaction with BRMS1 (breast cancer metastasis suppressor 1, Hurst et al., 2006) and HSP90 deacetylation (Bali et al., 2005; Fiskus et al., 2007), or its involvement in Akt-PP1 (protein phosphatase 1) mediated signaling (Brush et al., 2004; Chen et al., 2005; Park et al., 2008).

Chapter 1

The UBA domains of NUB1L are required for binding but not for accelerated degradation of the ubiquitin-like modifier FAT10

Gunter Schmidtke, Birte Kalveram, Elvira Weber[*], Petra Bochtler[‡], Sebastian Lukasiak, Mark Steffen Hipp[§] and Marcus Groettrup

Department of Biology, Division of Immunology, University of Constance, 78457 Konstanz, Germany

[‡]Present address: IZKF, Department of Internal Medicine I, University of Ulm, 89081 Ulm, Germany

[*]Present address: Department of Biological Sciences, Stanford University, Stanford, CA 94305, USA

Journal of Biological Chemistry. 281(29): 20045-20054. July 21, 2006.

Abstract

Proteins selected for degradation are labeled with multiple molecules of ubiquitin and are subsequently cleaved by the 26S proteasome. A family of proteins containing at least one ubiquitin-associated (UBA) domain and one ubiquitin-like (UBL) domain have been shown to act as soluble ubiquitin receptors of the 26S proteasome and introduce a new level of specificity into the degradation system. They bind ubiquitylated proteins via their UBA-domains and the 26S proteasome via their UBL-domain and facilitate the contact between substrate and protease. NEDD8 ultimate buster-1 long (NUB1L) belongs to this class of proteins and contains one UBL- and three UBA-domains. We recently reported that NUB1L interacts with the ubiquitin-like modifier FAT10 and accelerates its degradation and that of its conjugates.

Here we show that a deletion mutant of NUB1L lacking the UBL-domain is still able to bind FAT10 but not the proteasome and no longer accelerates FAT10 degradation. A version of NUB1L lacking all three UBA-domains, on the other hand, looses the ability to bind FAT10 but is still able to interact with the proteasome and accelerates the degradation of FAT10. The degradation of a FAT10 mutant containing only the C-terminal UBL-domain is also still accelerated by NUB1L, even though the two proteins do not interact. In addition, we show that FAT10 and either one of its UBL-domains alone can interact directly with the 26S proteasome. We propose that NUB1L not only acts as a linker between the 26S proteasome and ubiquitin-like proteins, but also as a facilitator of proteasomal degradation.

Introduction

Ubiquitin, a small protein of 76 amino acids is one of the most conserved proteins known and has been found in all eukaryotic cells studied. It is essential for a variety of cellular processes, including degradation, cell-cycle regulation, DNA repair, stress response, embryogenesis, apoptosis, signal transduction, and transmembrane- and vesicular transport. (Pickart, 2001; Hicke, 2001; Jesenberger and Jentsch, 2002; Lai, 2002; Ma and Hendershot, 2001; Koepp et al., 1999). Throughout the past years, a family of proteins containing structural motives related to ubiquitin has been described which can be grouped into the ubiquitin-like modifiers and the ubiquitin-domain proteins (Jentsch and Pyrowolakis, 2000). The ubiquitin-like modifiers have substantial sequence or structural homology to ubiquitin and form covalent conjugates with their target proteins. However, unlike ubiquitin, which can form large polymeric conjugates, usually only monomeric modifications are observed. As is the case for ubiquitin, a C-terminal diglycine motif is essential for conjugation of most modifiers to their target proteins (Yeh et al., 2000). Prominent members of this group include SUMO-1, which serves several functions including nuclear transport and budding, (Matunis et al., 1996; Müller et al., 2001), NEDD8, which regulates SCF ubiquitin-ligases via cullin modification (Osaka et al., 2000), ISG15, which plays a role in innate immunity and in the response to alpha interferon, (Ritchie et al., 2004; Kim et al., 2005) and FAT10, which is inducible with gamma interferon (IFN)-γ and tumour necrosis factor alpha (TNF)-α (Raasi et al., 1999; Liu et al., 1999), and has been shown to cause apoptosis upon ectopic expression (Raasi et al., 2001).

The ubiquitin-like protein FAT10 consists of two UBL domains in a head to tail formation, which are about 29% and 36% identical to ubiquitin, respectively. Several key features of ubiquitin, like the lysine residues 48, 63, and 29, which are required for polyubiquitin chain formation, are conserved in both UBL-domains (Fan et al., 1996). Its C-terminus bears a free diglycine motif, which is necessary for the conjugation to so far unidentified target proteins (Raasi et al., 2001). Like ubiquitin (Johnson et al., 1992), FAT10 causes rapid degradation of long-lived proteins when fused to the N-terminus (Hipp et al., 2005). However, unlike ubiquitin, which is recycled from the degraded target proteins, FAT10 is digested along with its substrates. FAT10 thus has a relatively short half life (Hipp et al., 2004), which decreases dramatically by coexpression of a member of the group

of ubiquitin-domain proteins named NEDD8 ultimate buster 1 long (NUB1L) (Kamitani et al., 2001; Kito et al., 2001).

Several ubiquitin-domain proteins consist of an N-terminal UBL-domain which binds to the 19S regulator of the 26S proteasome (Schauber et al., 1998) and one or more UBA-domains that bind mono- or polyubiquitin (Hofmann and Bucher, 1996; Raasi et al., 2005). Members of this group include Rad23, which is involved in nucleotide excision repair, and Dsk2, which plays a role in spindle pole duplication (Miller et al., 1982; Raasi et al., 2004; Biggins et al., 1996). It has been suggested that these ubiquitin-domain proteins serve as linkers of ubiquitylated proteins and the 26S proteasome (Miller and Gordon, 2005), but the role of these proteins in degradation is still controversial. Some artificial reporter substrates accumulate in rad23-deleted and dsk2-deleted cells, as do high molecular weight ubiquitin conjugates (Wilkinson et al., 2001; Chen and Madura, 2002; Funakoshi et al., 2002; Rao and Sastry, 2002; Saeki et al., 2002a), but even in rad23/rpn10 doubly deleted cells, the bulk turnover of short-lived proteins is not affected (Lambertson et al., 1999). Overexpression of either hPlic or Rad23 leads to inhibition of substrate turnover by the 26S proteasome (Kleijnen et al., 2000; Ortolan et al., 2000), and an excess of Rad23 inhibits the *in vitro* degradation of Ub_5-DHFR by the 26S proteasome (Raasi and Pickart, 2003). A recent study suggested that UBL-UBA proteins, acting as multiubiquitin chain binding proteins (MCBP), define a new layer of substrate specificity, where different MCBP are involved in the degradation of different proteins (Verma et al., 2004a). The UBA-domains are usually essential for this function. Rad23 lacking its UBA-domains cannot inhibit degradation *in vitro* anymore (Raasi and Pickart, 2003), nor can it bind polyubiquitin. The UBL-domains, on the other hand, are required for binding to the 26S proteasome (Schauber et al., 1998). For example, only Rad23 with both UBA- and UBL-domains can rescue degradation by either Rad23- or Rpn10-depleted proteasomes *in vitro* (Verma et al., 2004a).

In this study we investigated the impact of the UBL- and UBA-domains of NUB1L on the binding and degradation of FAT10 as well as the role of the two UBL-domains of FAT10. We were able to show that all three UBA-domains of NUB1L are required for FAT10 binding whereas the NUB1L UBL-domain mediates interaction with the 26S proteasome. Surprisingly, a NUB1L mutant lacking the UBA-domains was still able to accelerate the degradation of FAT10, even though the two proteins no longer interacted. This apparent contradiction could be reconciled by the finding that FAT10 and NUB1L as well as both UBL-domains of FAT10 separately interacted with the 26S proteasome. Taken together, we found

no correlation between the binding of target proteins to NUB1L and the ability of NUB1L to accelerate their degradation, suggesting that NUB1L, by binding to the proteasome via its UBL domain, functions as a facilitator of proteasomal degradation of FAT10 without the necessity to serve as a linker.

Results

All three UBA-domains of NUB1L are required for the interaction with FAT10, but the UBL-domain is dispensable

We recently showed that NUB1L interacts with FAT10 and accelerates its degradation and that of FAT10-conjugated proteins (Hipp et al., 2004, 2005). To elucidate the role of the different UBL- and UBA-domains, we created several deletion mutants of NUB1L. It should be pointed out that NUB1 is a natural splicing variant of NUB1L, which has a deletion of 14 amino acids, encompassing the C-terminal third of a UBA-domain (UBA2 in Fig. 6) (Tanaka et al., 2003). This flexibility in the structure should allow us to remove all three UBA-domains together (NUB1LΔUBA1-3), or two of them (NUB1LΔUBA2/3, NUB1LΔUBA1/3, NUB1LΔUBA2/3) or only one of them (NUB1LΔUBA3, NUB1LΔUBA2, NUB1LΔUBA1) without compromising the folding. We also deleted the ubiquitin-like domain (NUB1LΔUBL) as indicated in figure 6. First we analysed the interaction of FAT10 and the NUB1L mutants *in vitro*. After *in vitro* transcription and translation 10% of the reactions were analysed by SDS-PAGE and autoradiography. All analysed mutants appeared as a single band and were expressed as soluble proteins in amounts comparable to wild-type NUB1L (Fig. 6B). Half of the remainder of the reaction was incubated with Glutathione-S-transferase (GST) coupled to glutathione (GSH)-sepharose, the other half was incubated with GST-FAT10 coupled to GSH-sepharose. After washing, the bound proteins were analysed by SDS-PAGE and autoradiography. None of the analysed proteins could be detected after pull-down with GST alone (Fig. 6C). Only wild-type NUB1L, NUB1and NUB1LΔUBL were pulled down in significant amounts by GST-FAT10. NUB1LΔUBA3 was also bound, but to a much lesser extent, whereas none of the other mutants interacted with GST-FAT10 in this assay (Fig. 6D).

To study the interaction of FAT10 and NUB1L *in vivo*, we transfected wild-type and mutant HA-NUB1L either alone or together with His_6-tagged FAT10 into HEK293T cells. After metabolic labelling with [^{35}S]-methionine, the cells were lysed and subjected to immunoprecipitation with anti-HA antibodies. The re-

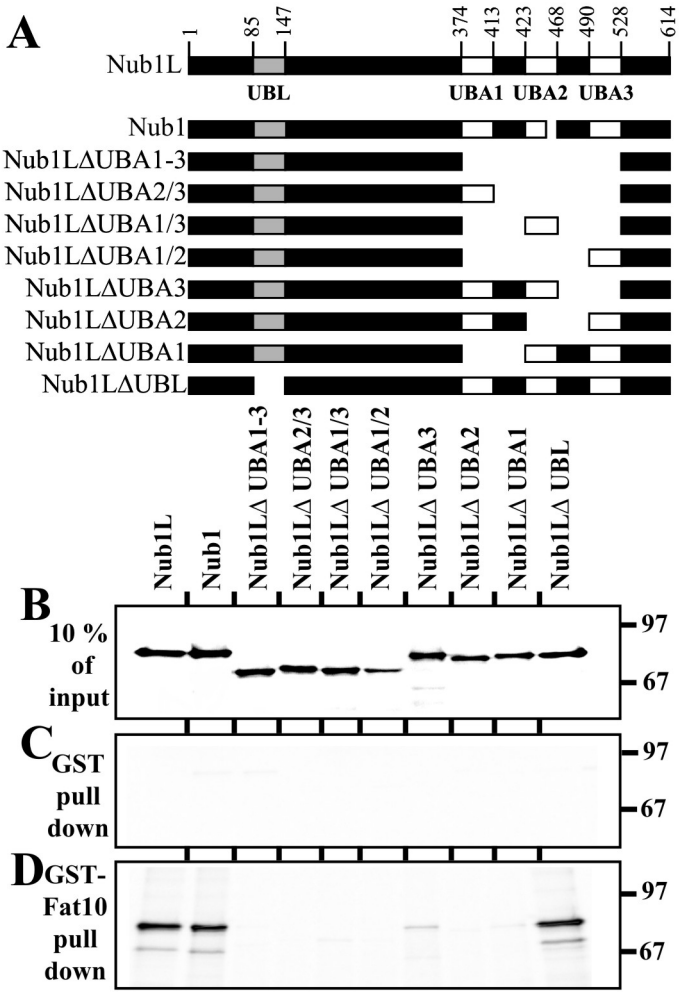

Figure 6: Domain structure of NUB1 and NUB1L, some deletion mutants, and their interaction with GST and GST-FAT10. (A) The positions of the domains of NUB1L are indicated by the number of the amino acids (aa). The ubiquitin-like (UBL) domains are shown in grey, the ubiquitin-associated (UBA) domains are shown in white. **(B)** Autoradiography of *in vitro* transcribed and translated NUB1L mutants after separation by SDS-PAGE. A 10% aliquot of each reaction was loaded to demonstrate the amount available for the GST pull-down. The positions of molecular weight markers (in kD) are indicated on the right. **(C)** Autoradiography of the NUB1L mutants shown in A after incubation with GST coupled GSH-sepharose, washing and separation by SDS-PAGE. The lane occupation is the same as in B. **(D)** Autoradiography of the NUB1L mutants shown in A after incubation with GST-FAT10 coupled GSH-sepharose, washing and separation by SDS-PAGE. Lane occupation is the same as in B. Only wild-type NUB1L, NUB1, and NUB1LΔUBL interact strongly, NUB1LΔUBA3 interacts weakly with GST-FAT10. The experiments were repeated three times with similar outcomes.

covered proteins were separated by SDS-PAGE and analysed by autoradiography. As can be seen in figure 7A, C and 9C, only wild-type NUB1L, NUB1, and NUB1LΔUBL were able to pull down His_6-FAT10 from the lysates. A subsequent immunoprecipitation of the supernatants with anti-His_6 antibody demonstrated that sufficient His_6-FAT10 was available in all reactions, so lack of expression can be excluded as a reason for the negative results. From the experiments presented in figure 6, figure 7 and figure 9C, D we conclude that the interaction of FAT10 and NUB1L depends on the presence of all three UBA-domains, but is independent of the UBL-domain of NUB1L. The deletion of only 14 amino acids in NUB1, which is about one third of the UBA2 domain is not sufficient to abrogate the interaction of NUB1 and FAT10.

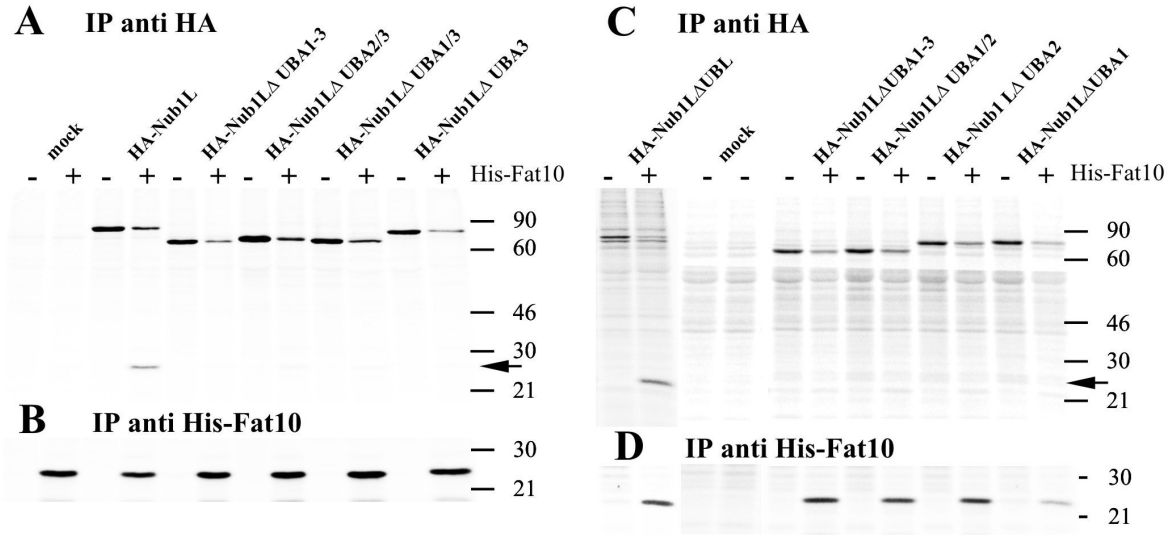

Figure 7: Co-immunoprecipitation of NUB1L mutants and FAT10. (A, C) Empty vector (mock) or HA-tagged NUB1L mutants lacking one or more UBA-domains were transfected either alone (- His-FAT10) or together with His_6-tagged FAT10 (+ His-FAT10) into HEK293T cells. The cells were lysed and an anti-HA immunoprecipitation was performed. The proteins bound by the antibody were separated by SDS-PAGE and analyzed by autoradiography. The NUB1L mutants appear between the 60 and the 90 kD molecular weight markers indicated at the right. An arrow on the right side of the gel denotes the position of co-immunoprecipitated FAT10. Only wild-type HA-NUB1L and HA-NUB1LΔUBL coprecipitated significant amounts of His_6-FAT10. **(B, D)** To analyze the amount of FAT10 available, the supernatants after the immunoprecipitation shown in A and C were precipitated with anti-His_6 antibodies, and the bound proteins separated by SDS-PAGE. Lane occupation is the same as in A and C, respectively. His_6-FAT10 was present in all FAT10 transfected cells. The experiments were repeated three times yielding similar results.

Only the UBL-domain of NUB1L is essential for the accelerated degradation of FAT10

To analyze the impact of the UBA- and UBL-domains of NUB1L on the accelerated degradation of FAT10, we cotransfected NUB1LΔUBA1-3 and NUB1LΔUBL together with FAT10 in HEK293T cells and determined the half-life of FAT10 by pulse-chase analysis. For comparison, we also transfected FAT10 alone and in combination with wild-type NUB1L (Fig. 8). As can be seen in figure 8A and B, wild-type NUB1L accelerates the degradation of FAT10 by a factor of about 4, which is consistent with our results previously obtained in HeLa cells (Hipp et al., 2004). In contrast, the cotransfection of NUB1LΔUBL did not have an effect on the half-life of FAT10 (compare Fig. 8A and C). Unexpectedly, the cotransfection of NUB1LΔUBA1-3 – which does not interact with FAT10 – accelerated the degradation of FAT10 almost as potently as wild-type NUB1L (compare Fig. 8B and D, for quantifications on a radio-imager see Fig. 8E). We also analysed the impact of the small splicing variant NUB1 on FAT10 degradation. We found that NUB1 is able to accelerate the degradation of FAT10 as potently as NUB1L (Fig. 9).

NUB1L does not influence protein degradation in general

We already published that expression of NUB1L does not have any effect on the degradation of the model substrates Ubiquitin-GFP and Ubiquitin-DHFR (Hipp et al., 2005). To extend this study and to investigate the role of NUB1L in proteasome dependent protein degradation we analysed the degradation of short lived proteins in mock transfected cells and NUB1L transfected cells. Western blot analysis of lysates from these cells showed a clear overexpression of NUB1L in the NUB1L transfectant (Fig. 10A). Aliquots of these cells were labeled with [^{35}S]-methionine, washed and chased for one hour. After this incubation cells were treated with TCA, and the acid soluble radioactivity, representing the amount of degraded protein, was counted. Mock transfected cells converted 31% (+/-5%) and NUB1L transfected cells 27% (+/-4%) of the activity into acid soluble counts. The ubiquitin-proteasome system is responsible for degradation of about 75% of bulk cellular proteins occuring within one hour after synthesis. Hence, a major effect of NUB1L overexpression on degradation by the ubiquitin-proteasome system should have been detectable in this assay. Since this was not the case, NUB1L is unlikely to generally affect ubiquitin mediated degradation. Moreover, the intracellular proteasome activity as measured by degradation of the cell permeable fluorogenic proteasome substrate MeO-Suc-GLF-AMC was not affected by NUB1L overexpression.

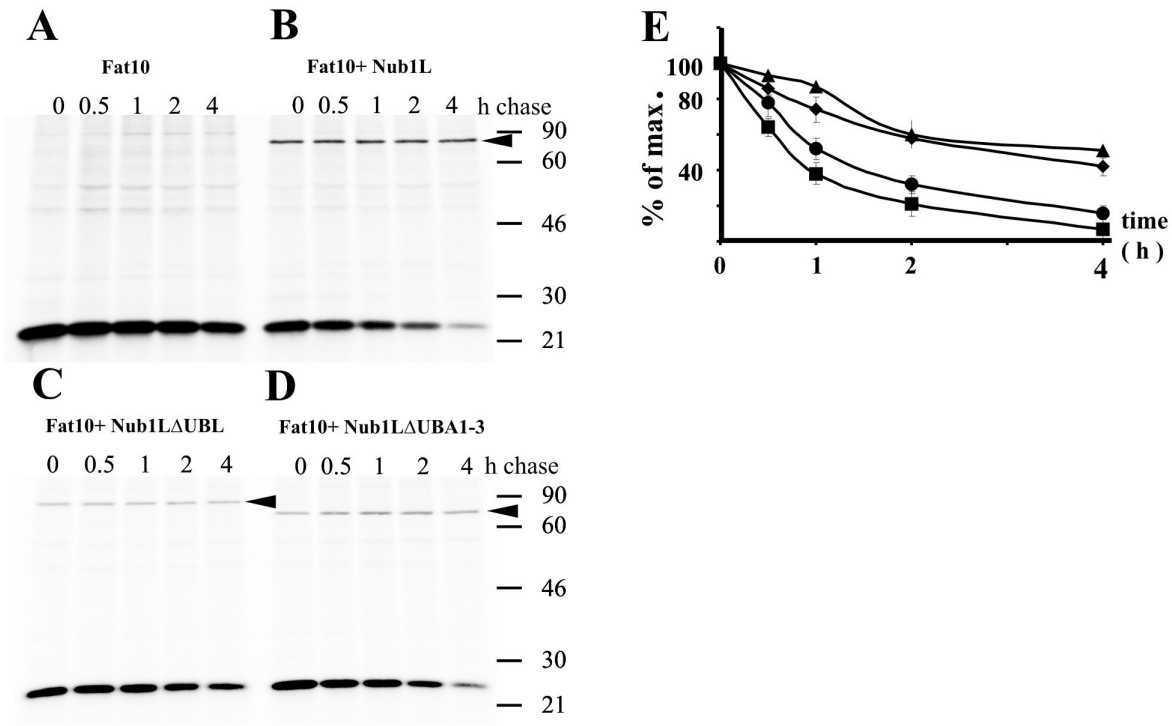

Figure 8: Accelerated degradation of FAT10 by NUB1L and NUB1LΔUBA1-3, but not by NUB1LΔUBL. (A) Pulse-chase analysis of FAT10 degradation. HEK293T cells were transfected with HA-FAT10 and labeled with (^{35}S)-methionine. At indicated time points of chase, aliquots of the cells were lysed and anti-HA immunoprecipitations were performed. Bound proteins were analyzed by SDS-PAGE and autoradiography.**(B)** Same experimental setup as in A, but HA-NUB1L was cotransfected. An open arrow at the right of the gel denotes the position of NUB1L, a closed arrow denotes FAT10. Positions of molecular weight markers from 21 to 90 kD are at the right of the gel. **(C)** Same experimental setup as in A, but HA-NUB1LΔUBL was cotransfected. **(D)** Same experimental setup as in A, but HA-NUB1LΔUBA1-3 was cotransfected. **(E)** Graphic representation of degradation rates as determined for FAT10 alone in A (diamonds), with NUB1L in B (squares), with NUB1L ΔUBL in C (triangles) and with NUB1LΔUBA1-3 in D (filled circles). The amount of radioactivity recovered at 0 hours was set to 100%. The activity immunoprecipitated at 0.5, 1, 2 and 4 hours was calculated relative to the 0 hour value. Values represent the mean of five independent experiments +/- SEM.

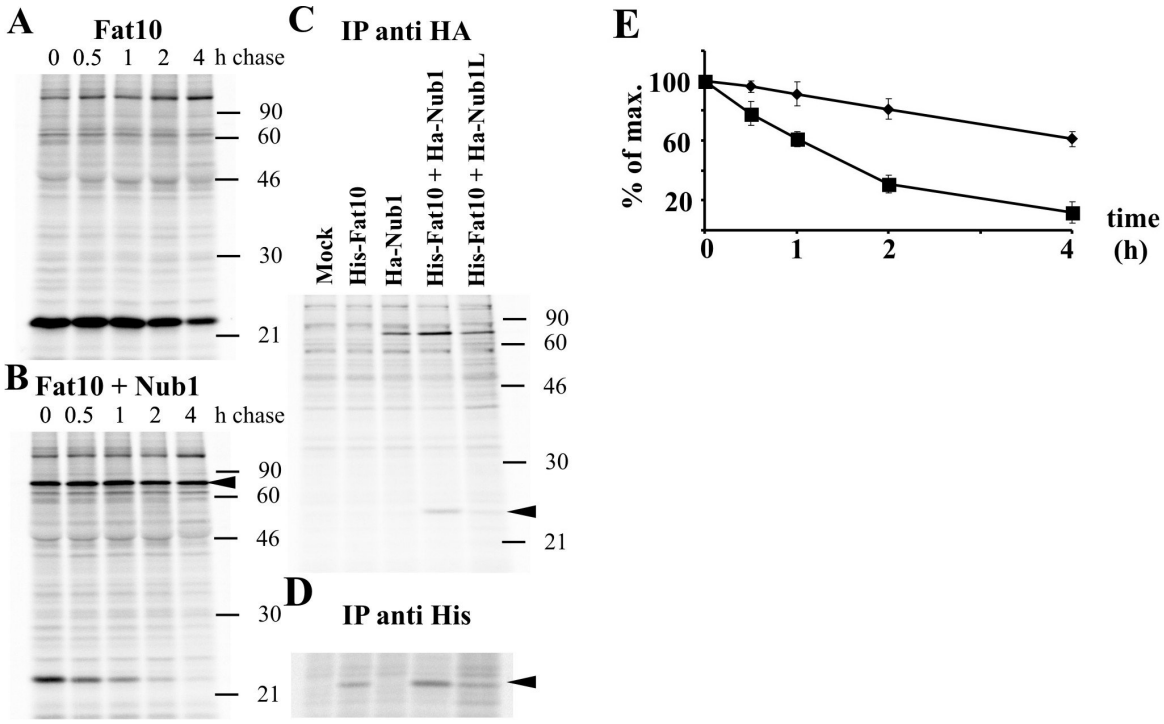

Figure 9: NUB1 interacts with FAT10 and accelerates its degradation. (A) HEK293 T cells were transiently transfected with HA-FAT10. After pulse labelling with (^{35}S)-methionine, aliquots of the cells were harvested at the indicated time points of chase, lysed and anti-HA immunoprecipitations were performed. Bound proteins were analyzed by SDS-PAGE and autoradiography. **(B)** Same experiment as in A, but NUB1 was co-expressed. The position of NUB1 is indicated by an arrowhead. Molecular weight markers (in kD) are shown at the right. **(C)** Co-immunoprecipitation of HA-NUB1 and His-FAT10. Empty vector (mock), or His-Fat10 or HA-tagged NUB1 were transfected either alone or together with His-FAT10 (His-FAT10 + HA-Nub1) into HEK293T cells. As a positive control we used His-FAT10 and HA-NUB1L. The cells were lysed and an anti-HA immunoprecipitation was performed. The proteins bound by the antibody were separated by SDS-PAGE and analyzed by autoradiography. An arrowhead on the right side of the gel denotes the position of co-immunoprecipitated FAT10. **(D)** The supernatants of C were immunoprecipitated with anti His_6-antibodies to show the amount of FAT10 available, the position of which is indicated by an arrowhead. **(E)** Graphic evaluation of the different degradation rates of FAT10 as determined in A (diamonds) and B (squares).

Treatment with IFN-γ and TNF-α enhances the expression of NUB1L and the degradation of endogenous FAT10

Next we investigated whether the endogenous upregulation of NUB1L expression by TNF-α and IFN-γ suffices to accelerate the degradation of endogenous FAT10. The combined treatment of HeLa cells with IFN-γ and TNF-α for one day resulted in an over nine fold increase in FAT10 mRNA expression and over five fold increase in NUB1L mRNA expression as determined by qRT PCR (Fig. 10C). Also on protein level we detected an upregulation of NUB1L by western analysis (Fig. 10B). The degradation rate of endogenous FAT10 was then analysed by pulse-chase analysis using an anti-FAT10 antibody. As shown in figure 10E andF, FAT10 degradation was accelerated threefold as compared to FAT10 transfected HeLa cells without cytokine mediated NUB1L induction (Fig. 10D). Transient FAT10 transfection of unstimulated HeLa cells was necessary because in the absence of cytokine stimulation no FAT10 protein was detectable. Taken together, we find a threefold acceleration of FAT10 degradation in cytokine treated cells which correlates with an upregulation of NUB1L.

The N-terminal UBL-domain of FAT10 is sufficient for interaction with NUB1L

We previously reported that the interaction of NUB1L with FAT10 is specific for this protein, because binding of NUB1L to NEDD8, SUMO-1, and ubiquitin was not detected by co-immunoprecipitation (Hipp et al., 2004). FAT10 consists of two ubiquitin-like domains in tandem array (Bates et al., 1997). To determine whether the N- and the C-terminal domains can interact with NUB1L independently, we performed co-immunoprecipitation experiments. However, the persistence of these single UBL proteins was so short that we could only detect them in the presence of proteasome inhibitors (data not shown). To overcome this obstacle, we fused each of them to the N-terminus of green fluorescent protein (GFP), as we did for FAT10 as positive and SUMO-1 as negative control (Fig. 11). Mock transfected cells, or cells transfected with the constructs mentioned above either alone or together with HA-NUB1L were metabolically labeled, lysed and subjected to anti-GFP immunoprecipitation. After washing, the bound proteins were analysed by SDS-PAGE and autoradiography. The supernatants of this first precipitation were then subjected to immunoprecipitation with anti-HA antibodies to determine the level of NUB1L expression. As shown in figure 11A, only the N-terminal UBL-domain of FAT10 (FAT10-N-GFP) and FAT10-GFP coprecipitated NUB1L. There was no NUB1L signal in mock transfected cells and cells express-

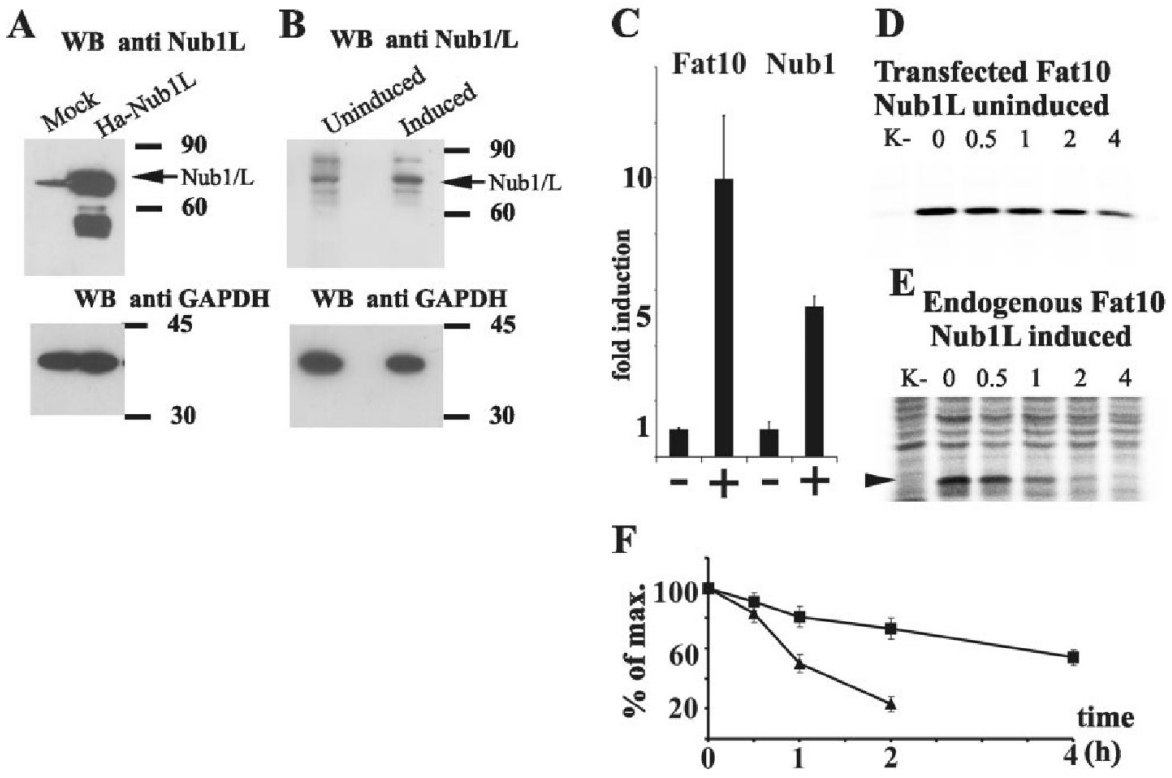

Figure 10: Treatment with IFN-γ and TNF-α upregulates NUB1L expression and accelerates the degradation of FAT10. (A) Anti-NUB1L Western blot of lysates from mock transfected and HA-NUB1 transfected HEK293T cells (top panel), Western analysis of GAPDH protein is used as loading control (bottom panel). **(B)** Anti-NUB1L Western blot of lysates from untreated HeLa cells and HeLa cells induced with IFN-γ and TNF-α for one day. An arrow at the right indicates the position of NUB1L (top panel); the same lysates probed with anti-GAPDH antibodies serves as loading control (bottom panel). **(C)** Real time RT-PCR analysis of FAT10 and NUB1L mRNA expression in HeLa cells before (-) and after (+) treatment with TNF-α and IFN-γ for one day. **(D)** HeLa cells were transfected with an HA-FAT10 expression construct and the degradation rate of FAT10 was determined in a pulse-chase experiment. K- denotes an IP with irrelevant antibody. **(E)** Analysis of the degradation rate of endogenous FAT10 after induction of FAT10 and NUB1L by IFN-γ and TNF-α. The pulse-chase experiment was performed as in E using an anti-FAT10 antibody. K- is an IP with pre-immune serum. The position of FAT10 is indicated by an arrowhead. **(F)** Graphic evaluation of the different degradation profiles of FAT10 as determined in D (squares) and E (triangles).

ing SUMO-1-GFP or the C-terminal UBL-domain of FAT10 (FAT10-C-GFP). Figure 11B demonstrates that the amounts of NUB1L available were sufficient in all co-expression reactions to allow detection if bound to the respective GFP fusion protein.

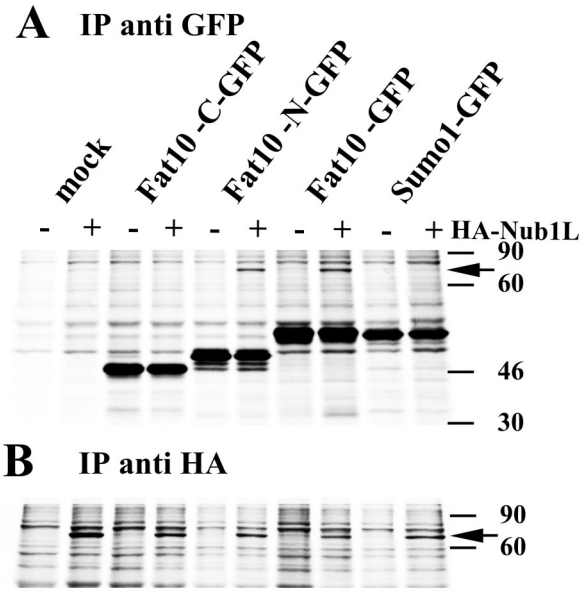

Figure 11: The N-terminal-, but not the C-terminal UBL-domain of FAT10 interacts with NUB1L. (A) Empty vector (mock), the C-terminal UBL-domain of FAT10 (FAT10-C), the N-terminal UBL-domain of FAT10 (FAT10-N), wild-type FAT10 as positive- and SUMO-1 as negative control, all as GFP-fusions, were transfected either alone (- HA-NUB1L) or together with HA-tagged NUB1L (+ HA-NUB1L) into HEK293T cells. The cells were lysed and an anti-GFP immunoprecipitation was performed. The proteins bound by the antibody were separated by SDS-PAGE and analyzed by autoradiography. An arrow denotes the position of NUB1L. Molecular weight markers are shown at the right. **(B)** To analyze the amount of NUB1L available, the supernatants after the immunoprecipitation shown in A were precipitated with anti-HA antibodies, and the bound proteins separated by SDS-PAGE. Lane occupation is the same as in A. An arrow denotes the position of NUB1L. HA-NUB1L was present in all HA-NUB1L transfected cells. The experiments were repeated two times with similar outcome.

NUB1L accelerates both FAT10-N-GFP and FAT10-C-GFP degradation

To analyse the impact of NUB1L expression on the half-lives of the two isolated UBL-domains of FAT10, we first determined the rate of degradation of FAT10-N-GFP and FAT10-C-GFP alone. As can be seen in figure 12A and B, the degradation rates of the two UBL-domain-GFP fusion proteins in HEK293T cells were significantly different from each other. FAT10-C-GFP was degraded with a rate comparable to that of wild-type FAT10-GFP (Hipp et al., 2005) but slower than FAT10 itself (compare Fig. 8E and Fig. 12I). FAT10-N-GFP, in comparison, is a

stable protein showing only minimal degradation within 5 hours. Co-expression of NUB1L lead to degradation of both UBL-domain-GFP fusion proteins at almost the same rate (Fig. 12C, D and I). In the presence of NUB1L, FAT10-C-GFP degradation was accelerated by a factor of two to three. The enhancement in FAT10-N-GFP degradation caused by NUB1L was much higher, as it was degraded very slowly alone. To determine whether the degradation of FAT10-N-GFP and FAT10-C-GFP is mediated by the proteasome and not by another protease, we repeated the experiments in the presence of the proteasome inhibitor lactacystin. As shown in figure 12E and F, both UBL-domain-GFP fusion proteins were not degraded at all. Even co-expression of NUB1L did not lead to detectable degradation of either protein in the presence of lactacystin.

FAT10 and NUB1L interact with the 26S proteasome

To investigate why NUB1LΔUBA1-3, but not NUB1LΔUBL, is able to accelerate the degradation of FAT10, we tested the working hypothesis that FAT10 may interact directly with the proteasome and that NUB1L with its UBL domain serves as a facilitator of degradation of FAT10 by the 26S proteasome. Binding of NUB1 to the S5a (Rpn10) subunit of the 26S proteasome has been shown *in vitro* before, as well as detection of NUB1 in preparations of purified 26S proteasome (Kamitani et al., 2001). We decided to use co-immunoprecipitation from transfected HEK293T cells to determine whether FAT10, NUB1L and their mutants are able to interact with the 26S proteasome. We used a bi-directional vector expressing GFP from one side, and FAT10 or NUB1L from the other site of the promoter. Aliquots of lysates from transfected cells were analysed for expression of the respective proteins (Fig. 13A lane 2 and 3 for NUB1L and FAT10, and Fig. 11B lane 5 and 6 for GFP). After immunoprecipitation with the monoclonal antibody MCP444 specific for the β-type proteasome core subunit HN3 (β7), we looked for coprecipitation of the expressed proteins with the proteasome. FAT10 and NUB1L, but not GFP, were co-immunoprecipitated by MCP444, indicating the specificity of the interaction (Fig. 13C lane 2 and 3 for NUB1L and FAT10, and Fig. 13D lane 5 and 6 for GFP). We also performed this experiment with FAT10 and NUB1L expressed together by the bi-directional promoter, and found that both can be co-immunoprecipitated at the same time (Fig. 13C lane 4). To determine the binding of the NUB1L mutants, we used NUB1L as control for NUB1LΔUBA1-3 and NUB1LΔUBL, which were all expressed from the vector pcDNA3.1. After the immunoprecipitation with MCP444, we found that NUB1LΔUBA1-3 interacted with the proteasome, but not NUB1LΔUBL (Fig. 13C lanes 5-7). A western blot against a subunit of the 19S regulatory com-

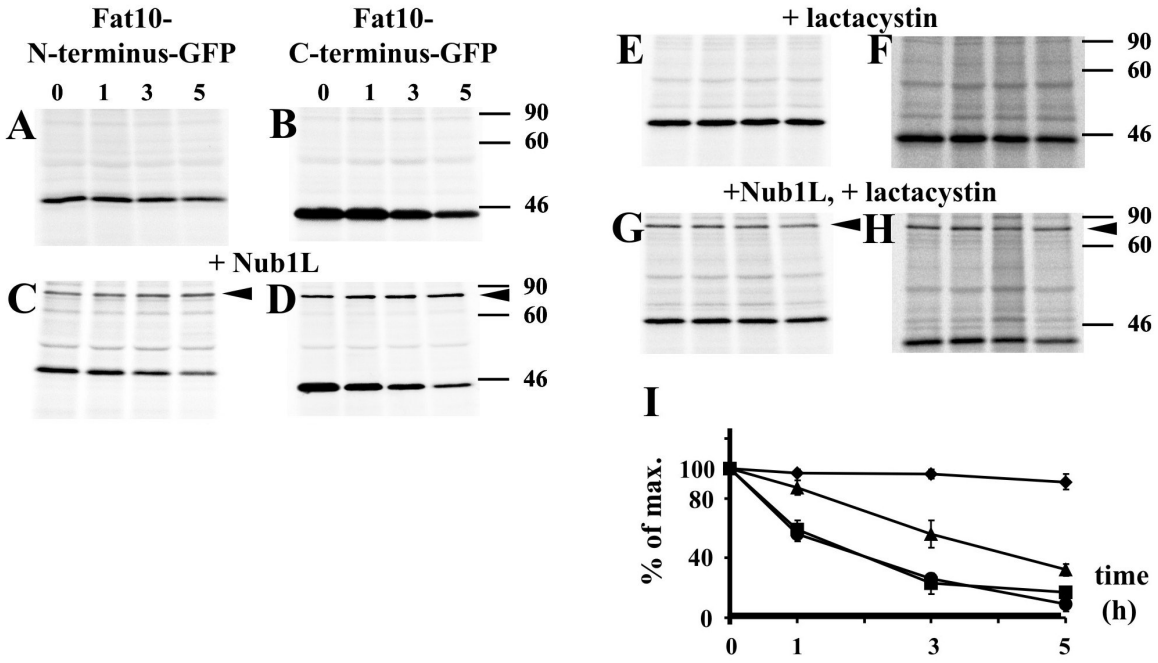

Figure 12: Accelerated degradation of the FAT10 UBL-domain-GFP fusion proteins by NUB1L. (A) Pulse-chase analysis of the FAT10-N-terminal UBL-domain fused to GFP. HEK293T cells were transfected with HA-FAT10-N-terminus-GFP and labeled with (^{35}S)-methionine. After indicated time periods of chase, aliquots of the cells were lysed and anti-HA immunoprecipitations were performed. Bound proteins were analyzed by autoradiography after SDS-PAGE. An arrowhead at the right denotes the position of the GFP fusion proteins. **(B)** Same experimental setup as in A, but HA-FAT10-C-terminus-GFP was transfected. The positions of the molecular weight markers are shown on the right. **(C)** Same experimental setup as in A, but HA-NUB1L was cotransfected. **(D)** Same experimental setup as in B, but HA-NUB1L was cotransfected. An open arrow at the right indicates the position of NUB1L. **(E, F)** Experiments were performed as in A and B, but in the presence of 50 μM lactacystin. **(G, H)** Experiments were performed as in C and D, but in the presence of 50 μM lactacystin. **(I)** Graphic representation of degradation rates as determined for FAT10-N-terminus-GFP alone in A (diamonds), for FAT10-C-terminus-GFP in B (triangles), for FAT10-N-terminus-GFP with NUB1L in C (squares) and for FAT10-C-terminus-GFP with NUB1L in D (closed circles). The amount of radioactivity recovered at 0 hours was set to 100%. The activity immunoprecipitated at 1, 3 and 5 hours was calculated relative to the 0 hour value. Values represent the means of three experiments +/- SEM.

plex, Rpt6, demonstrates successful immunoprecipitation of the 26S proteasome in all cases (Fig. 13E and F). The ability to interact with the 26S proteasome was shown for FAT10-N-GFP and FAT10-C-GFP in the same manner, using GFP alone as negative and FAT10-GFP as positive control (Fig. 13B and D). The specificity of the binding was again demonstrated by the lack of co-immunoprecipitation of GFP alone, despite successful immunoprecipitation of the 26S complex (Fig. 13F).

To investigate whether the interaction between FAT10 and the proteasome is direct, an *in vitro* pull-down assay was performed where recombinant GST-FAT10 was incubated together with purified 26S proteasome. Only GST-FAT10, but not GST alone, was able to pull down the proteasome, as determined by a western blot against the 20S subunit iota (α1, Fig. 13G) although the same amount of proteasomes was available for interaction as demonstrated by western blotting (Fig. 13H).

Discussion

The role of proteins which contain both a UBL domain and one or more UBA domains for the recruitment of polyubiquitylated substrates for degradation by the proteasome is currently a subject of intensive investigations (Miller and Gordon, 2005). While it was previously believed that polyubiquitylation is a sufficient label for docking to the 26S proteasome via the subunits Rpn10 (van Nocker et al., 1996) or Rpt5 (Lam et al., 2002), it is now becoming clear that UBL-UBA proteins, which bind to proteasomes via their UBL domain, can be required to target a subset of ubiquitylated substrates to the proteasome thus introducing a further layer of regulation. Here we investigated the molecular interactions required for a novel proteasomal targeting system consisting of the ubiquitin-like protein FAT10 and the UBL-UBA protein NUB1L. In table 1 we summarize the data we obtained while dissecting the different domains of NUB1L and FAT10 for interaction and accelerated degradation.

When we identified NUB1L as a non-covalent interaction partner of FAT10 that contains three bona fide UBA domains, it was an obvious assumption that these are required for the interaction with FAT10. Since the alternative splice variant NUB1 can be viewed as a 'naturally occurring' deletion mutant of NUB1L, it appeared reasonable to delete the UBA domains singly, in pairs, and altogether. We found in GST-pulldown experiments (Fig. 6B) and co-immunoprecipitation

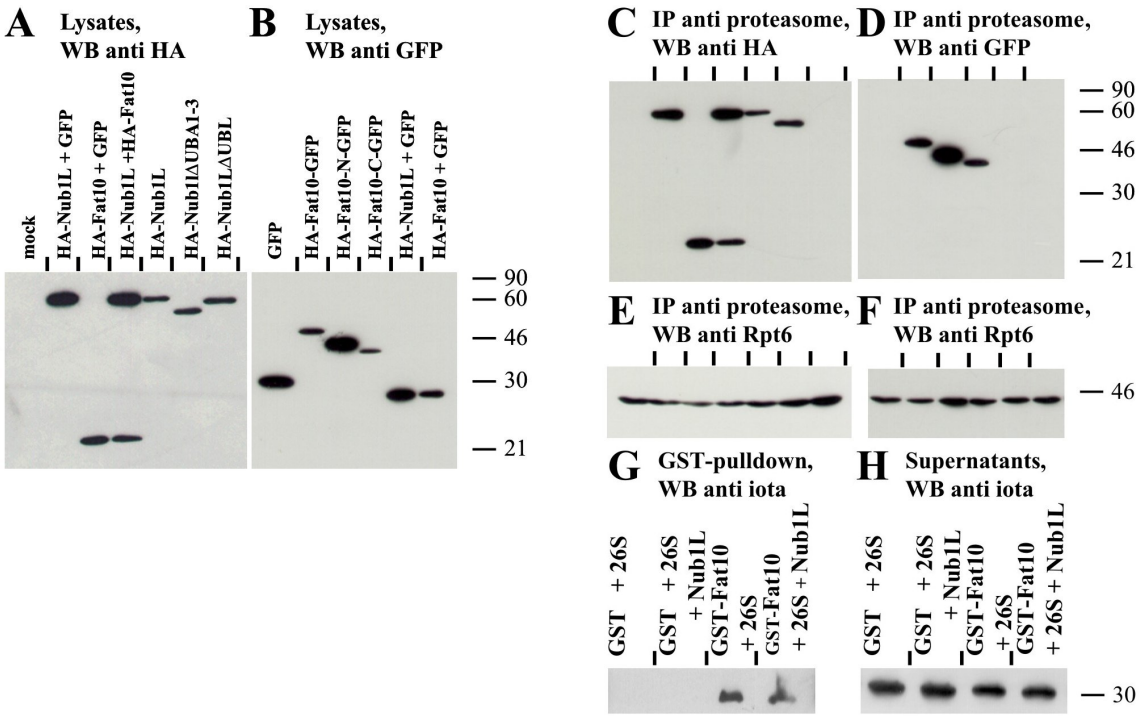

Figure 13: Co-immunoprecipitation of NUB1L, NUB1LΔUBA1-3, and FAT10, but not of NUB1LΔUBL with the 26S proteasome. **(A)** HEK293T cells were transfected with empty vector (mock), HA-NUB1L together with GFP (vector: pBI), HA-FAT10 together with GFP (vector: pBI), HA-NUB1L together with FAT10 (vector: pBI), HA-NUB1L (vector: pcDNA3.1), HA-NUB1LΔUBA1-3 (vector: pcDNA3.1) and HA-NUB1LΔUBL (vector: pcDNA3.1). The cells were then lysed and about 2% of the lysate was analyzed by SDS-PAGE and anti-HA Western blotting (WB). **(B)** HEK293T cells were transfected with GFP, HA-FAT10-GFP fusion protein, HA-FAT10-N-terminal UBL domain-GFP fusion protein (HA-Fat10-N-GFP), HA-FAT10-C-terminal UBL domain-GFP fusion protein (HA-FAT10-C-GFP), HA-NUB1L together with GFP (vector: pBI) and HA-FAT10 together with GFP (vector: pBI). The cells were lysed and about 2% of the lysate was analyzed by SDS-PAGE and anti-GFP Western blotting (WB). The positions of molecular weight markers are shown on the right side of the gel. **(C, D)** The lysates shown in A and B were subjected to immunoprecipitation with an antibody against the 20S proteasome subunit β7 (MCP444, anti-HN3) under conditions preserving the 26S proteasome. The bound proteins were analyzed by WB with an anti-HA antibody in C, or with an anti-GFP antibody in D. The lane occupation in C is the same as in A, the lane occupation in D is the same as in B. **(E, F)** To demonstrate the successful immunoprecipitation of the 26S proteasome, the samples shown in C and D were also analyzed by WB with an antibody recognising the 19S regulator subunit Rpt6. The lane occupation in E is the same as in A; the lane occupation in F is the same as in B. **(G)** GST-pull down experiment. GST (lanes 1 and 2) or GST-FAT10 (lanes 3 and 4) were incubated with purified 26S proteasome in the presence or absence of recombinant His_6-NUB1L and analyzed by WB with an antibody recognizing the 20S proteasome subunit iota (α1). **(H)** Supernatants of the GST-pull down shown in G were analyzed on a Western blot for iota content. The data were confirmed in three independent experiments.

	binding to FAT10	binding to proteasome	accelerated degradation of FAT10
NUB1L	+	+	+
NUB1ΔUBA1-3	-	+	+
NUB1ΔUBL	+	-	-
FAT10-GFP	+	+	+
FAT10-N-GFP	-	+	+
FAT10-C-GFP	+	+	+

Table 1: A summary of the results obtained. Results are classified with (+) for a positive result in a binding assay or for accelerated degradation and with (-) for a negative result.

studies (Fig. 7) that all three UBA-domains of NUB1L were required for the binding of FAT10, whereas the UBL-domain was dispensable for this interaction. We were able to detect a weak interaction of FAT10 and NUB1LΔUBL3 in pull-down studies, suggesting that the combination of the first two UBA domains can mediate a weak interaction, but since this interaction was not confirmed in co-immunoprecipitation studies *in vivo*, the significance of this interaction remains uncertain. Interestingly, the deletion of the 14 amino acids occuring in the natural splice variant NUB1 was insufficient to abolish the binding to FAT10.

While studying the interaction of isolated UBA domains with polyubiquitin chains, Raasi et al. divided the UBA-domains into four different groups, depending on their ability to discriminate between differently linked polyubiquitin chains and monoubiquitin. The members of the third group – which included all three UBA domains of NUB1L - were not able to interact with ubiquitin at all and may hence be in charge of recognizing ubiquitin-like proteins instead (Raasi et al., 2005). While most reports about UBL-UBA domain proteins focus on ubiquitin or polyubiquitylated substrates, very little is known about their interaction with ubiquitin-like modifiers. In the three first reports on this issue, NUB1 and NUB1L were found to bind to the ubiquitin-like modifier NEDD8 and to accelerate its degradation (Kamitani et al., 2001; Kito et al., 2001; Tanaka et al., 2003). Unexpectedly, the interaction of NUB1 and NEDD8 was not mediated by the three UBA domains but rather by a short C-terminal domain. Only the second UBA domain of NUB1L appeared to interact weakly with NEDD8 but it was not required to promote NEDD8 degradation (Tanaka et al., 2003). Subsequently, we reported the robust non-covalent interaction between FAT10 and NUB1L, but in the same series of experiments we failed to detect an interaction of NEDD8 and NUB1L (Hipp et al., 2004). In this study we found that the concerted action of three UBA

domains of NUB1L is required for the binding of FAT10, a ubiquitin-like protein containing two UBL domains.

In order to determine if only one or both of the UBL domains of FAT10 are required for binding NUB1L, co-immunoprecipitation studies were performed. These experiments revealed that only the N-terminal but not the C-terminal UBL-domain of FAT10 interacted with NUB1L (Fig. 11). The residues L8, I44, and V70 of ubiquitin, known to be important for the interaction of ubiquitin with other UBA domains, (Vijay-Kumar et al., 1987; Beal et al., 1996; Sloper-Mould et al., 2001; Raasi et al., 2004), are only partially conserved in FAT10. The N-terminal UBL-domain of FAT10 contains the L8 residue and bears a leucine in position 44, but a threonine in position 70. The C-terminal domain, in contrast, shows in the corresponding residues G8, T44, and A70. While this seems to be in good agreement with our results, it can not be excluded that different residues might be responsible for the interaction between NUB1L and ubiquitin-like modifiers, especially since it could be shown that NUB1L does not bind a ubiquitin-GFP fusion protein (Hipp et al., 2004) or polyubiquitin-chains (Raasi et al., 2005).

While interaction of monoubiquitin to UBA domain proteins has been reported (Wilkinson et al., 2001), usually polyubiquitylated proteins are better binders of UBL-UBA domain proteins. This can be rationalized by data on the binding affinity between ubiquitin and the UBL-UBA protein Rad23, where the strength of binding increased exponentially when the chain length of ubiquitin was extended from 1 to 6 units (Raasi et al., 2004). We take our result that one of the two FAT10 UBL domains is sufficient for mediating the interaction with NUB1L (Fig. 11) as further support for the specificity of this interaction. Our data suggest that this interaction is not merely a result of an increase in avidity by connecting two ubiquitin-like domains and thus mimicking a short polyubiquitin chain. Nevertheless, since the binding assays performed in our study are of qualitative rather than quantitative nature, we can not rule out that FAT10 or FAT10-GFP bind with a higher affinity than FAT10-N-GFP.

Several reports about the influence of UBL-UBA proteins on degradation have already appeared. The deletion of these proteins lead to an inhibition of degradation and accumulation of high molecular weight ubiquitin conjugates (Wilkinson et al., 2001; Chen and Madura, 2002; Funakoshi et al., 2002; Rao and Sastry, 2002; Saeki et al., 2002a). Conversely, overexpression of Rad23 or Dsk2 lead to inhibition of substrate turnover by the 26S proteasome (Kleijnen et al., 2000;

Ortolan et al., 2000), and Rad23 inhibited the *in vitro* degradation of Ub_5-DHFR (Raasi and Pickart, 2003). With respect to the function of UBA-UBL proteins in degradation it was proposed that they could operate as inhibitors of multiubiquitin chain assembly (Ortolan et al., 2000), inhibitors of deubiquitylation (Raasi and Pickart, 2003), linkers to the proteasome, and substrate carriers (Wilkinson et al., 2001). A careful investigation based on the reconstitution of Rad23- and Rpn10-deficient proteasomes with recombinant proteins and analysis of the degradation of different substrates clearly showed a substrate specificity of the UBL-UBA proteins beyond the modification with polyubiquitin (Verma et al., 2004a). This study demonstrated that deletion of a specific UBL-UBA protein lead to a slow down but not to a complete inhibition of the proteolysis of some substrates, but left others unaffected. However, in all cases the effect of the UBL-UBA protein was strictly dependent on the presence of the UBA-domain.

Here we report the unexpected finding that the accelerated degradation of FAT10 by NUB1L is independent of all three of its UBA-domains. Since FAT10 and NUB1LΔUBA1-3 could not be co-immunoprecipitated, this enhancement in degradation does not depend on the interaction of both proteins. Moreover, NUB1L was able to accelerate the degradation of the two isolated UBL-domains of FAT10 when fused to GFP. Since only the N-terminal UBL-domain of FAT10 bound to NUB1L (Fig. 11), this is the second independent experiment in which we found no correlation between the ability of NUB1L to bind a FAT10 variant and to accelerate its degradation. Therefore, a role of NUB1L as a proteasomal receptor for FAT10 can not be the only mode of action. Because FAT10 degradation occurs also independently of ubiquitylation (Hipp et al., 2005), a role for NUB1L in the protection from deubiquitylation is unlikely as well. Also a protection from putative FAT10-specific proteases is unlikely, since we failed to obtain evidence for their existence in two independent cell lines in the presence or absence of IFN-γ (Hipp et al., 2005). In our experiments, the ability of NUB1L to accelerate FAT10 degradation relied solely on the UBL domain-dependent interaction with the 26S proteasome, since both NUB1L and NUB1LΔUBA1-3 had a similar effect on the degradation rate of FAT10 while NUB1LΔUBL was ineffective (Fig. 8). Given that NUB1L and FAT10 can bind independently to the 26S proteasome (Fig. 13), we favour the hypothesis that binding of NUB1L to the 26S proteasome with its N-terminal UBL domain induces a conformational change in the 19S regulator that favours the binding and/or degradation of FAT10 and FAT10-conjugated proteins at an independent docking site. This scenario would be analogous to the one suggested by Verma et al. who showed that binding of the VWA domain of Rpn10 serves to facilitate the degradation of polyubiquitylated substrates delivered by

Rad23 (Verma et al., 2004a). In order to address this hypothesis for NUB1L and FAT10, it will be important to map the binding site of FAT10 at the 26S proteasome.

Curiously, the mutant FAT10-N-GFP is quite a stable protein (Fig. 12A), despite its ability to interact with the proteasome (Fig. 13D). Degradation of FAT10-N-GFP, however, can be readily induced by coexpression of NUB1L. These results combined argue against the recently proposed model that mere binding to the proteasome is sufficient to target for proteasomal degradation (Janse et al., 2004). Verma et al. found that the polyubiquitylated proteasome substrate Sic1 bound to Rpn10-deficient 26S proteasomes in dependency of Rad23, but no degradation was observed (Verma et al., 2004a). Thus binding seems to be a necessary but not a sufficient prerequisite for proteasomal degradation of at least some substrates. For the proteolysis of such substrates like Sic1 or FAT10, the binding of their respective facilitators Rpn10 or NUB1L to the proteasome appears to be important.

Experimental Procedures

Antibodies. The anti-HA mAb clone HA7 (Sigma) was used for immunoprecipitation in figures 7, 8, 9, 10, 11, 12 and for the Western blot in figure 13A. The anti-His_6 mAb clone BMG His-1 (Roche) was used for immunoprecipitation shown in figures 7B, D and 9D. A mixture of monoclonal anti-GFP clones 7.1 and 13.1 (Roche) was used for the immunoprecipitation in figure 11A and for the western blot in figure 13B. An anti-HA mAb clone HA7 antibody peroxidase-conjugate (Sigma) was used for the western blot shown in figure 13C, and a polyclonal rabbit anti-GFP antibody (Sigma) for the western blot in figure 13D. The western blots presented in figure 13E and F were performed with a rabbit polyclonal anti-Rpt6 (S8) from Biomol. The immunoprecipitation of the proteasome was performed with 5 μl of ascitis fluid of the anti-HN3 antibody MCP444 (Hendil et al., 1995). The mouse monoclonal anti-iota antibody 27K was kindly provided by Dr. Klaus Scherrer (Paris). Anti-FAT10 antibody has been described (Hipp et al., 2005), anti-NUB1 antibody was a gift from Dr. Michael E. Cheetham (London). The anti-GAPDH antibody was purchased from Ambion. All antibodies were coupled to EZview Red Protein A or G Affinity Gel (Sigma) for immunoprecipitation. All horseradish peroxidase-conjugated secondary antibodies were purchased from DAKO.

Tissue culture. HEK293T and HeLa cells were kept in IMDM. Induction of FAT10 and NUB1L was performed by over night incubation with interferon-γ (IFN-γ, Endogen) at a final concentration of 200 U/ml and tumor necrosis factor-α (TNF-α, Endogen) at 400 U/ml.

qRT-PCR. The RNA was isolated with a kit from Machery-Nagel and the cDNA was generated with a kit from Promega according to the instruction of the manufacturer. We use the following primers and conditions: for FAT10 forward primer: 5'-TTGTTCTTGTGGAGTCAGGTG-3'; reverse primer: 5'-AGTAAGTTGCCCTTT CTGATGC-3' with cycling parameters 95°C 10 min, 95°C 15 s, 60°C 5 s, 72°C 9 s 40 times; for NUB1L forward primer: 5'-AAAGGGATGGGCTACTCCAC-3', reverse primer: 5'-CGTCTGTTGAGGCACTAGAGG-3' with cycling parameters 95°C 10 min, 95°C 15 s, 60°C 5 s, 72°C 13 s 40 times; for GAPDH forward primer: 5'-GAAGGTGAAGGTCGGAGTC-3', reverse primer: 5'-GAAGATGGTGATGGGATTTC-3', with cycling parameters 95°C 10 min, 95°C 15 s, 60°C 5 s, 72°C 11 s 40 times.

Generation of cDNA constructs. The generation of HA-NUB1L (Figs. 6-11) and His_6-FAT10 (Fig. 7) both in pcDNA3.1, HA-FAT10 in pBI, HA-FAT10 in pBI+GFP, HA-NUB1L in pBI+GFP, HA-FAT10+HA-NUB1L in pBI, FAT10-GFP, SUMO-1-GFP and GST-FAT10 has been described (Hipp et al., 2004). The GST-expressing vector pGEX-4T-3 and the GFP-expressing vector pN1EGFP are commercially available from Amersham Biosciences and Clontech. Generation of expression constructs for NUB1LΔUBA1, NUB1LΔUBA2, NUB1LΔUBA3, NUB1LΔUBA1/2, NUB1LΔUBA1/3, NUB1LΔUBA2/3, NUB1LΔUBA1-3, NUB1LΔUBL and NUB1 was performed by PCR. A list of the primers used will be available on request. First we made the deletion mutant NUB1LΔUBA1-3. The parts of the DNA from the 5'-end of the full length cDNA to the 5'-end of UBA1, and from the 3'-end of UBA3 to the 3'-end of the wild-type cDNA were amplified separately by PCR. A short overlap of the primers flanking the region to be deleted allowed for assembly of these two fragments that were completed by amplification using the 5' and 3' primers or the full length cDNA. The short overlap of the two primers contained three unique restriction sites, which were introduced by conservative mutations. The UBA domain or domains of the other mutants were amplified by PCR and introduced into NUB1LΔUBA1-3 via the unique restriction sites. Nub1LΔUBL was generated the same way as NUB1LΔUBA1-3, but different primers were used. FAT10-N-GFP and FAT10-C-GFP were generated by PCR amplification of the N-terminal (FAT-N-GFP) or C-terminal (FAT10-C-GFP) UBL domain of FAT10 and replacing FAT10 in a

FAT10-GFP expressing vector by restriction digestion. The two domains were cloned into pcDNA3.1 as well. All sequences were verified by sequencing.

Immunoprecipitation. Co-immunoprecipitation of NUB1L mutants and His_6-FAT10, and NUB1L and FAT10 mutants was performed as previously described (Hipp et al., 2004). For the immunoprecipitation (IP) of the 26S proteasome, one well of a 6-well plate of transfected cells was used per IP. Cells were lysed in 25 mM Tris pH 7.8, 2 mM $MgCl_2$, 20% glycerol, 1 mM DTT, and 2 mM ATP by sonification. After centrifugation for 15min at 20000 × g, the supernatant was supplemented with BSA to a final concentration of 1 mg/ml, 15 mM creatine phosphate and 15 U/ml creatine kinase. After preincubation of the lysates for one hour with Sepharose CL-4B (Amersham), the supernatant was immunoprecipitated for four hours with 5 μl of MCP444 ascitis fluid. After washing three times with lysis buffer, the matrix was washed once with 25 mM Tris pH 7.8, 2 mM $MgCl_2$, 20% glycerol, 1 mM DTT, 2 mM ATP, 150 mM KCl, and 0.05% Triton X-100. Bound proteins were eluted by boiling in SDS sample buffer and analysed by western blotting.

Pulse-chase experiments. Tissue culture and transfection of HEK293T cells, metabolic labelling, and pulse-chase analysis were performed as described (Hipp et al., 2004).

GST-pulldown assays. Glutathione Sepharose 4B (Amersham) and recombinant GST or GST-FAT10 Hipp et al., 2004, purified as previously described in were incubated over night at 4°C with 20 μg 26S proteasome in the presence or absence of recombinant His_6-NUB1L Hipp et al., 2004, purified as previously described in. The incubation buffer contained 20% glycerol, 2 mM ATP, 1 mM DTT, and 100 μM LLnL (Roche). The matrix was washed four times with incubation buffer and analysed by western analysis for the 20S subunit iota. All other GST-pulldown assays and coupled *in vitro* transcription/translation reactions were performed as described (Hipp et al., 2004).

Purification of 26S proteasomes. Purification of 26S proteasomes was performed as detailed elsewhere (Khan et al., 2004).

Analysis of intracellular protein degradation and proteasome activity. The experiments were performed exactly as previously described (Moradpour et al., 2001).

Acknowledgements

We thank Elisabeth Naidoo for excellent technical support and Selina Khan for contributing a preparation of 26S proteasome. Klaus Hendil, Klaus Scherrer, and Michael E. Cheetham are acknowledged for the contribution of antibodies. This work was supported by Deutsche Forschungsgemeinschaft (grants GR1517/2-1 and GR1517/3-1) and the Fritz Thyssen Foundation.

Chapter 2

Degradation of FAT10 by the 26S proteasome *in vitro* is independent of ubiquitylation but relies on NUB1L

Gunter Schmidtke*, Birte Kalveram* and Marcus Groettrup

Department of Biology, Division of Immunology, University of Constance, 78457 Konstanz, Germany

*The authors contributed equally to this work

Manuscript submitted.

Abstract

FAT10 is a ubiquitin-like protein which is encoded in the major histocompatibility complex class I locus and is synergistically inducible with interferon-gamma and tumor necrosis factor-alpha. It encompasses two ubiquitin-like domains connected by a short linker, and bears a free diglycine-motif at its C-terminus through which it forms covalent conjugates with its target proteins. Previously, we have shown that both monomeric FAT10 as well as its conjugates are rapidly degraded by the proteasome in intact cells and their degradation was further accelerated by expression of the UBL-UBA domain protein NEDD8 ultimate buster 1-long (NUB1L). This degradation was independent of a ubiquitin activating enzyme and did not rely on the lysine residues of FAT10, suggesting that poly-ubiquitylation was not involved. Here we show that the 26S proteasome readily degrades the model substrate FAT10-dihydrofolate reductase (DHFR) but not ubiquitin-DHFR *in vitro*, demonstrating conclusively that FAT10-mediated degradation does not rely on poly-ubiquitylation. Interestingly, the purified 26S proteasome could only degrade FAT10-DHFR when NUB1L was present. Knockdown of NUB1L attenuated the degradation of FAT10-DHFR, suggesting that NUB1L modulates the degradation rate of FAT10-linked proteins in cells. In conclusion, our data establish FAT10 as a ubiquitin-independent but NUB1L-dependent targeting signal for proteasomal degradation.

Introduction

The proteasome is responsible for the turnover of the majority of intracellular proteins in eukaryotes and is essential for the degradation of misfolded proteins and the destruction of short-lived regulatory proteins. Most proteins are degraded by the 26S proteasome, a 2.4M Da multi-subunit complex consisting of the 20S proteasome core particle capped by one or two 19S regulatory particles (Hanna and Finley, 2007). The 20S proteasome is a cylindrical stack of four 7-membered rings around a central pore, where subunits α1-α7 make up the outer and subunits β1-β7 the inner two rings. Six of those subunits – two copies of β1, β2 and β5 – are catalytically active, and their active sites point toward the central lumen of the core particle. The 19S regulator, also known as PA700, can be further subdivided into the proximal "base", which abuts to the outer α-rings of the 20S proteasome, and the distal "lid". The "base" consists of six AAA-family ATPases (Rpt1-Rpt6) and four non-ATPase subunits (Rpn1, 2, 10 and 13). The ATPases form a hexameric ring, which mediates ATP-dependent opening of the pores formed by the α-subunit rings and unfolding of substrate proteins. The remainder of the approximately 20 PA700 subunits make up the "lid"; and while some of them could be shown to display deubiquitylating activity, most of their functions are unknown.

Proteins are targeted for proteasomal degradation by the covalent attachment of a chain of ubiquitin molecules by way of a multi-enzyme cascade. Ubiquitin first gets activated by an E1 enzyme, then it is transferred to an E2 enzyme and finally, through the help of an E3 enzyme, becomes conjugated to an acceptor lysine of a target protein. After attachment of a single ubiquitin molecule, additional ubiquitins can become conjugated to each of its seven lysine residues to form a polyubiquitin chain. Polyubiquitin chains linked through K48 are the principal targeting signal, with the attachment of a tetraubiquitin chain serving as the minimal signal required for proteasomal degradation (Thrower et al., 2000). Substrate recognition of the proteasome is mediated by four subunits of the 19S regulator; S5a/Rpn10 and S6'/Rpt5, which directly recruit K48-linked polyubiquitin chains (Deveraux et al., 1994; Lam et al., 2002) as well as S1/Rpn2 and S2/Rpn1, which indirectly recognize substrates by binding to linker proteins such as Rad23/hHR23 and Dsk2/hPLIC (Elsasser et al., 2002; Saeki et al., 2002b; Walters et al., 2002).

Aside from this canonical mode of proteasomal degradation, a few alternative routes into the proteasome exist. The most prominent and well-studied case is that of ornithine decarboxylase (ODC), the first and rate-limiting enzyme in the

synthesis of polyamines. Cellular ODC levels are controlled through a negative feedback mechanism involving the polyamine-induced inhibitor antizyme (AZ) (Murakami et al., 1992). AZ serves to inactivate ODC by two different mechanisms. Firstly, it disrupts the enzymatically active ODC homodimer, forming an inactive AZ/ODC heterodimer instead. Secondly, it alters ODC conformation, exposing a C-terminal segment which, in combination with the bound AZ, serves as a recognition signal for the 26S proteasome. Analogous to ubiquitin, AZ is not degraded along with ODC but can promote its destruction even in substoichiometric amounts (Zhang et al., 2003a).

A small group of proteins can be degraded by the proteasome without the need for prior attachment of a polyubiquitin chain or the intervention of a negative regulator such as AZ. Among them are $p21^{Waf1/Cip1}$, thymidylate synthase, IκBα, c-Jun, and α-synuclein, with their common denominator being the presence of a loosely folded, disordered domain, which in some cases suffices as a signal for proteasomal processing (Forsthoefel et al., 2004; Liu et al., 2003; Asher et al., 2005). Furthermore, the proteasome regulator PA28γ has been shown to facilitate the ubiquitin- and ATP-independent degradation of p21 (Li et al., 2007; Chen et al., 2007) and the steroid receptor coactivator-3 (Li et al., 2006).

A different case entirely is that of the ubiquitin-like modifier FAT10, which encompasses two ubiquitin-like domains connected by a short linker. FAT10 lies encoded in the major histocompatibility complex class I locus (Fan et al., 1996) and is inducible with the proinflammatory cytokines IFN-γ and TNF-α (Raasi et al., 1999; Liu et al., 1999). FAT10 can become activated by the E1 type enzyme UBA6 (E1-L2, UBE1L2) and becomes covalently conjugated to a number of so far unidentified target proteins through a free diglycine-motif at its C-terminus (Raasi et al., 2001; Chiu et al., 2007). Both monomeric FAT10 as well as FAT10-conjugates are rapidly degraded by the proteasome in a ubiquitin-independent manner; and N-terminal fusions of FAT10 to long-lived proteins such as GFP and DHFR are degraded with a kinetic similar to that of ubiquitin-fusions (Hipp et al., 2005). In addition, degradation of FAT10 can be further accelerated by the UBL-UBA domain protein NEDD8 ultimate buster 1-long (NUB1L) (Hipp et al., 2004), which interacts with both FAT10 and the 26S proteasome (Tanji et al., 2005). Since FAT10 can also directly interact with the 26S proteasome and since NUB1L can promote FAT10 degradation even without binding to FAT10, we postulated that NUB1L may serve as a facilitator of FAT10 degradation (Schmidtke et al., 2006).

From our previous data it appeared that FAT10 functions as an inducible alternative to ubiquitin-mediated proteasomal degradation, but it needs to be rigorously investigated whether the FAT10 system can operate independently of ubiquitin conjugation. Two approaches have been used so far to address this issue in intact cells: the first was the mutation of all 17 lysine residues to arginine which did not affect proteasomal degradation of FAT10 (Hipp et al., 2005). Although we could not detect any ubiquitylation of lysineless FAT10, one can not absolutely exclude that residual ubiquitylation of the N-terminus of FAT10 below detection level may contribute to proteasome targeting. The second approach was the investigation of FAT10 degradation in E36ts20 cells which bear a temperature sensitive mutation of the ubiquitin activating enzyme UBE1. In these cells FAT10 degradation occured normally at the restrictive temperature (Hipp et al., 2005). However, the recent discovery of UBA6 (UBE1L2, E1-L2) as a second ubiquitin activating enzyme (Pelzer et al., 2007; Chiu et al., 2007; Jin et al., 2007) opens the possibility that ubiquitylation of FAT10 may rely on UBA6 activity thus rendering experiments in ts20 cells inconclusive.

In this study we have addressed whether FAT10 can target a linked protein to the 26S proteasome independently of ubiquitylation *in vitro*. We found that an N-terminal FAT10-DHFR fusion protein can be degraded *in vitro* by purified 26S proteasomes, but only in the presence of the UBL-UBA domain protein NUB1L. Experiments in NUB1L knock-down cells show that NUB1L is indispensable for proteasome-mediated FAT10 turnover in cells. The herein presented results conclusively demonstrate the ubiquitin-independence of FAT10-mediated degradation and, given that FAT10 can also directly interact with the proteasome, allow for the conclusion that mere association of FAT10 with the 26S proteasome is not enough to promote its degradation.

Results

In order to investigate whether purified 26S proteasome can degrade a FAT10-linked protein in the absence of ubiquitylation we decided to use an N-terminal fusion of FAT10 to DHFR as a model substrate because Ub_5-DHFR has been shown to be a well behaved substrate for degradation by 26S proteasomes *in vitro* (Thrower et al., 2000) and because HA-FAT10-DHFR fusions could be degraded in a proteasome-dependent manner in intact cells (Hipp et al., 2005). To exclude any residual ubiquitylating activity in our reactions, we decided on Ub-DHFR as a negative control. In cells, both yeast and mammalian, Ub-DHFR is readily

polyubiquitylated and rapidly degraded by the proteasome (Johnson et al., 1995; Hipp et al., 2005), however, a single ubiquitin moiety is insufficient to promote proteasomal degradation by 26S proteasomes *in vitro* (Thrower et al., 2000). A C-terminal fusion of FAT10 to GST (GST-FAT10) was selected as a second negative control on the premise that, if the C-terminal attachment of ubiquitin to a protein has no effect on its degradation (Lévy et al., 1996), the same should also hold true for FAT10.

FAT10-DHFR, Ub-DHFR as well as GST-FAT10 were recombinantly produced in *E. coli* and metabolically labeled with [^{35}S]-methionine. Degradation was measured by the release of acid soluble counts and was linear over time (data not shown). [^{35}S]-labeled, *in vitro* transcribed/translated and affinity purified ornithine decarboxylase (ODC) served as the positive control for degradation. The proteinaceous components of our *in vitro* degradation assays are depicted in figure 14. In panel A a coomassie staining of the purified proteins is shown while in panel B the autoradiogram of the same proteins is presented.

In accordance with the literature (Zhang et al., 2003a), degradation of ODC already occurred to a minor extent when incubated with 26S proteasome alone (Fig. 15A, compare bars 1 and 3) and could be greatly increased by the addition of recombinant, unlabeled AZ (Fig. 15A, bar 4). Incubation of the reaction mix in the presence of the proteasome inhibitor epoxomycin reduced the release of acid soluble counts to background levels (Fig. 15A, bar 5). The observed degradation of ODC in the absence of AZ is most likely due to the degradation of monomeric ODC by dissociated 20S proteasome (Asher et al., 2005), and native SDS-PAGE did indeed reveal low levels of 20S proteasome in our preparations of 26S proteasome (data not shown). Fig. 15B reveals our assay to be devoid of any ubiquitylating activity, as Ub-DHFR was not degraded by the proteasome under any of the conditions investigated.

In a previous study, we were able to show FAT10 to be capable of direct interaction with the 26S proteasome (Schmidtke et al., 2006), however, incubation of FAT10-DHFR with purified 26S proteasome alone was not sufficient to promote its degradation over background level *in vitro* (Fig. 15C, bar 2) which also occured in the presence of epoxomycin (Fig. 15C, bar 5). Remarkably, the addition of purified, recombinant NUB1L was able to induce degradation of FAT10-DHFR by the 26S proteasome in a dose dependent manner (Fig. 15C, bar 3 and 4). In contrast, FAT10-DHFR was completely stable when incubated with purified 20S proteasomes, even in the presence of recombinant NUB1L (Fig. 15C, bars 8 and

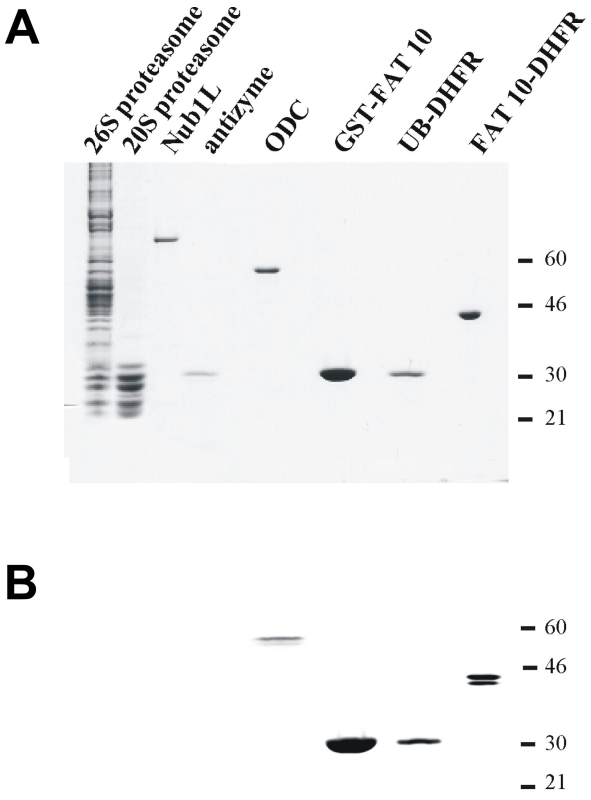

Figure 14: Purified components for in vitro degradation. (A) Silver stained SDS-gel of purified 26S proteasome (about 500ng), purified 20S proteasome (about 250ng) and the recombinant purified proteins NUB1L, antizyme, ornithine decarboxylase (ODC), GST-FAT10, ubiquitin-dihydrofolate reductase (Ub-DHFR) and FAT10-DHFR (between 10 and 50ng each). **(B)** Autoradiogram of the radioactively labelled ODC, GST-FAT10, Ub-DHFR, and FAT10-DHFR.

9). Experiments with GST-FAT10 as a substrate showed that modification with a C-terminal FAT10-tag was insufficient to promote degradation even under conditions where N-terminal fusions were efficiently degraded, and despite the ability of GST-FAT10 to interact with both NUB1L and the 26S proteasome *in vitro* (Hipp et al., 2004; Schmidtke et al., 2006, and data not shown).

To determine whether NUB1L is essential for the degradation of FAT10-DHFR *in vivo*, we created HeLa cell transfectants stably expressing two shRNAs directed against both NUB1 as well as NUB1L. We selected three different clones with knock-down efficiencies of 91.2% (clone G6), 90.5% (clone F9) and 89.1% (clone H10), as determined by quantitative RT-PCR, to use in the subsequent pulse-chase experiments. Western blots of cell lysates probed with two different antibodies against NUB1 as well as an anti-HSP90 antibody as a loading control revealed faintly detectable levels of NUB1L protein in only one of the clones (F9) and with only one of the antibodies (Fig. 16A and C). Densitometric

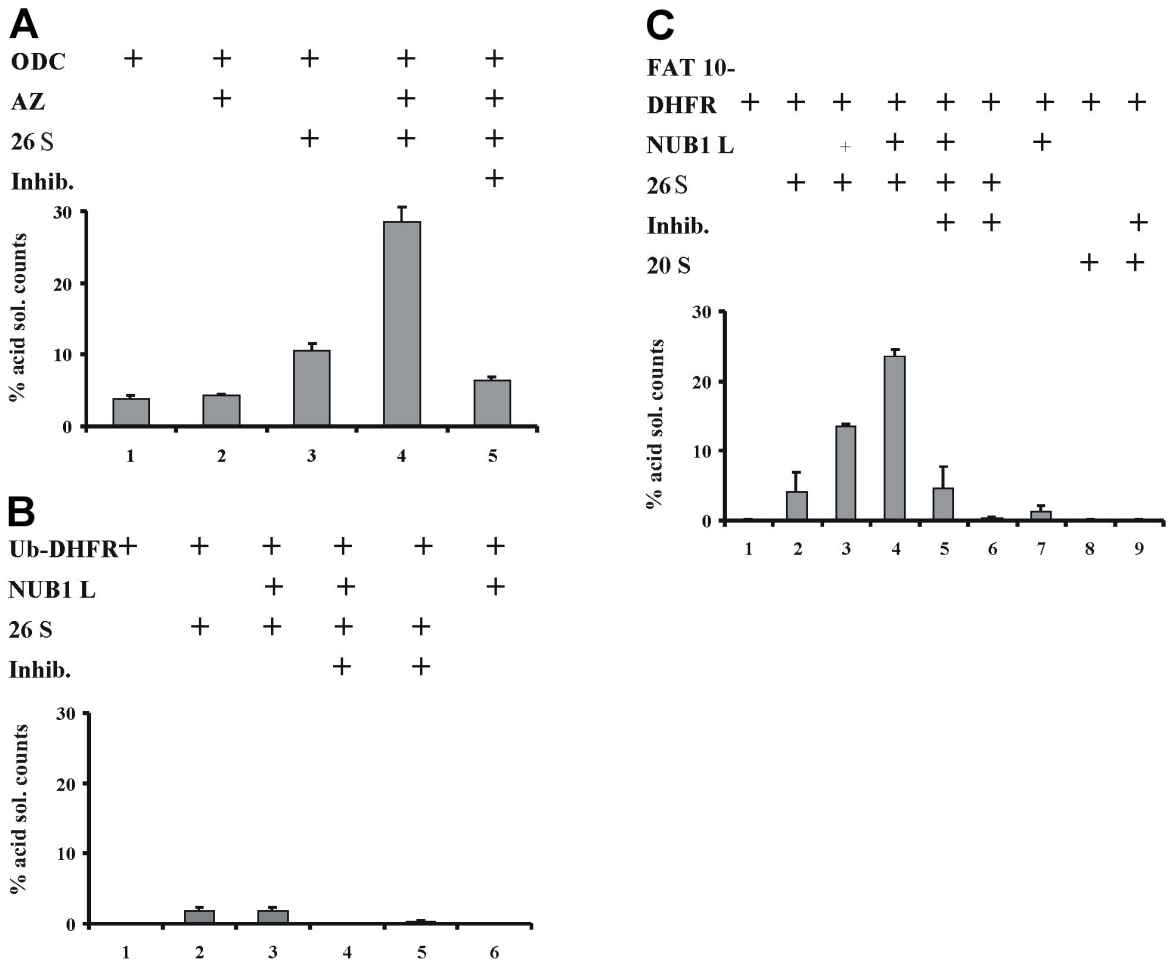

Figure 15: The degradation of FAT10-DHFR by the 26S proteasome *in vitro* is independent of ubiquitylation but relies on NUB1L. The Y-axis always represents percent of acid soluble counts per hour. The *in vitro* reactions were performed with the components indicated above each panel. Inhib. refers to degradation obtained in the presence of the specific proteasome inhibitor epoxomycine. (A) Antizyme (AZ) dependent degradation of ornithin decarboxylase (ODC) as positive control for 26S proteasome activity. **(B)** HA-Ubiquitin-DHFR (Ub-DHFR) is not significanly degraded by the purified 26S proteasome. **(C)** NUB1L-dependent degradation of HA-FAT10-DHFR by purified 26S proteasome. A small and a normal sized (+) sign designate degradation in the presence of low (2ng) and high (20ng) amounts of NUB1L, respectively.

evaluation of the NUB1L bands obtained by three dilutions of lysates on graded semi-quantitative Western blots (Fig. 16A) revealed that the residual expression of NUB1L protein in the shRNA transfectants was 2% (G6), 8.5% (F9), and 4% (H10), respectively. As NUB1L is the dominant isoform in HeLa cells, no NUB1 was detectable even in wild-type cells.

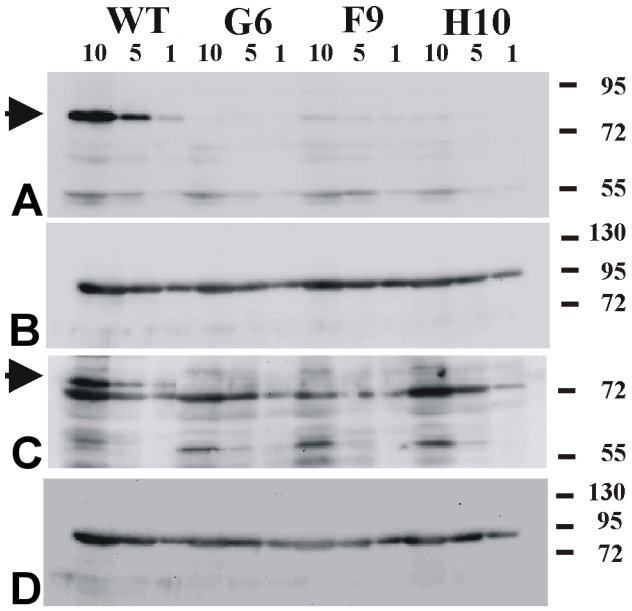

Figure 16: Efficient knock down of NUB1L in stable HeLa transfectants expressing two NUB1L shRNAs. Shown are Western blots of wild-type HeLa-cells (WT) and 3 different stable transfectants expressing two NUB1L specific shRNAs (clones F9, G6 and H10). 10, 5 and 1μl of cell lysate (indicated above the panels) were loaded for each cell type. **(A,C** Western blots probed with two different NUB1/NUB1L peptide specific antibodies (A, van der Spuy et al., 2003); (B, Biomol). The arrowheads on the left show the position of NUB1L.**(B, D** Loading control for panels (A) and (C) with anti-HSP90 antibody.

Next, we transiently transfected the three NUB1L knock-down clones as well as wild-type HeLa cells with an expression contruct for HA-FAT10-DHFR (Hipp et al., 2005). Subsequent to transfection, the degradation of HA-FAT10-DHFR was monitored in pulse-chase experiments. As shown in figure 17, the degradation of HA-FAT10-DHFR was markedly slowed down in the three NUB1L knock-down clones compared to wild-type HeLa cells, and the reduction in HA-FAT10-DHFR degradation correlated with the extent of NUB1L deficiency. This result strongly suggests that in intact cells, NUB1L is required for the degradation of FAT10-linked proteins by the proteasome.

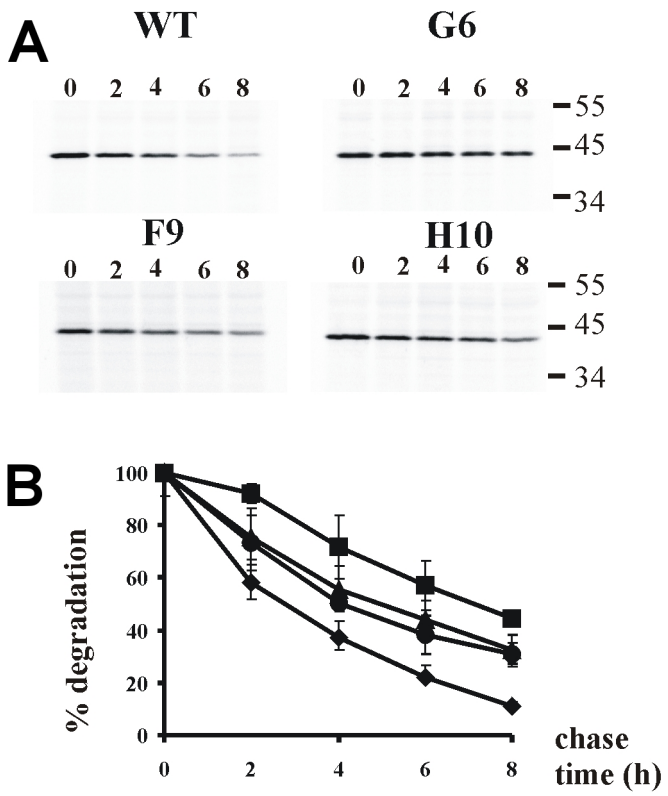

Figure 17: Knock-down of NUB1L attenuates the degradation of HA-FAT10-DHFR. (A) Shown are autoradiograms of HA-FAT10-DHFR immunoprecipitations from wild-type HeLa cells (WT) and the NUB1L shRNA transfected clones G6, F9, und H10 described in figure 3. Cells were pulse labeled with (^{35}S)-methionine/cysteine for one hour and subsequently chased for the indicated time periods (in h). **(B)** Graphic representation of the phosphorimager-assisted quantitative evaluation of three different experiments as exemplified in panel **(A)**; the extent of FAT10 degradation in percent is plotted versus the chase time. Shown are the means +/-SD for HeLa wild-type cells (diamonds), and the transfectants F9 (dots), H10 (triangles), and G6 (cubes).

Discussion

Ubiquitin has long lost its unique status as the sole mediator of proteasomal degradation. While other, non-proteolytic functions of ubiquitin have been discovered, several alternative routes into the proteasome have also been scouted. The ubiquitin-like modifier FAT10 was shown to be as potent as ubiquitin in targeting artificial fusion proteins for proteasomal degradation. The present study shows that FAT10-linked proteins are efficiently degraded by the 26S proteasome *in vitro*, but only in the presence of the UBL-UBA domain protein NUB1L.

Degradation by the proteasome can be divided into two main categories: inducible destruction, which is chiefly mediated by attachment of a K48-linked polyubiquitin chain to the target protein, and degradation “by default” of pro-

teins which contain intrinsic targeting signals (Asher et al., 2006). A diverse group of proteins has been described which can be characterized by the presence of one or more loosely folded domains and which can be degraded by the 20S proteasome without the need for prior ubiquitylation or ATP-dependent unfolding. Members of this group include IκBα (Alvarez-Castelao and Castaño, 2005), p53 (Asher et al., 2005), p21$^{\text{Waf1/Cip1}}$ (Touitou et al., 2001), α-synuclein (Tofaris et al., 2001), thymidylate synthase (Forsthoefel et al., 2004), and ODC (Asher et al., 2005). As many of these proteins function as part of a multimeric complex, and "default" degradation can only be observed when they are present in monomeric form, it has been suggested that assembly into a larger complex masks the unstructured regions – which are considered to function as the targeting signal – and thereby protects them from degradation. It is interesting to note that most, if not all of these proteins can also be actively targeted to the 26S proteasome by attachment of a polyubiquitin chain or – in the case of ODC – by interaction with AZ.

The structure of FAT10 remains yet to be solved, however, the high sequence similarity to ubiquitin and ISG15 suggests that it is in all likelihood composed of two ubiquitin-fold domains (Narasimhan et al., 2005), which are anything but loosely folded. One can thus safely assume that FAT10 has evolved as a component of a specialized regulatory system responsible for targeting a subset of proteins for proteasomal degradation, and is not merely degraded due to an intrinsic instability. This notion is further supported by the finding that purified 20S proteasome – which was fully competent in the cleavage of short peptide substrates (data not shown) – was unable to degrade HA-FAT10-DHFR *in vitro* (Fig. 15C), and that C-terminal attachment of a FAT10-tag does not promote degradation (data not shown).

The precise mechanism by which FAT10 is targeted to the proteasome has somewhat remained a mystery. Discovery of the UBL-UBA domain protein NUB1L as a non-covalent interaction partner and an accelerator of FAT10 degradation (Hipp et al., 2004) suggested that it might interact with FAT10 through its C-terminal UBA domains and with the 19S regulator through its N-terminal UBL domain and thus physically link FAT10 to the proteasome. It was soon revealed, however, that while NUB1L did interact with FAT10 through all three of its UBA domains, only the UBL domain was required to accelerate its degradation, and that FAT10 was perfectly able to interact with the 26S proteasome on its own (Schmidtke et al., 2006). Recent studies investigating other members of this family, most notably Rad23/hHR23 and Dsk2/hPLIC, have revealed functional redundancy in

the targeting of polyubiquitylated substrates to the proteasome (Elsasser et al., 2004) and have uncovered, in at least some cases, an uncoupling of proteasomal anchoring and degradation (Verma et al., 2004a). The current results provide the final piece of evidence that the same also applies to the degradation of FAT10 and its conjugates. While the 26S proteasome is able to directly interact with FAT10, it fails to degrade FAT10-DHFR *in vitro*. Nevertheless, the addition of NUB1L is sufficient to facilitate FAT10 degradation (Fig. 15C). It remains subject to investigation whether the requirement for a facilitator applies to all of FAT10's conjugates or whether it can perhaps be circumvented by the presence of intrinsic degradation signals in some of the target proteins.

As of yet, the binding sites of FAT10 and NUB1L to the proteasome are still unknown. Although NUB1 was shown to interact with S5a/Rpn10 through a short C-terminal region between amino acids 536 and 584 (Tanji et al., 2005), other studies demonstrated an absolute requirement of the N-terminal UBL domain for its interaction with the 26S proteasome (Schmidtke et al., 2006). Interestingly, binding of the UBL domain does not seem to be mediated by S5a/Rpn10. Likewise, S5a/Rpn10, S6'/Rpt5 and S2/Rpn1 are no likely candidates as receptors for FAT10, as they all failed to interact in GST-pulldown assays (data now shown). Because DHFR needs to be unfolded in an ATP-dependent manner before it can be processed by the proteasome (Liu et al., 2002), PA700 is the most likely candidate for regulating FAT10 access to the proteasome, as it is the only regulator which contains ATPases to confer unfoldase activity.

The important role for NUB1L in mediating the degradation of FAT10 and FAT10-linked protein has been confirmed in three independent HeLa clones stably expressing two different NUB1L shRNAs each. Compared to the parental cells the degradation rate of HA-FAT10-DHFR was reduced by approximately 50% (Fig. 17), indicating that the expression of NUB1L mRNA and protein, which was reduced by over 90%, became a rate limiting factor for HA-FAT10-DHFR degradation (Fig. 16). It hence appears, that both *in vitro* and *in vivo*, NUB1L is indispensable for the proteasomal degradation of HA-FAT10-DHFR. Whether the residual degradation of HA-FAT10-DHFR relies on a second factor that can mediate degradation of this substrate by the proteasome or whether it is due to the residual expression of minute amounts of NUB1L in the knock-down lines remains to be determined in NUB1L gene deficient mice which are not yet available.

Combined with our studies on FAT10 degradation in UBE1 mutant ts20 cells and the fact that deletion of all lysines of FAT10 abolished the prominent mono-ubiquitylation and faint poly-ubiquitylation of wild-type FAT10 in HEK293 cells but nevertheless had not effect on FAT10 degradation (Hipp et al., 2005), the present *in vitro* studies establish FAT10 as the second member of the ubiquitin family that serves as an autonomous signal for targeting proteins for degradation by the 26S proteasome.

Materials and methods

Proteasome purification. Purification of the 20S proteasome was performed exactly as described elsewhere (Schmidtke et al., 1996). 26S proteasome was purified as described (Ben-Shahar et al., 1999) with the following modifications: all initial purification procedures were performed at 4°C. 26S proteasome was prepared from 10 livers of 8-13 week old C57BL/6 mice. The livers were cut and homogenized in 10 ml/liver of buffer A (20 mM Tris-HCl (pH 7.5), 1 mM DTT, 1 mM EDTA, 1.5 mM ATP, and 0.25 M Sucrose) using a blender and a Potter-Elvehjem grinder. After ammonium sulfate precipitation as described (Ben-Shahar et al., 1999), gel filtration chromatography was performed at 15°C on a Sepharose 6B fast-flow column (1.6 × 100 cm, GE Healthcare) equilibrated in buffer B (20 mM Tris-HCl (pH 7.5), 1 mM DTT, 1 mM ATP, and 20% (v/v) glycerol). The pellet of the 38% ammonium sulfate precipitation was dissolved in 10 ml of buffer B and was loaded onto the column. 10 ml fractions were collected, and 26S proteasome activity was assayed with 50 μl samples of column fractions as described previously (Schmidtke et al., 2000). The fractions with proteasome peak activity were combined and loaded onto a 6 ml Resource-Q column (GE Healthcare) equilibrated in buffer B. The column was then washed with 5 column volumes of buffer B and developed with a linear gradient from 0 to 0.8 M NaCl in buffer B over 60 ml. The 26S proteasome eluted from the column between 0.35 and 0.4 M salt. The proteolytically active fractions from the ion exchange column were concentrated to 500 μl by ultrafiltration in a Centricon 100 device (Amicon). The sample was loaded onto a 20-40% (v/v) glycerol gradient in buffe B (12.5 ml in a 14 × 89 mM tube). After centrifugation at 28,000rpm for 18 h at 4°C, fractions of 0.6 ml were collected, and 26S proteasome activity was assayed in 20 μl samples. The quality of the preparation was tested with *in vitro* transcribed/translated ODC and recombinant antizyme. The proteasome preparation was stored in aliquots at 80°C.

Expression constructs. Plasmids for ODC and antizyme were kindly provided by Dr. Philip Coffino (San Francisco, USA). Expression constructs for GST-FAT10 and His-NUB1L have been described (Hipp et al., 2004). HA-FAT10-DHFR and HA-ubiquitin-AV-DHFR expression constructs (Hipp et al., 2005) were amplified by PCR and cloned into an expression vector with a Tev-protease cleavage site after the GST reading frame, which was kindly provided by Dr. Michael Groll (Munich, Germany). Because the HA-ubiquitin-AV-DHFR construct could not be cleaved with the Tev-protease, it was also cloned into the pQE30 vector (Qiagen).

Generation of shRNA constructs. Three siRNA oligonucleotides against NUB1L were designed and provided by Dharmacon Inc. and tested in transient transfection using HeLa cells and X-tremeGENE siRNA (Roche) for transfection. The degree of RNA repression was determined by quantitative reverse transcriptase PCR (qRT PCR) as described (Schmidtke et al., 2006). The most effective of our oligonucleotides (5'-CCTCAGATGTGGTGGTTAA-3') and one reported earlier (5'-CGATGGTGCTTGAACTAAA-3') (Tanji et al., 2006) were selected for shRNAi expression. Overlapping double-strand DNA oligonucleotides with these sequences and the antisense sequences separated by the hairpin loop were generated, the missing parts from the overlap filled with Pfu-polymerase and the constructs were cloned into pSUPER vector (Oligoengine) via BamHI and HindIII. From these constructs we cleaved out the H1 promoter and the shRNA oligo via EcoRI and XhoI and cloned them into the vectors pRETRO-SUPER (Screeninc) and pMSVneo (Clontech). This allowed us to transfer and express both shRNA constructs with two different retroviruses in parallel into the same cell and select with two different resistance markers. Packing of the shRNA constructs into retroviruses, propagation, titration, and transfection was performed exactly as described by the supplier (Clontech). Tissue culture and selection of stable clones has been described elsewhere (Schmidtke et al., 2006).

Expression and purification of recombinant proteins. The plasmids coding for the respective proteins were transformed into BL21 (DE3) [pLysE] cells. Each transformation was allowed to grow over night in 200 ml LB-medium. The next morning, the culture was diluted 1:200 in 500 ml fresh LB-medium and allowed to grow until an OD_{600} of 0.6 to 0.8 was reached. The expression of the proteins was induced with IPTG(1 mM final concentration) for 4-6 hours. Next, the culture was centrifuged at 5000 × g for 10 minutes, the supernatant removed and the pellet washed once in PBS. The pellets were frozen at -80°C if not immediately processed.

Recombinant expression of radioactively labelled proteins was a modification of methods described previously (Ben-Shahar et al., 1999; Zhang et al., 2003a). Plasmids were transformed into the methionine-auxotroph *E. coli* strain B834 (DE3) (Novagen Inc.) and allowed to grow over night in 200 ml of LB-medium. The next morning, the culture was diluted 1:200 in 100 ml fresh LB-medium and allowed to grow to an OD_{600} of 0.5. The culture was centrifuged at 5000 × g for 10 minutes and the pellet washed twice in PBS. After the final wash the cells were resuspended in 50 ml M9 minimal medium supplemented with thiamine (20 μg/ml) and all amino acids (except methionine and cysteine) at 50 or 100 mg/l and incubated for 1 hour at 37°C with agitation. The expression of the proteins was induced with IPTG (1 mM final concentration) for 4-6 hours in the presence of 1 mCi TranS^{35} Label (ICN). After the expression, the culture was processed as described above.

Purification of His-NUB1L, His-antizyme1 (AZ), His-ornithine decarboxylase (ODC), and His-ubiquitin-dihydrofolatereductase (DHFR). After bacterial expression in *E. coli*, the cell pellets were resuspended in PBS and lysozyme (100ng/ml) was added. The suspension was kept on ice for 30 min followed by sonication and centrifugation at 20000 × g for 20 min. The supernatants were adjusted to 500 mM NaCl and 0.1% Triton X-100 before loading on Protino Ni-IDA resin (Macherey Nagel). The resin was washed with PBS containing 500 mM NaCl and 1% Triton X-100, followed by 50 mM Tris-HCl (pH 7.5), 2 mM DTT, 5 mM $MgCl_2$, 10% glycerol. The proteins were eluted with 50 mM Tris-HCl (pH 7.5), 2 mM DTT, 5 mM $MgCl_2$, 20% glycerol, 200 mM Imidazole. The samples were concentrated and the imidazole was removed by ultrafiltration in a Centricon 10 or Centricon 30 concentrator (Millipore).

Purification of GST-FAT10-DHFR and GST-FAT10. The cells were lysed as described above. Triton X-100 was added to the supernatant after centrifugation to a final concentration of 1%, and the proteins were incubated with GSH-Sepharose 4B (GE Healthcare) over night. The GSH-resin was washed with PBS/ Triton X-100. The GST-FAT10 preparation was washed with 50 mM Tris-HCl (pH 7.5), 2 mM DTT, 5 mM $MgCl_2$, 20% glycerol, and the bound protein eluted with the same buffer containing 20 mM reduced glutathione. The samples were concentrated and the glutathione was removed by ultrafiltration in a Centricon 10 concentrator (Millipore). The GST-FAT10-DHFR preparation was washed two times with Tev-protease buffer. A 50% slurry of beads in Tev-buffer was prepared and 2 units of Tev-protease (Invitrogen) were added. The reaction was allowed to proceed for six hours at room temperature. After the incubation the beads were

centrifuged, the supernatant was removed, and the beads were washed with Tev-buffer. The supernatant and the wash were combined and diluted in 50 mM Tris-HCl (pH 7.5), 2 mM DTT, 5 mM $MgCl_2$, 20% glycerol. The DTT was removed and the protein was concentrated by ultrafiltration. The Tev-protease was removed by Ni^{++}-affinity chromatography as suggested by the supplier (Invitrogen).

Preparation of radiolabeled *in vitro* transcribed/translated ODC was performed by a T7 polymerase-dependent transcription-translation (TNT)-coupled system from reticulocyte lysate (Promega) in the presence of TranS^{35} label as recommended by the supplier. Following the translation reaction, unincorporated [^{35}S]-labeled methionine/cysteine was removed and the buffer was exchanged to 50 mM Tris-HCl (pH 7.5), 2 mM DTT, 5 mM $MgCl_2$, 20% glycerol by gel filtration chromatography on a NICK column (GE healthcare). The protein was concentrated by ultrafiltration in a Centricon 30 unit. Specific activity for [^{35}S]-labeled proteins was estimated to be about 5×10^4 c.p.m./pmol. After buffer exchange to 50 mM Tris-HCl pH 7.5, 10 mM KCl, 5 mM $MgCl_2$, 1 mM DTT, 1 mM ATP and 20% glycerol, the concentration of labeled proteins was estimated by SDS-PAGE and coomassie blue staining, using unlabeled proteins as a standard.

***In vitro* degradation assays**. Protein degradation assays were performed as previously outlined (Ben-Shahar et al., 1999; Hoyt et al., 2006) with some modifications. The assays were performed in 50 μl reaction volumes at 37°C for one hour and contained 50 mM Tris-HCl, pH 7.5, 5 mM $MgCl_2$, 1 mM ATP, 20% glycerol, an ATP regenerating system (2 mM dithiothreitol, 10 mM creatine phosphate, 1.6 mg/ml creatine kinase), 1 mg/ml acetylated bovine serum albumin (Promega) and proteasomes. Reactions were initiated by addition of substrate (usually 20000cpm) and quenched by addition of 50 μl of 20% (w/v) trichloroacetic acid. The trichloroacetic acid-insoluble material was removed by centrifugation (14,000 × g, 15 min) at 4°C, and 3 × 30 μl of the supernatant was removed and released counts were measured in a scintillation counter. Percentage degradation of radiolabeled proteins was determined as the released counts/min divided by total input in counts/min. Total input counts were determined by substituting water for trichloroacetic acid in the reactions. Background counts/min were determined in reactions devoid of proteasomes, and were typically 1% to 3% of total input counts.

Western blot and immunoprecipitation. Determination of NUB1L protein expression was performed by Western blotting using anti-NUB1L peptide antibodies provided by Biomol and Dr. Michal E. Cheetham (London) (van der Spuy

et al., 2003), both at a 1:10000 dilution. Cells were harvested, washed, and lysed in 200 μl 50 mM Tris-HCl, pH 7.8 and 0.01% SDS. After sonication and centrifugation, the supernatant was removed and the OD at 260nm and 280nm determined. All lysates were diluted to an OD_{280} of 0.15 and 10, 5 and 1 μl was loaded onto SDS-PAGE. As a loading control the HSP90-specific antibody H-114 (Santa Cruz Biotechnology) was used. Cultivation and transfection of HeLa cells, pulse chase analysis, immunoprecipitation, SDS-PAGE and audioradiography have been described in detail before (Hipp et al., 2004).

Acknowledgements

We thank E. Naidoo for excellent technical support. We acknowledge Dr. P. Coffino and Dr. M. Groll for the donation of plasmids and Dr. M. E. Cheetham for contributing the NUB1 antibody. This work was funded by the German Research Foundation (grants GR1517/2-3 and GR1517/3-1).

Chapter 3

The ubiquitin-like modifier FAT10 interacts with HDAC6 and localizes to aggresomes under proteasome inhibition

Birte Kalveram, Gunter Schmidtke and Marcus Groettrup

Department of Biology, Division of Immunology, University of Constance, Universitätsstrasse 10, 78457 Konstanz, Germany

Journal of Cell Science, 121(24): 4079-4088. December 15, 2008.

Abstract

During misfolded protein stress, the cytoplasmatic protein Histone Deacetylase (HDAC) 6 functions as a linker between the dynein motor and polyubiquitin to mediate the transport of polyubiquitylated cargo to the aggresome. Here we identify a new binding partner of HDAC6, the ubiquitin-like modifier FAT10, which is cytokine-inducible and – like ubiquitin – serves as a signal for proteasomal degradation. *In vivo*, the two proteins only interacted under conditions of proteasome impairment. The binding of HDAC6 to FAT10 was mediated by two separate domains, its C-terminal ubiquitin-binding zinc-finger (BUZ domain) as well as its first catalytic domain, even though catalytic activity of HDAC6 was not required for this interaction. Both endogenous and ectopically expressed FAT10 as well as the model conjugate FAT10-GFP localized to the aggresome in a microtubule-dependent manner. Furthermore, FAT10-containing as well as ubiquitin-containing aggresomes were reduced in both size and number in HDAC6 deficient fibroblasts. We conclude that if FAT10 fails to subject is target proteins for proteasomal degradation, an alternative route is taken to ensure their sequestration and possibly also their subsequent removal by transporting them to the aggresome via the association with HDAC6.

Introduction

The ubiquitin-proteasome system (UPS) is responsible for the targeted destruction of the majority of intracellular proteins. Proteasomal degradation is a tightly controlled process and can serve either of the following two functions in the cell – it can have a regulatory role by destroying and thus inactivating specific proteins such as cell cycle regulators, key enzymes and transcription factors (Hershko and Ciechanover, 1998), or it can ensure the removal of non-functional, damaged or misfolded proteins from the cell (Goldberg, 2003). Substrates are targeted to the 26S proteasome by covalent modification with Lys48-linked polyubiquitin chains. Enzymatic cascades involving a ubiquitin-activating enzyme (E1), a ubiquitin-conjugating enzyme (E2), and a ubiquitin-ligase (E3), catalyze the formation of an isopeptide bond between the ε-amino group of a lysine residue in the target protein and the C-terminal diglycine motif of ubiquitin. Specificity in ubiquitin conjugation is conferred by a multitude of different E3 enzymes, which recruit one of a limited number of E2 enzymes as well as the target protein, to facilitate attachment of the polyubiquitin chain (Hershko and Ciechanover, 1998; Pickart and Fushman, 2004). While Lys48-linked polyubiquitylation is the main route of targeting for proteasomal degradation, there are a few exceptions to this rule. These include the ubiquitin-independent degradation of select proteins such as ornithine decarboxylase (Murakami et al., 1992) or p21 (Chen et al., 2004) as well as the attachment of polyubiquitin chains of unconventional linkage, such as Lys29-linked chains (Pickart and Fushman, 2004), or the modification with the ubiquitin-like modifier FAT10 (Hipp et al., 2005).

Under normal condidions, the proteasome is responsible for the destruction of the majority of misfolded proteins in the cell. However, when the capacity of the proteasome is exceeded, the resulting accumulation of aggregation-prone misfolded proteins tends to have deleterious effects on the cell, which might contribute to a variety of conformational diseases such as Parkinson's disease, amyotrophic lateral sclerosis or dementia with Lewy bodies (Gregersen et al., 2006). Over the past few years, evidence has been uncovered for a compensatory mechanism by which, under conditions where proteasomal degradation is no longer possible, misfolded proteins are transported to pericentriolar inclusions termed aggresomes via dynein-dependent retrograde transport along the microtubule network (Johnston et al., 1998, 2002; Garcia-Mata et al., 2002). Once sequestered in the aggresome, these proteins can now be removed by the lysosomal pathway via autophagy (Iwata et al., 2005; Pandey et al., 2007b). Making the connec-

tion between the UPS and aggresome formation is one of the proposed functions of histone deacetylase 6 (HDAC6) which, in addition to two catalytic domains, contains a ubiquitin binding zinc finger (BUZ, also known as PAZ, ZnF-UBP or DAUP domain) and a dynein binding domain. The latter two domains are utilized by HDAC6 to function as a linker between the dynein motor complex and polyubiquitylated cargo during its transport to the aggresome (Hook et al., 2002; Seigneurin-Berny et al., 2001; Kawaguchi et al., 2003). In addition to its function as a linker, HDAC6 is also involved in aggresome formation and protein quality control in other ways – it mediates microtubule stability by deacetylation of α-tubulin (Hubbert et al., 2002), it is involved in the transport of components of the autophagy apparatus to the aggresome (Iwata et al., 2005) and it is required for the induction of major cellular chaperones via HSF1 after misfolded protein stress (Boyault et al., 2007). In addition, it can also deliver proteins to the aggresome directly, even under conditions where the proteasome is functioning normally, if they are marked with a Lys63-linked polyubiquitin chain (Olzmann et al., 2007).

In addition to ubiquitin, the ubiquitin-like modifier FAT10 can serve as a signal for proteasomal degradation (Kerscher et al., 2006). Like ubiquitin, FAT10 can become covalently conjugated to its target proteins via a free diglycine motif at its C-terminus (Raasi et al., 2001; Chiu et al., 2007). It is encoded in the major histocompatibility class I locus, encompasses two ubiquitin-like domains (UBLs) connected by a short linker (Fan et al., 1996) and can be induced with the proinflammatory cytokines IFN-γ and TNF-α (Raasi et al., 1999; Liu et al., 1999). Overexpression of FAT10 leads to apoptosis in a conjugation-dependent manner (Raasi et al., 2001). Attachment of FAT10 causes the rapid degradation of long-lived proteins, which is dependent on the 26S proteasome but occurs independently of ubiquitylation (Hipp et al., 2005). In contrast to ubiquitin, FAT10 has a relatively short half-life since it is also subject to proteasomal degradation in its monomeric form and, additionally, it is probably not recycled but instead degraded along with its substrates (Hipp et al., 2004).

The herein presented results uncover a role for HDAC6 not only in the transport of polyubiquitylated cargo, but also in the transport of the ubiquitin-like modifier FAT10 and a FAT10-linked protein. We show that, after inhibition of proteasome activity, FAT10 interacts with HDAC6 and localizes to the aggresome in a microtubule-dependent manner. This interaction is mediated by the ubiquitin-binding zinc finger and the first catalytic domain of HDAC6 as well as both ubiquitin-like domains of FAT10 and is not dependent on catalytic activity

of HDAC6. Combined with previous findings, these results suggest that the role of FAT10 is the rapid and inducible destruction of its target proteins via conjugation and subsequent degradation. If the primary way of degradation by the proteasome fails, an alternative route is taken to ensure their removal by sequestering them in the aggresome.

Results

FAT10 interacts with HDAC6 after proteasome inhibition

A yeast two-hybrid screen using FAT10 as a bait against a human lymph node cDNA library (Hipp et al., 2004) identified HDAC6 as a novel interaction partner of FAT10. Sequencing of the plasmid recovered from the transformant revealed that the insert did not encode a full length copy of HDAC6 but rather an N-terminal truncation containing only the last 106 amino acids of the protein. This C-terminal part of HDAC6 encompasses little more than the zinc-finger domain (BUZ) which is responsible for the interaction with free ubiquitin and ubiquitin conjugates (Seigneurin-Berny et al., 2001; Hook et al., 2002). To confirm the interaction with FAT10 *in vivo*, we transfected HEK293T cells with FLAG-tagged HDAC6 as well as hemagglutinin (HA)-tagged FAT10 and treated them with proteasome inhibitor before performing co-immunoprecipitation experiments. In accordance with the finding that HDAC6 only associated non-covalently with polyubiquitylated proteins if the proteasome is impaired (Kawaguchi et al., 2003), we observed robust interaction of FAT10 with wild-type HDAC6 only after proteasome inhibition (Fig. 18A, lanes 1 and 2). As shown in figure 18B, transiently transfected HDAC6 was also capable of interacting with endogenous FAT10 after proteasome inhibition. To our surprise, deletion of the BUZ domain did not abolish the interaction between FAT10 and HDAC6 (Fig. 18A, lanes 3 and 4), suggesting that – while being able to bind FAT10 on its own as shown by the yeast two-hybrid screen – the BUZ domain is not the only domain of HDAC6 which is capable of binding to FAT10.

HDAC6 has no influence on the rate of FAT10 degradation

Since overexpression of the other interaction partner discovered in the yeast-two hybrid screen, the ubiquitin-domain protein NEDD8 ultimate buster-1 long (NUB1L), leads to a marked acceleration of FAT10 degradation (Hipp et al., 2004), and since HDAC6 is able to attenuate the proteasomal degradation of poly-

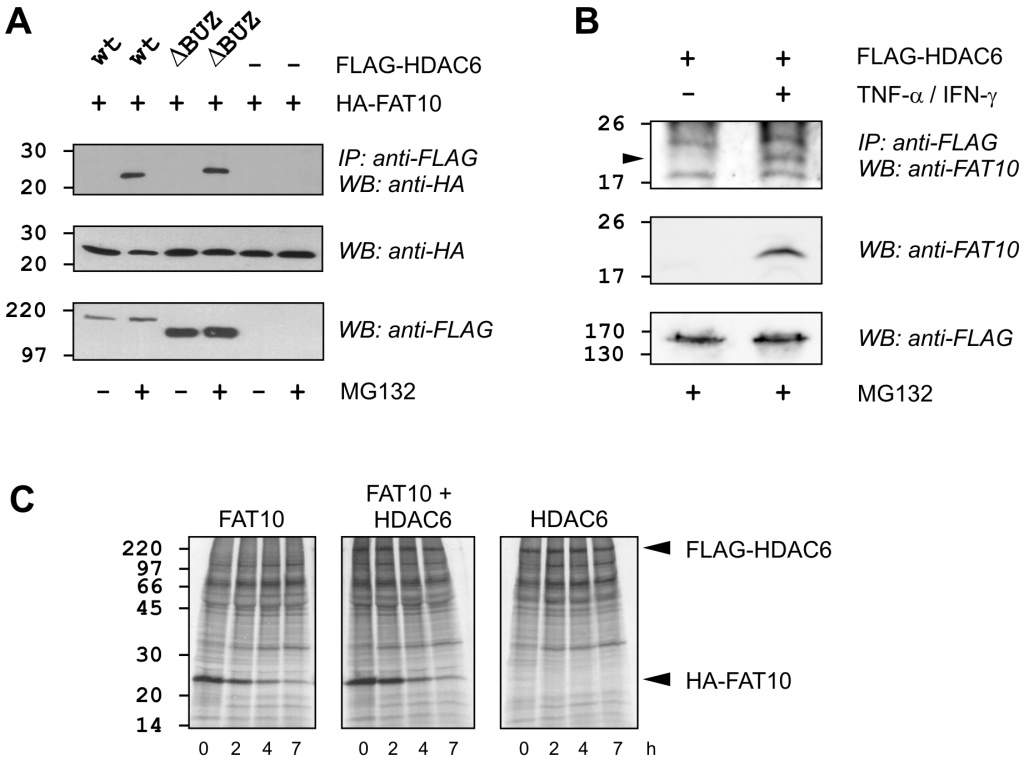

Figure 18: HDAC6 interacts with FAT10 only under proteasome inhibition and has no influence on the degradation rate of FAT10. (A) HEK293T cells, transiently transfected with HA-FAT10 and either wild-type (wt) FLAG-HDAC6, a ΔBUZ mutant, or empty vector, were treated with 5μM of the proteasome inhibitor MG132 or DMSO as a negative control for 6 hours before lysis, anti-FLAG immunoprecipitation (IP) and analysis by Western blot (WB). **(B)** HEK293T cells were transiently transfected with FLAG-HDAC6 followed by treatment with 500 U/ml TNF-α and 200 U/ml IFN-γ for 16 hours and 5μM MG132 for another 6 hours before lysis, anti-FLAG immunoprecipitation (IP) and analysis by Western blot (WB). **(C)** HEK293T cells transfected with either HA-FAT10 alone (left panel), HA-FAT10 and FLAG-HDAC6 together (center panel) or FLAG-HDAC6 alone (right panel) were pulse labeled with (^{35}S)-methionine and chased for the indicated times. Cell lysates were subjected to anti-HA and anti-FLAG immunoprecipitation followed by SDS-PAGE and autoradiography.

ubiquitylated misfolded proteins (Boyault et al., 2006), we decided to investigate whether overexpression of HDAC6 had an effect on the rate of FAT10 degradation. We performed pulse-chase assays with FAT10 in the presence or absence of HDAC6, however, as can be seen in 18C, coexpression of HDAC6 did not affect the degradation of FAT10.

HDAC6 binds FAT10 via the zinc finger (BUZ) and the first catalytic domain (CAT1)

To identify additional FAT10-binding domains of HDAC6, we performed co-immunoprecipitation experiments with truncation mutants of HDAC6. To this aim, cells were transfected with FAT10 and each of the HDAC6 mutants depicted

in figure 19B and treated with proteasome inhibitor. In these experiments, we were able to identify the first deacetylase (CAT1) domain of HDAC6 as a second domain responsible for interacting with FAT10. Interestingly, this is not the domain which exhibits α-tubulin deacetylase activity (Haggarty et al., 2003). Both the isolated BUZ as well as the CAT1 domain were able to associate with FAT10 after proteasome inhibition, but not as strongly as the full length protein. However, the longer proteins which lack only the N-terminal (ΔN) or C-terminal (ΔBUZ) domain were able to precipitate amounts of FAT10 which were comparable to those pulled down by wild-type HDAC6. The 1-503 mutant showed weak interaction with FAT10 only in some of the experiments performed, while the 1-840 mutant was never able to bind FAT10, which might be explained by incorrect folding or the formation of multimers which could result in blockage of the FAT10 binding site.

To confirm the results obtained in cell lines in an *in vitro* setting, we performed a GST-pulldown assay using recombinant GST-FAT10 and *in vitro* transcribed and translated [^{35}S]-methionine labeled HDAC6. As shown in figure 20A, only GST-FAT10, but not GST alone, was able to pull down the CAT1 and the BUZ domain as well as full length HDAC6. Both of the isolated domains showed robust interaction with FAT10, while the isolated BUZ domain only interacted weakly in the co-immunoprecipitation experiments. *In vitro* as well as in intact cells, the full length protein displayed the highest affinity for FAT10. Taken together, these results demonstrate that both the BUZ as well as the CAT1 domain are sufficient to bind FAT10 on their own, but do so much more efficiently in the context of the full length protein.

Binding of FAT10 to HDAC6 is not mediated through its C-terminal diglycine motif

Previous studies have suggested the interaction between HDAC6 and ubiquitin to be largely mediated by its free C-terminal diglycine (Pai et al., 2007; Reyes-Turcu et al., 2006), therefore we decided to investigate whether the C-terminal diglycine motif of FAT10 was required for its interaction with HDAC6. As demonstrated in figure 20C, both wild-type FAT10 as well as a mutant lacking the C-terminal diglycine were able to pull down comparable amounts of radiolabeled HDAC6. Further evidence that its C-terminal diglycine is not required comes from experiments in which a linear fusion of FAT10 to GFP was transiently transfected into HEK293T cells. In this fusion protein, the two C-terminal glycines of FAT10 were exchanged for alanine and valine (AV), yet it was still able to localize to aggresomes (Fig. 23A) and could still be coprecipitated with HDAC6 (Fig. 26A).

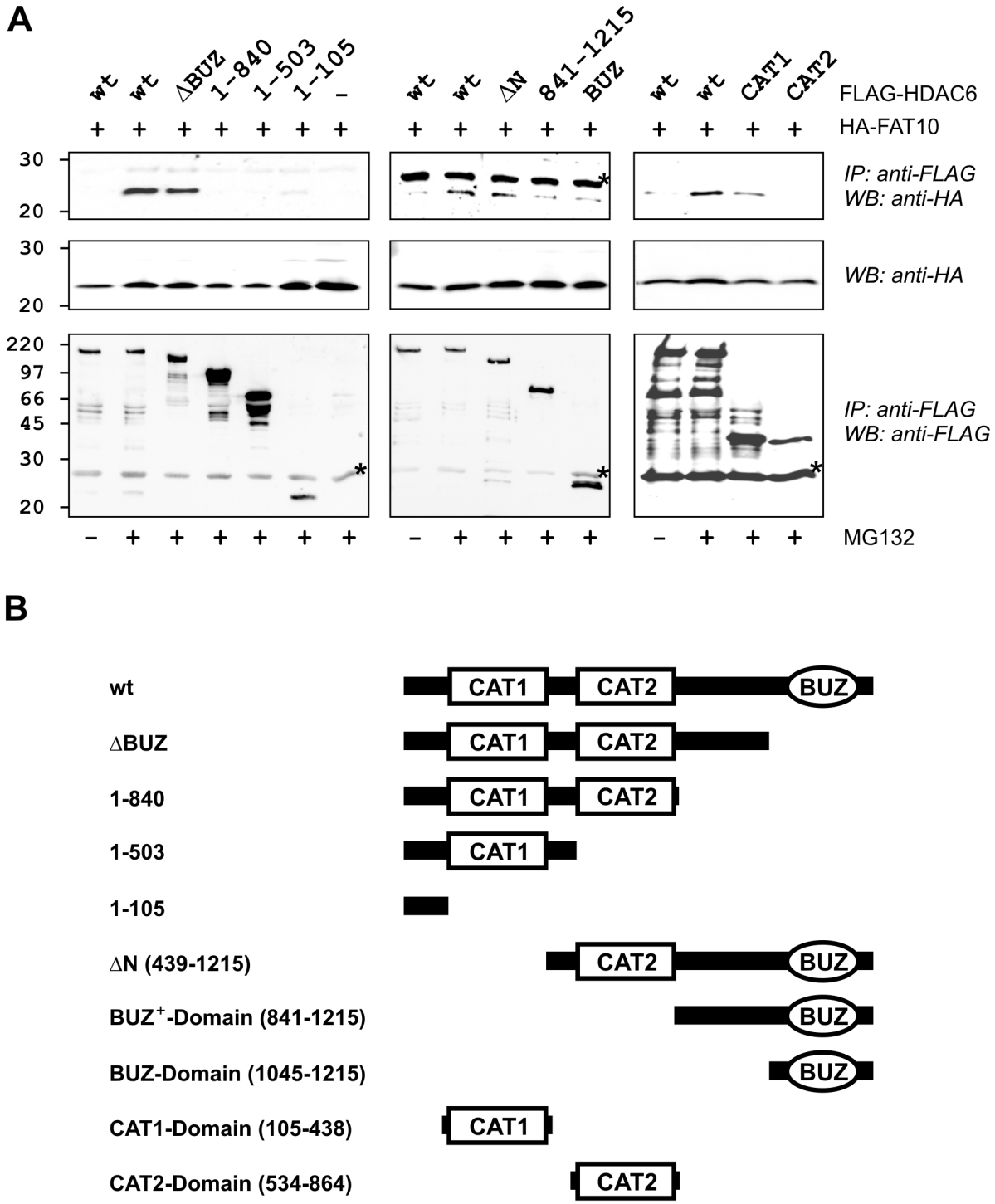

Figure 19: Both the BUZ domain and the first catalytic domain (CAT1) of HDAC6 are able to bind FAT10. (A) HEK293T cells, transfected with HA-FAT10 and the indicated FLAG-HDAC6 mutants, were treated with 5μM MG132 or DMSO as a negative control for 6 hours. Cell lysates were subjected to anti-FLAG immunoprecipitation (IP) and analysis by Western blot (WB). Asterisks denote the position of antibody light chains. **(B)** Schematic representation of the mutants used in A. CAT1 = first catalytic domain, CAT2 = second catalytic doman, BUZ = ubiquitin binding zinc finger.

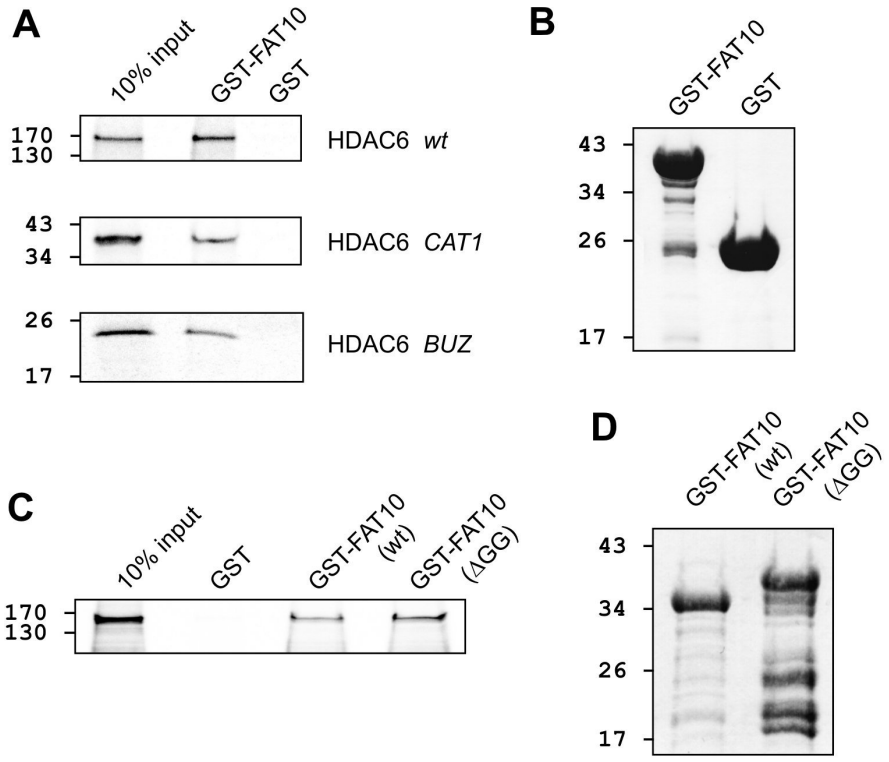

Figure 20: Both full length HDAC6 as well as the isolated CAT1 and BUZ domains interact with FAT10 *in vitro*. The diglycine motif of FAT10 is not required for its interaction with HDAC6. (A) GST-pulldown of (^{35}S)-methionine labeled *in vitro* transcibed and translated HDAC6 mutants with recombinant FAT10. Bound proteins were analyzed by SDS-PAGE and autoradiography. CAT1 = first catalytic domain, BUZ = ubiquitin binding zinc finger. **(B)** Coomassie-staining of the recombinant proteins used in A. **(C)** GST-pulldown of (^{35}S)-methionine labeled HDAC6 with recombinant wild-type FAT10 or FAT10 lacking the C-terminal diglycine motif (ΔGG). **(D)** Coomassie-staining of recombinant FAT10 used in C.

The catalytic activity of HDAC6 is not required for interaction with FAT10

The role of the deacetylase activity of HDAC6 in aggresome formation remains somewhat mysterious. On one hand, reintroduction of either the ΔBUZ or a catalytically inactive mutant into HDAC6 knock-down cells resulted in little to no rescue of aggresome formation. On the other hand, formation of ubiquitin-free aggresomes, which appear after expression of the aggregation-prone GFP chimera GFP-250, which is not ubituitylated (Garcia-Mata et al., 1999), does not seem to require HDAC6 at all (Kawaguchi et al., 2003). Then again, the inhibition of tubulin deacetylase activity has a profound effect on the transport of LC3, a component of the autophagy apparatus, to the aggresome, but affects the transport of polyubiquitylated misfolded huntingtin to a much lesser extent (Iwata et al., 2005). We therefore decided to investigate whether the catalytic activity

of HDAC6 was required for its interaction with FAT10. In fact, this turned out not to be the case. A catalytically dead mutant, in which the deacetylase activity was inactivated by two point mutations in the active sites, interacted with FAT10 just as well as the catalytically active wild-type HDAC6 (Fig. 21A). Treatment of cells with the broad-spectrum deacetylase inhibitor trichostatin A even lead to an increased association of HDAC6 with FAT10, which could already be observed in the absence of proteasome inhibition (compare Fig. 21B lanes 1 and 2 vs. 5 and 6). To elucidate whether this increase was a direct effect of HDAC6 inhibition or a secondary consequence of inhibiting one or more of the many deacetylases also affected by TSA, we repeated the experiment using the HDAC6 specific tubulin deacetylase inhibitor tubacin (Haggarty et al., 2003). Treatment of cells with tubacin had hardly any effect on the association of FAT10 with HDAC6 although it markedly increased the level of acetylated α-tubulin (Fig. 21C). The addition of neither inhibitor affected HDAC6-FAT10 interaction in *in vitro* pull-down experiments (Fig. 28), suggesting that the inhibition of catalytic activity has no influence on the binding capacity of HDAC6 for FAT10. We therefore conclude that the deacetylase activity of HDAC6 is dispensable for its interaction with FAT10.

FAT10 is acetylated, but acetylation is not required for interaction with HDAC6

The findings that (1) HDAC6 interacts with FAT10 through one of its catalytic domains, that (2) treatment with trichostatin A slightly increases the interaction between the two proteins and that (3) two-dimensional gel electrophoresis of FAT10 reveals several closely migrating bands with a similar molecular weight but distinct isoelectric points (Raasi et al., 2001) collectively raise the question if FAT10 is acetylated and whether this might be a prerequisite for its interaction with HDAC6. To address this question, we investigated whether immunoprecipitated FAT10 showed reactivity with an antibody against acetylated lysine. As can be seen in Fig. 29A, FAT10 can indeed be acetylated, although this is in all likelihood not a very dynamic process, as treatment of cells with trichostatin A for 6 hours did not change the level of FAT10 acetylation. In addition, FAT10 does not appear to be a substrate of HDAC6 either, since FAT10 exhibited similar levels of acetylation when expressed in the presence or absence of HDAC6 (Fig. 29B). The degree of FAT10 acetylation is estimated to be low as judged from 2D gels (Raasi et al., 2001) and since exposure times for the anti-acetylated lysine Western blots (Figs. 21E and 29) were at least 10-fold longer than for the anti-HA blots. In fact, the pool of FAT10 which interacted with HDAC6 after proteasome inhibition did not appear to be acetylated at all, as indicated by the complete absence of anti-acetyl-lysine reactivity of the FAT10 which co-

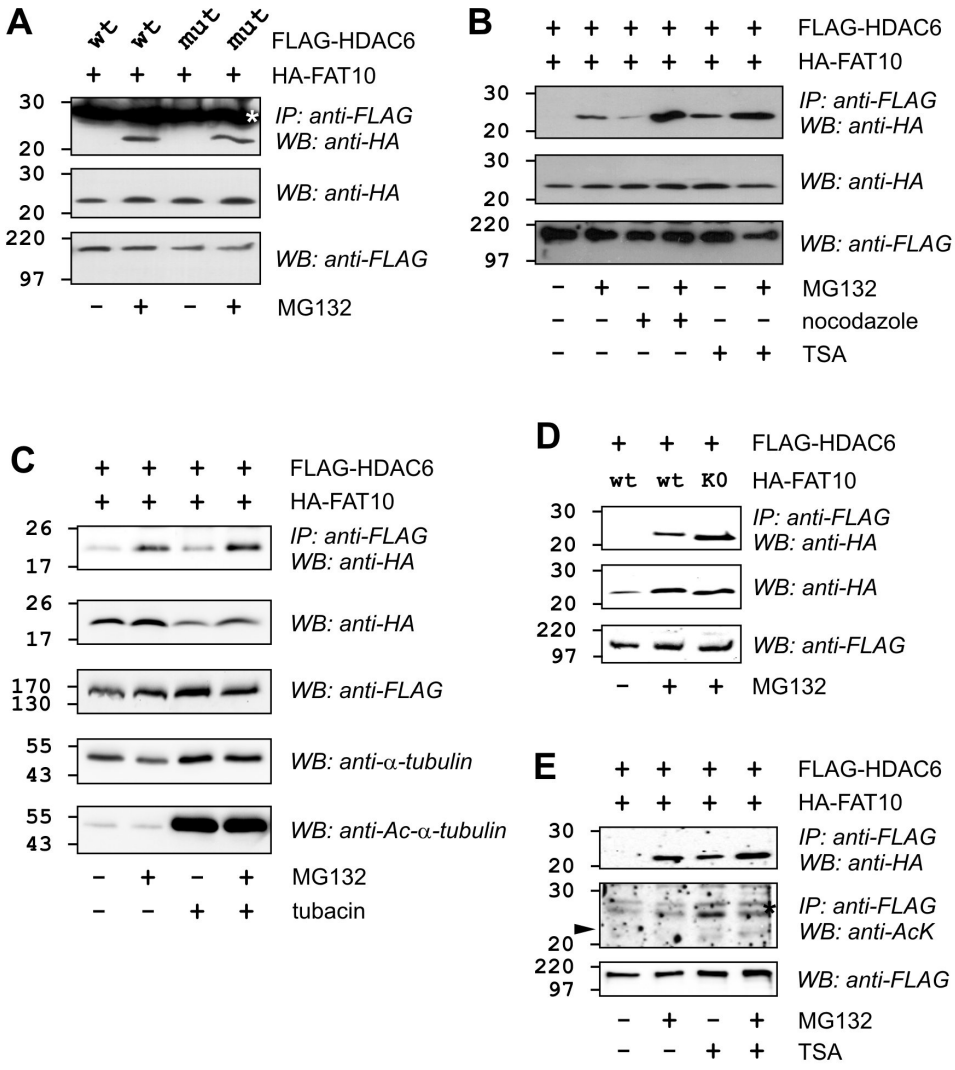

Figure 21: Neither acetylation of FAT10, nor catalytic activity of HDAC6 are required for interaction between the two proteins. (A) HEK293T cells transfected with HA-FAT10 and either wild-type (wt) FLAG-HDAC6 or a catalytically dead mutant (mut) were treated with 5μM MG132 or DMSO as a negative control for 6 hours before lysis, anti-FLAG immunoprecipitation (IP) and analysis by Western blot (WB). **(B)** HEK293T cells transfected with HA-FAT10 and FLAG-HDAC6 were treated with 5μM MG132, 1μM nocodazole, 5μM of the HDAC inhibitor trichostatin A (TSA) or mock treated for 6 hours before lysis, anti-FLAG immunoprecipitation (IP) and analysis by Western blot (WB). **(C)** HEK293T cells transfected with HA-FAT10 and FLAG-HDAC6 were treated with 5μM MG132, 20μM tubacin or mock treated for 6 hours before lysis, anti-FLAG immunoprecipitation (IP) and analysis by Western blot (WB). **(D)** HEK293T cells, transfected with FLAG-HDAC6 and either wild-type (wt) or a lysine-less HA-FAT10 mutant (K0), were treated with 5μM MG132 or DMSO for 6 hours before lysis, anti-FLAG immunoprecipitation (IP) and analysis by Western blot (WB). **(E)** HEK293T cells transfected with HA-FAT10 and FLAG-HDAC6 were treated with 5μM MG132, 5μM TSA or mock treated for 6 hours before lysis, anti-FLAG immunoprecipitation (IP) and analysis by Western blot (WB) with an acetyl-Lysine antibody (AcK). An asterisk denotes the position of the antibody light chain, an arrow the position of HA-FAT10 on the anti-AcK Western blot.

precipitates with HDAC6 (Fig. 21E). Moreover, a mutant of FAT10 in which all lysines were mutated to arginine (Hipp et al., 2005) – thus preventing it from being ubiquitylated or acetylated – was still able to interact with HDAC6 as well as, if not better than, wild-type FAT10 (Fig. 21D). Still, the ability of catalytically dead or inhibited HDAC6 to interact with FAT10 might solely be mediated through the C-terminal BUZ domain. To exclude this possibility, we performed co-immunoprecipitation experiments with an isolated, catalytically dead CAT1 domain. As can be seen in figure 27A, the mutated CAT1 domain was still able to pull down FAT10. In addition, the isolated CAT1 domain was still capable of interacting with the lysine-less mutant of FAT10. Figure 27B demonstrates that recombinant GST-FAT10 was able to pull down similar amounts of the wild-type and mutated *in vitro* transcribed and translated [^{35}S]-methionine labeled CAT1 domains. Together, these findings suggest that, while a small portion of the intracellular FAT10 is acetylated, acetylation is not required for its binding to HDAC6 nor is FAT10 a substrate of HDAC6 deacetylase activity.

FAT10 and FAT10-GFP localize to the aggresome after proteasome inhibition

As FAT10 interacts with HDAC6 after proteasome inhibition, and as HDAC6 is involved in the transport of polyubiquitylated proteins to the aggresome upon proteasome impairment (Kawaguchi et al., 2003), we investigated whether HDAC6 may likewise transport FAT10 to the aggresome. To test this hypothesis, we investigated whether treatment of transiently HA-FAT10-tranfected HEK293T cells with proteasome inhibitor had an influence on the subcellular localization of FAT10 as analyzed by confocal immunofluorescence microscopy. In untreated cells, FAT10 was evenly distributed throughout the cytoplasm and showed varying degrees of localization to the nucleus (Fig. 22A, a and i). HDAC6, on the other hand, was completely excluded from the nucleus and showed only cytoplasmatic localization (Fig. 22A, b). As reported by Kawaguchi et al., proteasome inhibition induced relocalization of HDAC6 to a single prominent juxtanuclear structure – and indeed also caused FAT10 to localize to the very same structure (Fig. 22A, e-h). To determine the identity of the observed inclusion bodies, we analyzed them for the presence of known aggresome markers other than HDAC6. We never observed formation of more than one of these inclusion bodies per cell, and combined with the observation that they colocalizd with γ-tubulin (Fig. 22A, m-p), a component of centromeres, this leads us to infer that they form at the microtubule organizing center. In addition, we observed a characteristic distortion and enlargement of the centromeres upon proteasome inhibition (compare Fig. 22A, j and n), which is another hallmark of aggresome formation (Johnston

et al., 1998). The colocalization with ubiquitin conjugates (Fig. 22A, q-t) and 20S proteasome (Fig. 22A, u-x) further substantiates the evidence that the observed inclusion bodies are indeed bona fide aggresomes.

To exclude the possibility that the localization of FAT10 to aggresomes is only an artefact of overexpression, we treated cells with TNF-α and IFN-γ to induce expression of FAT10 and examined whether the endogenous protein behaved similarly to the overexpressed version. The localization of both exogenous and cytokine-induced FAT10 in cells not treated with proteasome inhibitor was absolutely identical (compare Fig. 22A, a and Fig. 22B, a), and while the aggresomes formed in the absence of overexpression tended to be smaller, there is no question that endogenously expressed FAT10 also localized to aggresomes (Fig. 22B, e-h).

Since HEK293T cells produce extremely low levels of FAT10 conjugates (Hipp et al., 2005; Chiu et al., 2007), we assume the FAT10 observed in figure 22 to be mostly monomeric. To investigate whether FAT10 linked proteins are also transported to the aggresome, we transfected cells with our model conjugate – a linear, N-terminal fusion of FAT10 to GFP. This model conjugate is rapidly degraded by the proteasome (Hipp et al., 2005) and, as shown in figure 23A, m-p, also localized to the aggresome after proteasome inhibition. In fact, cells transfected with wild-type GFP did form aggresomes under proteasome inhibition, but these did not contain GFP (Fig. 23A, e-h), suggesting that FAT10mediated targeting to the aggresome is specific and not an artefact of protein overexpression in the face of proteasome inhibition. Quantification of three independent experiments revealed a statistically significant increase in the formation of GFP-containing aggresomes only after proteasome inhibition and transfection with FAT10-GFP but not GFP alone (Fig. 23B). Taken together, these data provide compelling evidence for a specific localization of FAT10 to the aggresome after proteasome inhibition.

Transport of FAT10 to aggresomes depends on an intact microtubule network

To test whether FAT10 also relies on the tubulin network for transport to aggresomes, we treated cells with the microtubule depolymerizing agent nocodazole in addition to proteasome inhibitors and observed the effect this had on the localization of FAT10. In accordance with the central role of retrograde microtubule-dependent transport in the formation of aggresomes (Kopito, 2000), depolymerization of microtubules also lead to the disruption of FAT10 containing aggresomes.

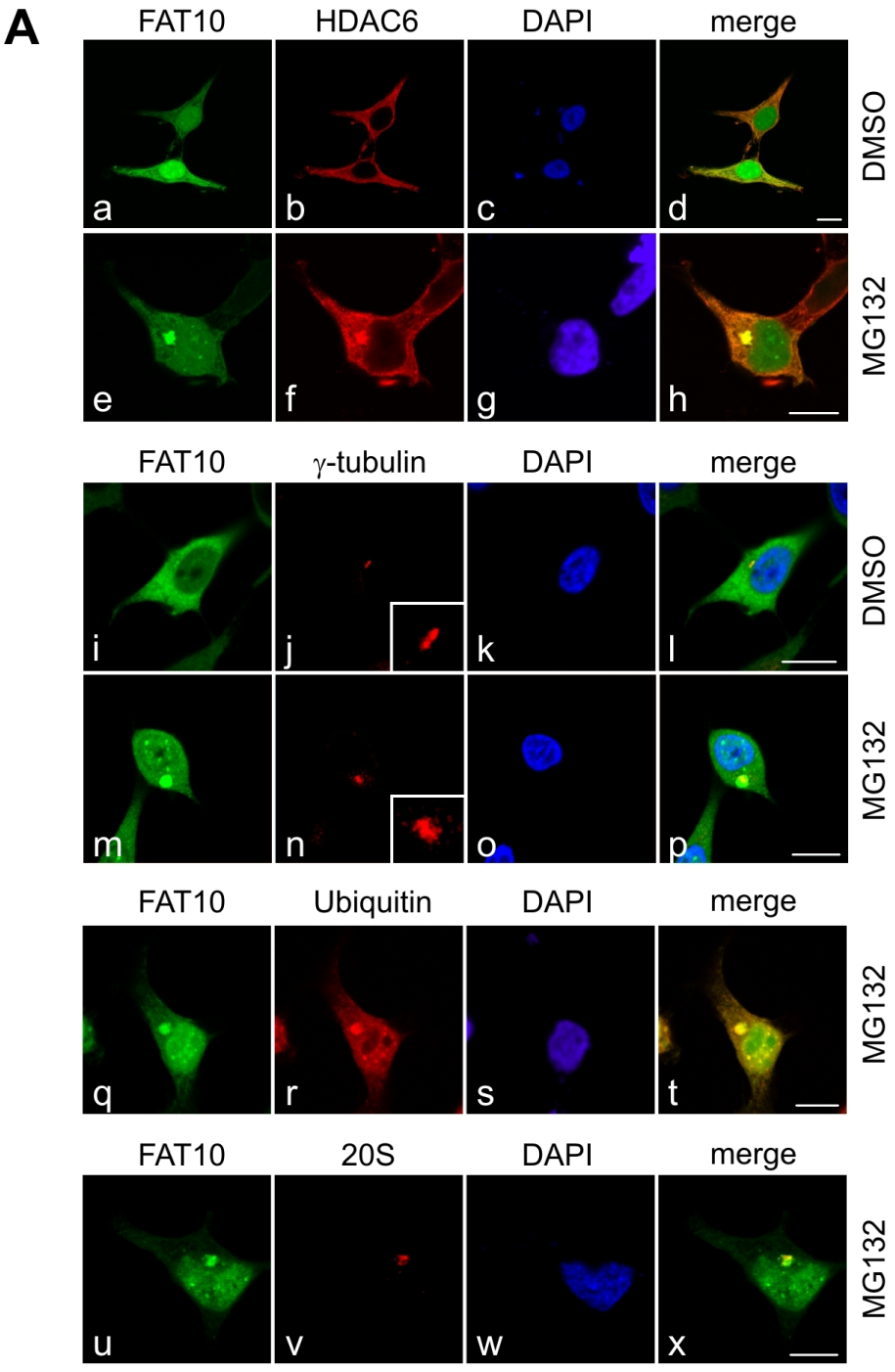
A
FAT10
HDAC6
DAPI
merge
DMSO
MG132
FAT10
γ-tubulin
DAPI
merge
DMSO
MG132
FAT10
Ubiquitin
DAPI
merge
MG132
FAT10
20S
DAPI
merge
MG132

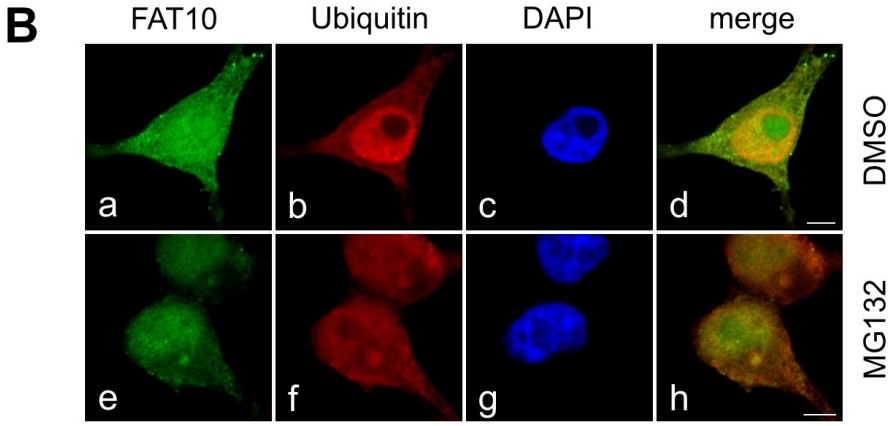

Figure 22: FAT10 localizes to aggresomes under proteasome inhibition. (A) HEK293T cells transiently transfected with HA-FAT10 and FLAG-HDAC6 were treated with 5μM MG132 or DMSO as a negative control for 6 hours and immunostained with antibodies for HA (green), FLAG (red) and DAPI (blue; a-h). HEK293T cells transfected with HA-FAT10 were treated with 5μM MG132 or DMSO for 6 hours and immunostained with anti-HA (green), DAPI (blue) and anti-γ-tubulin (red; i-p), anti-Ubiquitin (red; q-t) or anti-20S proteasome (red; u-x). **(B)** HEK293T cells treated with TNF-α and IFN-γ for 16 hours were incubated in the presence of 5μM MG132 or DMSO for an additional 6 hours and immunostained with antibodies against endogenous FAT10 (green), Ubiquitin (red) and DAPI (blue). Scale bars = 5μm.

Instead of localizing to one prominent juxtanuclear aggresome upon proteasome inhibition (Fig. 24A, d-f), FAT10 accumulated under nocodazole treatment in several microaggregates which were evenly dispersed throughout the cytoplasm (Fig. 24A, g-i).

Since catalytic activity of HDAC6 is required for the transport of polyubiquitylated proteins to the aggresome (Kawaguchi et al., 2003), but is dispensable for the interaction with FAT10 (Fig. 24 and 28), we set out to investigate the effect of the HDAC6 specific inhibitor tubacin (Haggarty et al., 2003) on the formation of FAT10 containing aggresomes. Unfortunately though, we were not able to draw many conclusions regarding the formation of aggresomes from this experiment, since the combination of tubacin and MG132 lead to profound cell death in FAT10 transfected cells already a few hours after treatment. Up until that point, however, the formation of aggresomes appeared to be comparable between cells treated with tubacin or the inactive control compound niltubacin (data not shown). Thus it is clear that the transport of FAT10 to the aggresome requires a functional microtubule network, but the question whether it also requires the deacetylase function of HDAC6 remains unsolved.

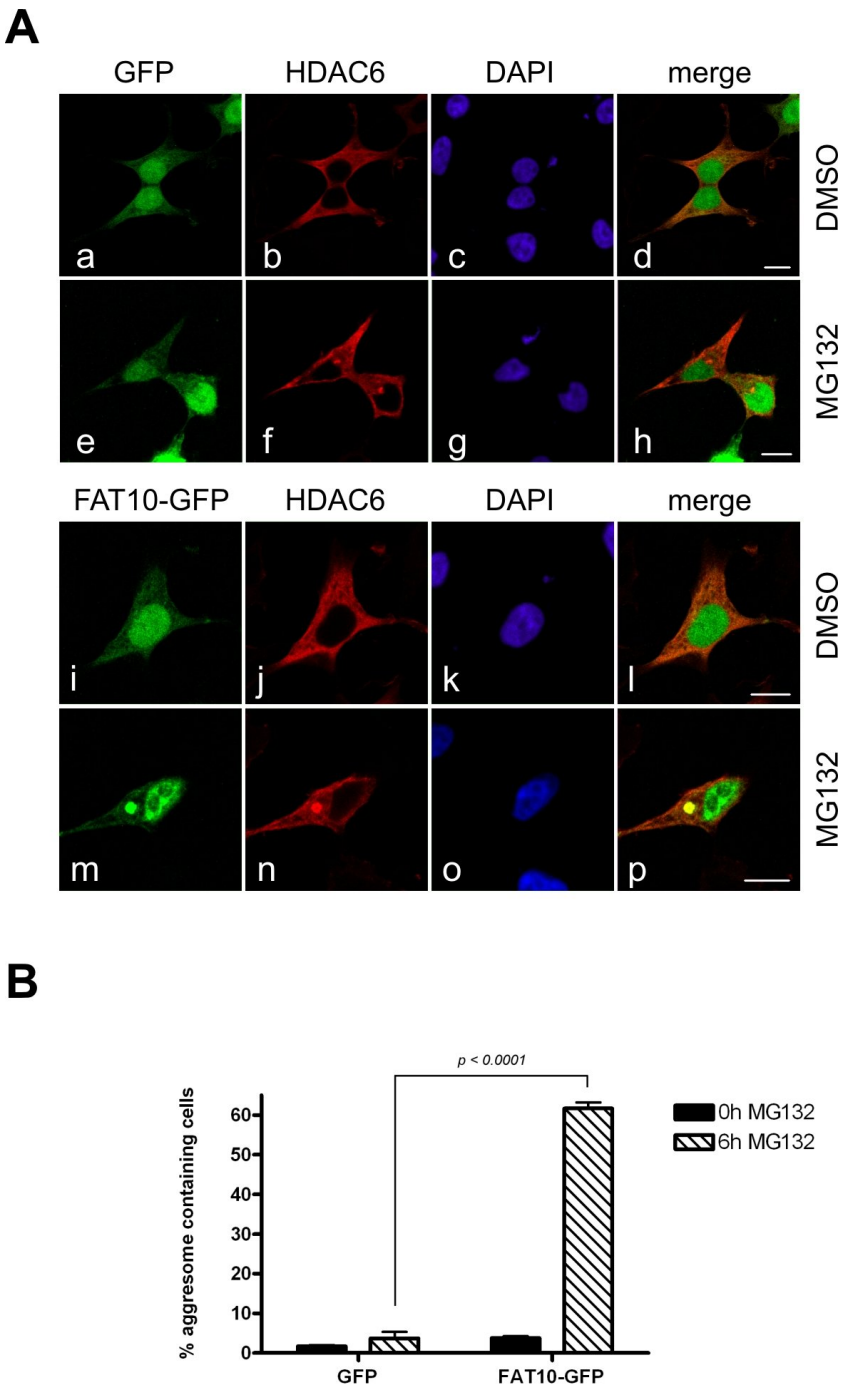

Figure 23: The model conjugate FAT10-GFP localizes to aggresomes under proteasome inhibition. (A) HEK293T cells transfected with FLAG-HDAC6, GFP or FAT10-GFP were treated with 5μM MG132 or DMSO for 6 hours and immunostained with anti-GFP antibody (green), anti-FLAG antibody (red) and DAPI (blue). Scale bars = 5μm. **(B)** Quantification of percentage of cells with GFP containing aggresomes, n $\geq$ 100. Error bars represent the standard error of the mean (s.e.m.), statistical analysis was carried out using Student's *t* test.

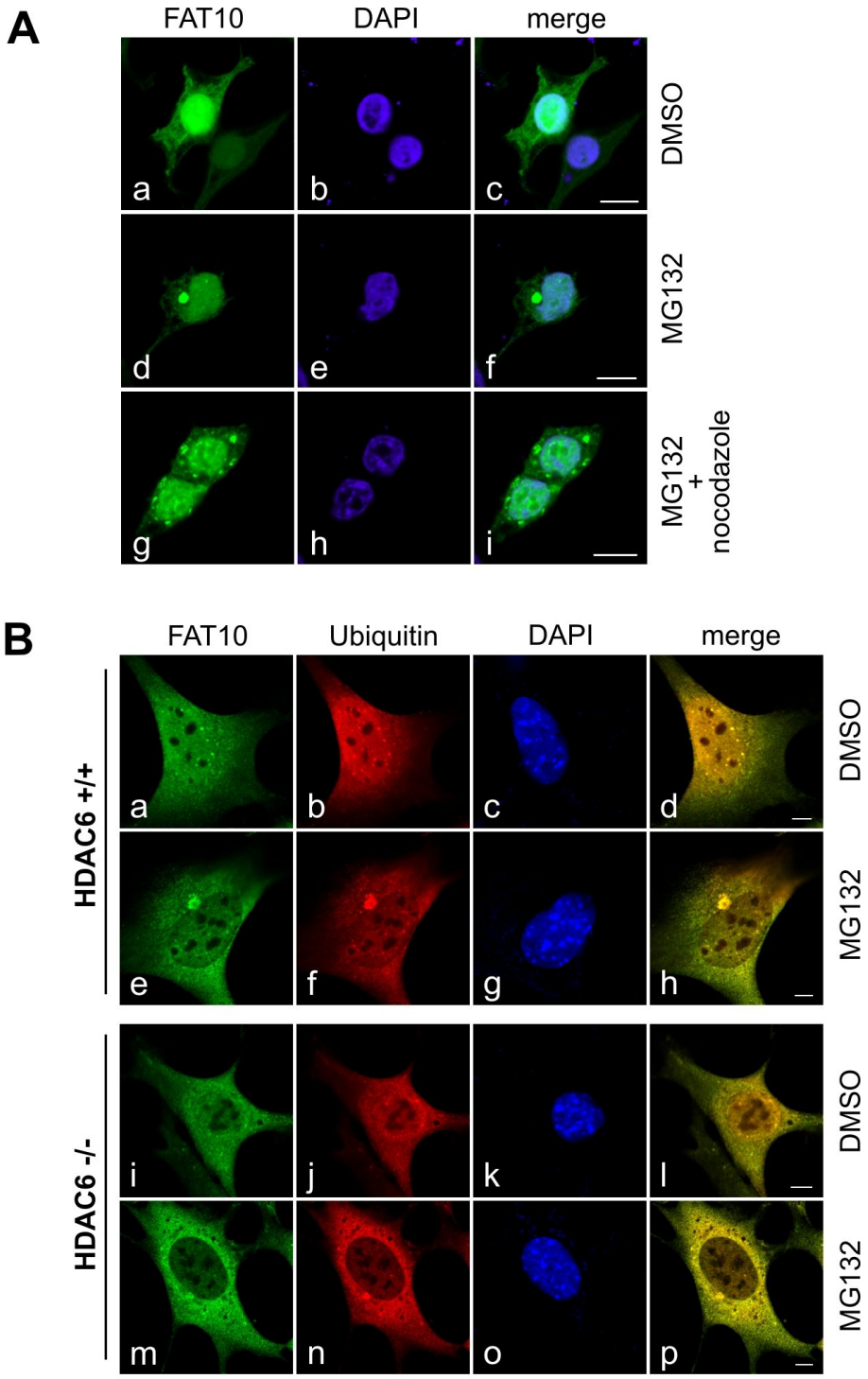

Figure 24: Localization of FAT10 to aggresomes is dependent on the tubulin network and on HDAC6. (A) HEK293T cells transfected with HA-FAT10 were treated with 5μM MG132, 1μM nocodazole or mock treated for 6 hours and immunostained with anti-HA antibody (green) and DAPI (blue). Scale bars = 5μm. **(B)** HDAC6 wild-type (a-h) or knock-out (i-p) cells were transiently transfected with HA-FAT10 followed by treatment with 5μM MG132 or DMSO for 4 hours and immunostained with anti-HA antibody (green), anti-Ubiquitin antibody (red) and DAPI (blue). Scale bars = 5μm.

HDAC6 is required for the proper formation of FAT10-containing aggresomes

To assay whether HDAC6 is essential for the localization of FAT10 to the aggresome, we set out to investigate the formation of aggresomes and subcellular localization of FAT10 in cells derived from mice lacking the *hdac6* gene (Zhang et al., 2008b). Cells stably expressing an siRNA directed against HDAC6 have previously been shown to be defective in the formation of polyubiquitin-containing aggresomes. After inhibition of the proteasome, in comparison to wild-type cells, fewer of these cells contained aggresomes and those aggresomes which did form were smaller in size (Kawaguchi et al., 2003). Our experiments revealed HDAC6-deficient cells to have a similar phenotype. When treated with 5 μM of the proteasome inhibitor MG132 for 4 hours, HDAC6 knock-out cells were still able to form polyubiquitin-containing aggresomes (Fig. 24B). However, fewer cells (approximately 40% less) contained an aggresome in comparison to HDAC6 wild-type cells (Fig. 25B) and the aggresomes which still formed were significantly smaller in size (Fig. 25C). In those cells which were transiently transfected with HA-FAT10, the subcellular localization – including the localization to aggresomes – of FAT10 mirrored that of polyubiquitin (compare Figs. 24B h and p). The quantification of aggresome size as determined by anti-HA immunofluorescence also revealed HDAC6 knock-out cells to have significantly smaller FAT10-containing aggresomes (Fig. 25D). As cells lacking HDAC6 are partially deficient in the formation of FAT10- as well as polyubiquitin-containing aggresomes, HDAC6 certainly plays an important role in their formation, even though it does not appear to be essential for the transport of neither polyubiquitin nor FAT10 to the aggresome or the formation of aggresomes in general.

Both ubiquitin-like domains of FAT10 interact with HDAC6 and localize to aggresomes under proteasome inhibition

Since the isolated ubiquitin-like domains of FAT10 exhibit differences in their ability to be degraded by the 26S proteasome and to interact with NEDD8 ultimate buster 1 long (Schmidtke et al., 2006), we decided to examine whether there were also differences in their ability to bind to HDAC6 or to localize to aggresomes. To investigate the interaction with HDAC6, we performed co-immunoprecipitation experiments similar to the ones described above, only this time we used wild-type HDAC6 and N-terminal fusions of either full length FAT10 or the isolated N- and C-terminal ubiquitin-like domains of FAT10 with GFP. We found that GFP-fusions with both the N- or C-terminal domain of FAT10 as well as full length FAT10 were able to interact with HDAC6 under proteasome inhibition (Fig. 26A). In addition, immunofluorescence studies revealed that both

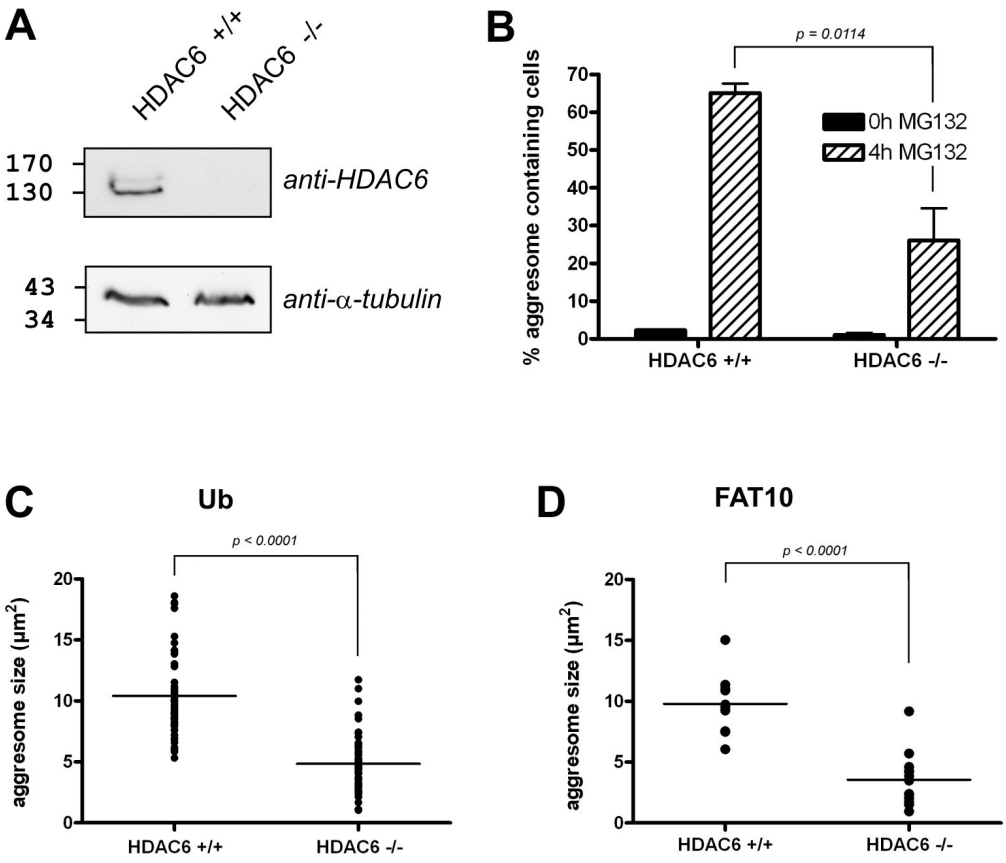

Figure 25: HDAC6-deficient cells have defects in aggresome formation. (A) Verification of HDAC6 knock-out by Western blot. **(B)** Quantification of the percentage of cells with ubiquitin containing aggresomes, n $\geq$ 100. **(C)** Quantitative evaluation of the size of ubiquitin containing aggresomes, n $\geq$ 50. **(D)** Quantitative evaluation of the size of FAT10 containing aggresomes, n $\geq$ 10. Error bars represent the standard error of the mean (s.e.m.), statistical analysis was carried out using Student's *t* test.

domains localized to aggresomes under proteasome inhibition (Fig. 26B). We can therefore conclude that each ubiquitin-like domain of FAT10 is sufficient to interact with HDAC6 and mediate localization to the aggresome.

Discussion

FAT10 is unique among the family of ubiquitin-like proteins as it is the only member – aside from ubiquitin – which can lead conjugated proteins directly to proteasomal degradation. Here we report the discovery of a third non-covalent interaction partner of FAT10, the cytosolic deacetylase HDAC6. HDAC6 has a binding domain for ubiquitin-like proteins in its C-terminus which belongs to the family of 'ubiquitin carboxyl-terminal hydrolase-like zinc finger' (Znf-UBP) do-

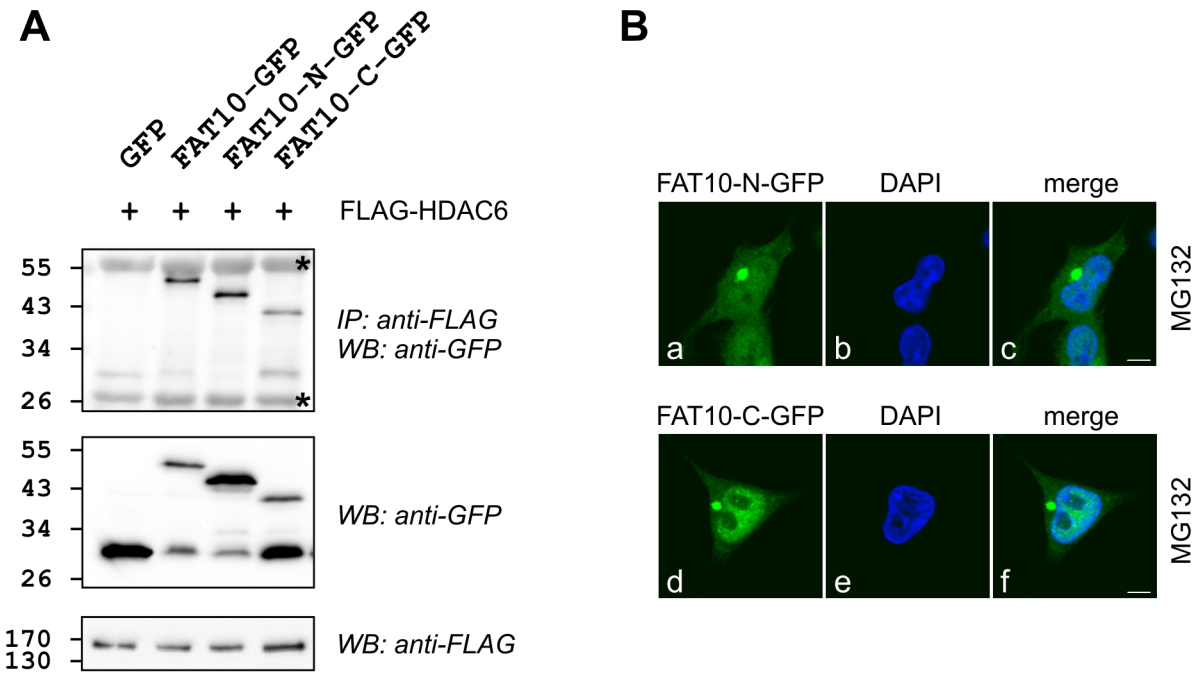

Figure 26: Both ubiquitin-like domains of FAT10 interact with HDAC6 and localize to aggresomes under proteasome inhibition. (A) HEK293T cells transfected with FLAG-HDAC6 and the indicated GFP-fusions were treated with 5μM MG132 for 6 hours before lysis, anti-FLAG immunoprecipitation (IP) and analysis by Western blot (WB). **(B)** HEK293T cells transfected with either the N-terminal (a-c) or C-terminal (d-f) domain of FAT10 fused to GFP were treated with 5μM MG132 for 6 hours and immunostained with anti-GFP antibody (green) and DAPI (blue). Scale bars = 5μm.

mains, also known as either 'deacetylase/ubiquitin-specific protease' (DAUP) domain, 'polyubiquitin-associated zinc finger' (PAZ) domain, or 'binder of ubiquitin zinc finger' (BUZ) domain.

Since NUB1L leads to an accelerated degradation of FAT10 (Hipp et al., 2004) and HDAC6 has been shown to be involved in the turnover of polyubiquitylated proteins (Kawaguchi et al., 2003; Boyault et al., 2006), we investigated whether the overexpression of HDAC6 would have an effect on the rate of FAT10 degradation – but this turned out not to be the case (Fig. 18C). We were able to obtain evidence that FAT10 is acetylated (Fig. 29), which may in part account for the isoelectric variants observed for FAT10 on two-dimensional gels (Raasi et al., 2001). However, the degree of acetylation was neither affected by the overexpression of HDAC6 nor by treatment of cells with the broad range deacetylase inhibitor trichostatin A (TSA), suggesting that the acetylation of FAT10 is not under dynamic regulation and that FAT10 is not a deacetylation substrate of HDAC6. Acetylation of FAT10 was also not required for the interaction with HDAC6 as (1) neither mutation of the active sites of HDAC6 nor treatment with TSA or tubacin abol-

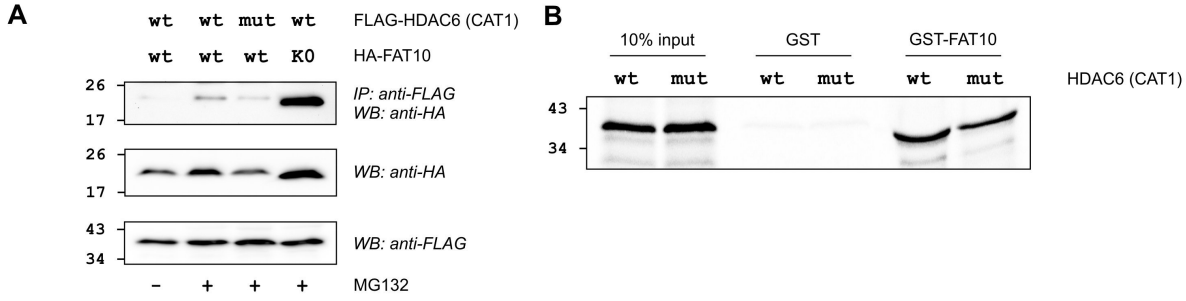

Figure 27: Neither acetylation of FAT10 nor catalytic activity of the CAT1 domain are required for its interaction with FAT10. (A) HEK293T cells were transfected with either catalytically active (wt) or inactive (mut) FLAG-CAT1 together with either wild-type or lysine-less (K0) HA-FAT10, followed by treatment with 5μM MG132 or DMSO for 6 h. Cell lysated were subjected to anti-FLAG immunoprecipitation and subsequent analysis by Western blot (WB). **(B)** GST-pulldown of an (^{35}S)-methionine labeled *in vitro* transcibed and translated active (wt) or inactive (mut) CAT1 domain by recombinant GST-FAT10.

ished FAT10 binding (Fig. 21A-C), as (2) the mutation of all lysine residues of FAT10 did not alter its association with HDAC6 (Fig. 21D), and as (3) acetylated FAT10 did not preferentially associate with HDAC6 (Fig. 21E).

Much more revealing were our experiments investigating the hypothesis that HDAC6 might also shuttle FAT10 to the aggresome in situations of misfolded protein stress or proteasome inhibition (Johnston et al., 1998; Kawaguchi et al., 2003). Indeed, proteasome inhibition lead to the accumulation of FAT10 or FAT10-linked GFP in a single, large juxtanuclear inclusion body. Compelling evidence has been collected that this inclusion body is an aggresome: firstly, FAT10 colocalized in this structure with typical constituent proteins of aggresomes such as HDAC6, γ-tubulin, polyubiquitin, and the proteasome (Fig. 21). Secondly, FAT10 localized to this inclusion body only when the proteasome was inhibited, and did so with a kinetic similar to the one reported for aggresome formation (Garcia-Mata et al., 1999, Fig. 22 and data not shown). Thirdly, the presence of an intact microtubule network, which is essential for the formation of aggresomes, was also required as treatment of cells with the microtubule depolymerizing agent nocodazole in addition to proteasome inhibition resulted in the formation of multiple FAT10 containing microaggregates in the cytosol (Fig. 24A). Evidence that the transport of FAT10 to aggresomes is not merely an artifact of overexpression comes from experiments in which endogenous FAT10, which was physiologically induced with IFN-γ and TNF-α, displayed a localization similar to that of the transiently transfected protein (Fig. 22B). In addition, co-immunoprecipitation

also revealed endogenous, cytokine-induced FAT10 to be associated with HDAC6 (Fig. 18B).

The question whether transport of FAT10 to the aggresome is solely dependent on HDAC6 was adressed in cells derived from HDAC6-deficient mice. A previous study with cells stably expressing an shRNA directed against HDAC6 (Kawaguchi et al., 2003) revealed HDAC6 to be required for the proper formation of polyubiquitin-containing aggresomes, as HDAC6 knock-down cells contained fewer and smaller aggresomes as compared to wild-type cells. However, it was impossible to determine whether the residual formation of aggresomes was due to an incomplete knock-down of HDAC6 or a functional redundancy. Our experiments in cells lacking the *hdac6* gene now point toward the latter, as these cells display a similar phenotype (Fig. 24B, 25B and C). We were able to demonstrate the transport of FAT10 and polyubiquitin to the aggresome to be equally dependent on HDAC6; both FAT10- as well as polyubiquitin-containing aggresomes were significantly reduced in size in HDAC6-deficient compared to wild-type cells (Fig. 25C and D).

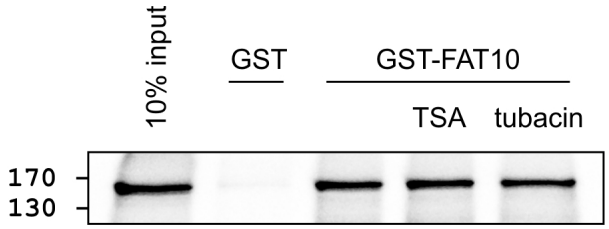

Figure 28: Inhibition of catalytic activity has no effect on the interaction between HDAC6 and FAT10 *in vitro* . GST-pulldown of (^{35}S)-methionine labeled *in vitro* transrcibed and translated HDAC6 with recombinant GST-FAT10 in the presence of 20μM TSA or 160μM tubacin.

The role of tubulin deacetylation in the transport of FAT10 to the aggresome however remains unclear. We attempted to investigate whether the deacetylase activity of HDAC6 was required for the transfer of FAT10 into aggresomes by using the HDAC6 specific inhibitor tubacin. Unfortunately, cells treated with proteasome inhibitor and tubacin at the same time did not survive long enough to investigate aggresome formation. We only can say for certain that the catalytic activity of HDAC6 is dispensable for its interaction with FAT10, as both inhibition as well as mutation of the active sites failed to abolish this interaction (Figs. 21 and 28). In fact, the association of HDAC6 with FAT10 was even increased after treatment of cells with the broad-spectrum deacetylase inhibitor TSA (Fig. 21B), which might be attributed to an increase in α-tubulin acetylation as well as non-specific effects

of TSA on other targets, especially as treatment of cells with tubacin has a much less pronounced effect (Fig. 21C).

The question arises why the interaction between HDAC6 and FAT10 can only be observed under proteasome inhibition. Boyault et al. have proposed a model in which HDAC6 senses an overload of polyubiquitylated proteins through the binding of polyubiquitin to its BUZ domain. This then results in the release of heat-shock factor 1 and HDAC6 from a complex also containing p97/VCP and HSP90 (Boyault et al., 2007). An alternative model (Pai et al., 2007) suggests that it is not the accumulation of polyubiquitylated proteins but rather the lack of unconjugated ubiquitin resulting from proteasome inhibition that facilitates the interaction of HDAC6 and polyubiquitin. Owing to a much higher affinity of the BUZ domain for the C-terminus of ubiquitin rather than for polyubiquitin-conjugates (Reyes-Turcu et al., 2006), the majority of HDAC6 would normally be bound to free ubiquitin. Under conditions of proteasome impairment, the decline in the level of monomeric ubiquitin releases HDAC6. In both models, HDACD6 would then be free to interact with polyubiquitin - and also FAT10-conjugates.

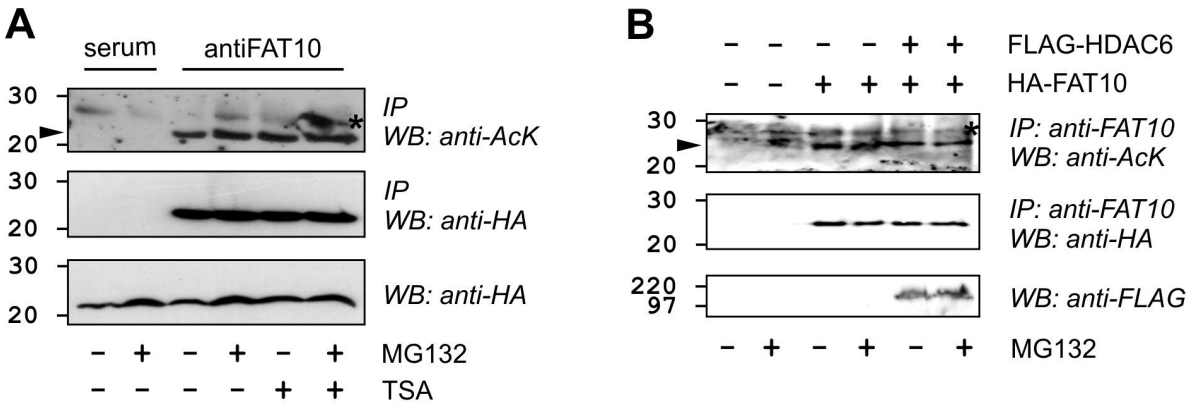

Figure 29: FAT10 is acetylated but does not appear to be a substrate of HDAC6-mediated deacetylation. (A) HEK293T cells transfected with HA-FAT10 were treated with 5μM MG132, 5μM TSA or mock treated for 6 h before lysis, immunoprecipitation (IP) with anti-FAT10 or control serum and subsequent analysis by Western blot (WB) with an acetyl-Lysine antibody (AcK). **(B)** HEK293T cells transfected with either HA-FAT10, FLAG-HDAC6 or empty vector were treated for 6 h with 5μM MG132 or DMSO before lysis, anti-FAT10 immunoprecipitation (IP) and analysis by Western blot (WB). Asterisks denote the position of antibody light chains, arrows the position of HA-FAT10 on the anti-AcK Western blots.

It is interesting that FAT10, which can target proteins for proteasomal degradation independently of the ubiquitin system, uses the same rescue strategy when the proteasome is overwhelmed. This implies that the rapid removal of FAT10

and/or its conjugates is essential for the cell, for example to protect it from the deleterious effects caused by an excess of free FAT10, which is suggested by the finding that the ectopic expression of FAT10 induces apoptosis in several cell types (Raasi et al., 2001; Ross et al., 2006).

The formation of ubiquitin-containing aggregates is a hallmark of many neurodegenerative diseases like Huntington's or Parkinson's disease (PD) and dementia with Lewy bodies (DLB). It is notable that NUB1L, another non-covalent interaction partner of FAT10 (Hipp et al., 2004), accumulates in Lewy bodies of PD and DLB (Tanji et al., 2007) and localizes to aggresomes under proteasome inhibition (data not shown). It will hence be interesting to investigate whether FAT10 is also a component of Lewy bodies and may even be responsible for targeting NUB1L to these sites. Since the basal expression of FAT10 in the brain is extremely low (Canaan et al., 2006), an involvement of FAT10 would rely on a strong induction of *fat10* expression with TNF-α and IFN-γ which is probably not prevalent in these chronic neurological disorders. Recently, FAT10 was shown to be highly upregulated in hepatocellular carcinoma (Lee et al., 2003), and in a drug induced mouse model of hepatocellular carcinoma FAT10 localized to Mallory-Denk bodies, which are a special form of aggresomes observed in a variety of liver diseases (Oliva et al., 2008; Zatloukal et al., 2007). On the other hand, the localization of the *fat10* gene in the major histocompatibility class I locus and the fact that it is inducible by proinflammatory cytokines point toward a function in the immune response. It remains subject to investigation whether FAT10 is perhaps involved in the formation of DALIS – which are transient aggresome like structures that function as storage compartments of antigenic proteins during the maturation of dendritic cells (Lelouard et al., 2002). In addition, as autophagy has been implicated in the innate as well as the adaptive immune response to intracellular pathogens, it is tempting to speculate whether FAT10 might be involved in those processes as well.

Materials and Methods

Tissue culture and transfection. Spontaneously immortalized HDAC6$^{+/+}$ and HDAC6$^{-/-}$ MEFs were generously provided by P. Matthias (Zhang et al., 2008b). MEFs and HEK293T cells were cultivated in DMEM supplemented with 10% FCS and 100 μg/ml penicillin/streptomycin (all from Invitrogen). HEK293T cells were transiently transfected using FuGENE 6 (Roche) according to the manufacturer's instructions. MEFs were transiently transfected using the Amaxa MEF2

Kit according to the manufacturer's instructions. For the induction of endogenous FAT10, cells were treated for 16-20 hours with 500 U/ml hTNF-α (Endogen) and 200 U/ml hIFN-γ (Endogen).

Yeast two-hybrid screen. The yeast two-hybrid screen was performed as previously described (Hipp et al., 2004).

Antibodies and reagents. The antibodies used in this study were anti-FLAG M2 (Sigma), anti-FLAG polyclonal (Sigma), anti-HA HA-7 (Sigma), anti-HA polyclonal (Sigma), anti-AcK 103 (Cell Signaling), anti-γ-tubulin GTU-88 (Sigma), anti-Ubiquitin FK2 (Biomol), anti-HC9/20S (Affinity), anti-HDAC6 polyclonal (Cell Signaling) and anti-GFP polyclonal (Sigma). The anti-FAT10 polyclonal antibody was generated as previously described (Hipp et al., 2005). Horse radish peroxidase coupled anti-HA HA-7 antibody was purchased from Sigma, anti-rabbit and anti-mouse antibodies from DAKO. The antibodies used in immunofluorescence, anti-HA 16B12, Alexa Fluor™ 488-coupled, goat anti-rabbit IgG (H+L), Alexa Fluor™ 488-coupled and goat anti-mouse IgG (H+L), Alexa Fluor™ 546-coupled were purchased from Molecular Probes. MG132, nocodazole and trichostatin A were purchased from Sigma.

Plasmids and generation of expression constructs. pcDNA3-FLAG-tagged wt, ΔBUZ, 1-840, 1-503 and ΔN HDAC6 as well as the catalytically dead mutant were a kind gift from T. P. Yao (Kawaguchi et al., 2003). The additional mutants were constructed by first inserting a FLAG-tag (5'-ATGGACTACAAGGACGACG ATGACAAG-3') between the KpnI and BamHI restriction sites of pcDNA3.1. The desired fragments of HDAC6 were then amplified by PCR using pcDNA3/FLAG-HDAC6 wt as a template and cloned into the vector via BamHI and XbaI restriction sites. The following primers were used for PCR: forward 5'-TAACGGATCCAC CTCAACCGGCCAGGATTC-3', reverse 5'-TAAGTCTAGATTAGAAGCTGTCAT CCCAGAGGCA-3' (1-105); forward 5'-TAACGGATCCTCTCCCAGTACACTGAT TGGG-3', reverse 5'-TAAGTCTAGATTAGTGTGGGTGGGGCATATCCTC-3' (BUZ); forward 5'-GTATGGATCCGACAGAGAAGGACCCTCCAG-3' (841-1215); forward 5'-TAACGGATCCCCGGAAGGCCCTGAGCGG-3', reverse 5'-TAACTCT AGATTAAAGAACCTCCCAGAAGGGCTCA-3' (CAT1); forward 5'-TCTAAGATC TGTACCCCAGCGCATCTTGC-3', reverse 5'-ACAGTCTAGATTATTCTACCTTC ATGACCCGTAAG-3' (CAT2). The catalytically inactive CAT1 domain was generated using the catalytically dead full-length protein as a template. All sequences were verified by dideoxy sequencing. pcDNA3.1/HA-FAT10 was generated as previously described (Raasi et al., 2001), as were pcDNA3.1/HA-FAT10 K0

(Hipp et al., 2005), pEGFP-N1/FAT10-AV-GFP and pGEX-4T-3/GST-FAT10 (Hipp et al., 2004), as well as EGFP-N1/FAT10-N-GFP and pEGFP-N1/FAT10-C-GFP (Schmidtke et al., 2006). pGEX-4T-3/GST-His_6-FAT10ΔGG was generated by mutating the C-terminal diglycine to AV. pEGFP-N1 was purchased from Clontech.

Pulse-chase experiments and immunoprecipitation. Pulse-chase experiments were performed as previously described (Hipp et al., 2004). For the immunoprecipitation experiments, transiently transfected cells were incubated for 6 hours in the presence of 5 μM MG132, 1 μM nocodazole, 5 μM trichostatin A or the respective solvent as a negative control. After harvesting, cells were lysed in 20 mM Tris/HCl pH 7.8 containing 0.1% Triton X-100, 1 μM pepstatin, 10 μM leupeptin, 5 μg/ml aprotinin, 100 μM PMSF, 20 μM MG132, 2 mM ATP and 2 mM $MgCl_2$ for 30 min on ice, followed by sonication, addition of 150 mM NaCl and centrifugation for 15 min at 20000 × g. Cleared lysates were subjected to preclearance with either protein A or protein G affinity gel (Sigma) for 30 min at 4°C followed by incubation over night at 4°C with 10 μg anti-FLAG M2 antibody and protein G or 15 μl anti-FAT10 or control serum and protein A, respectively. Immunoprecipitates were washed 5 times in lysis buffer and analysed by SDS-PAGE and Western blotting. For the experiments examining the acetylation of FAT10, 5 μM trichostatin A was included in the lysis buffer.

GST-pulldown assay. GST-FAT10 and GST were purified as previously described (Hipp et al., 2005). FLAG-tagged wild-type as well as mutant HDAC6 was *in vitro* transcribed and translated using the TNT® T7 Coupled Reticulocyte Lysate System (Promega) according to the manufacturer's instructions. After preclearance with GSH-Sepharose (GE Healthcare), half of each reaction was incubated with 30 μl GSH-Sepharose (blocked with 1 mg/ml BSA) and either 50 μg GST-FAT10, GST-His_6-FAT10 (ΔGG) or GST as a negative control in 200 μl of the lysis buffer used in the immunoprecipitation experiments. Samples were incubated over night at 4°C, washed 5 times and analysed by SDS-PAGE followed by autoradiography.

Immunofluorescence and confocal microscopy. For the anti-γ-tubulin (dilution 1:500) and anti-20S proteasome (dilution 1:100) stainings, HEK293T cells were grown on poly-L-lysine (Fluka) coated cover slips, incubated with 5 μM MG132 or solvent only for 6 hours and fixed with ice-cold MeOH:acetic acid (3:1) for 10 min. For the anti-FLAG M2 (dilution 1:300), anti-Ubiquitin FK2 (dilution 1:100), anti-GFP (dilution 1:200) and anti-FAT10 (dilution 1:200) stainings, cells were grown on poly-L-lysine coated cover slips, incubated with 5 μM MG132, 1 μM

nocodazole or solvent only for 6 hours (HEK293T cells) or 4 hours (MEFs), fixed with 4% paraformaldehyde for 30 min and permeabilized with 0.1% Triton X-100 for 10 min at room temperature. Cells were first labeled with the primary antibodies, followed by washing and incubation with the respective Alexa Fluor™ labeled secondary antibodies (dilution 1:300), followed by washing and incubation with the Alexa Fluor™ labeled anti-HA antibody (dilution 1:300) where applicable. All antibodies were diluted in 0.2% gelatine, except for the anti-γ-tubulin and anti-FAT10 stainings, were 1.5% normal goat serum was added. All incubations were carried out for 1 h at room temperature. Images were aquired and analyzed with a LSM 510 confocal laser-scanning microscope (Carl Zeiss) using a 63× plan-apochromat, oil-immersion objective (NA=1.4). Statistical analysis of the number of aggresome-containing cells was performed by randomly selecting approximately 100 cells and scoring them for the presence of a large, juxtanuclear aggresome. Statistical analysis of aggresome size was carried out by randomly selecting approximately 50 (for the anti-ubiquitin staining) or 10 (for the anti-HA staining after HA-FAT10 transfection) aggresome-containing cells. Aggresome sizes were then quantified using ImageJ (Rasband, 1997).

Acknowledgements

We thank Dr. P. Matthias for the donation of HDAC6$^{-/-}$ cells, Dr. T. P. Yao for the donation of plasmids, Dr. M. Langhorst for the kind instruction in confocal microscopy and Dr. S. L. Schreiber for the gift of tubacin and niltubacin. This work was supported by the German Research Foundation (DFG) grant GR1517/2-3.

Chapter 4

FAT10-deficient mice display a prolonged $CD8^+$ T-cell response after LCMV infection

Birte Kalveram, Michael Basler and Marcus Groettrup

Unpublished results.

Introduction

Nearly all types of cells present on their surface an array of peptides representative of their physiological state, which will be scanned by cytotoxic ($CD8^+$) T cells or natural killer (NK) cells for potential abnormalities, such as infection by viruses or intracellular bacteria. These peptides are derived from endogenous proteins, which include all normal cellular constituents as well as foreign antigens introduced into the cell as components of the invading pathogen (Germain, 1994). The targeting and degradation of these antigens is mostly achieved through polyubiquitylation and subsequent proteasomal degradation (Kloetzel, 2004). The peptides produced by the proteasome are then translocated into the endoplasmatic reticulum (ER) by the MHC locus-encoded transporters associated with antigen processing (TAPs) (Townsend and Trowsdale, 1993) and are further trimmed to the correct size by a set of ER resident aminopeptidases (Kloetzel and Ossendorp, 2004). With the help of several chaperones, such as tapasin as well the more ubiquitous chaperones calnexin and calreticulin, the generated peptides are finally loaded onto MHC class I molecules and subsequently transported to the surface (Antoniou et al., 2003).

For a cytotoxic T cell to take action upon recognizing an infected cell, however, it first needs to become activated through the action of a professional antigen-presenting cell. In most cases, this activation is mediated through the action of dendritic cells (DCs), which in their immature form patrol through peripheral organs and continuously sample their surroundings via phagocytosis or macropinocytosis. Upon contact with specific pathogen-associated molecular patterns such as LPS – which are recognized through Toll-like receptors (TLRs) – they become activated, mature and migrate to the lymph knode, where they present their collected antigens to circulating T cells. As professional antigen-presenting cells, DCs not only present endogenous antigens on their MHC class I molecules but are also able to load them with exogenous antigens in a process termed “cross presentation”. In addition, mature DCs express a number of co-stimulatory molecules (such as CD80, CD86 or CD40) on their surface, which, in combination with the recognition of their cognate peptide-MHC complex, mediate activation of circulating T cells. Following its activation, the T cell proliferates vigorously and its decendants proceed to patrol the periphery and kill infected cells upon recognition of their cognate peptide-MHC complex (Guermonprez et al., 2002).

Once the infection is cleared, massive cell death of of antigen-activated T cells occurs in order to maintain homeostasis and only a few cells which have been exposed to the antigen remain and develop into memory T cells. Removal of superfluous T cells is either mediated by activation-induced cell death (AICD), in which restimulation of expanded T cells in the absence of appropriate co-stimulation and in combination with the engagement of death receptors such as Fas or TNFR triggers apoptosis, or by activated cell-autonomous death (ACAD), in which the absence of survival signals such as IL-2 leads to the induction of apoptosis via the intrinsic pathway (Krammer et al., 2007).

Due to the localization of its gene in the MHC class I locus (Fan et al., 1996), as well as its expression profile (mainly restricted to DCs and mature B cells, Bates et al., 1997) and cytokine inducibility (Raasi et al., 1999), the ubiquitin-like modifier FAT10 has been suggested to play a role in MHC class I mediated antigen presentation. Until now, however, evidence supporting this hypothesis has remained sparse. Prompted by the findings that FAT10 is capable of targeting proteins for proteasomal degradation (Hipp et al., 2005) as well as inducing apoptosis (Raasi et al., 2001; Ross et al., 2006), we set out to determine whether it was possibly involved in the targeting of viral or bacterial antigens for degradation and subsequent presentation, or perhaps in the downregulation of the immune response after elimination of the pathogen.

To this aim, we used infection with lymphocytic choriomeningitis virus (LCMV) to study antigen presentation and antiviral response in FAT10-deficient mice, which have previously been shown to exhibit minor differences in the number of DCs as well as the apoptosis of lymphocytes (Canaan et al., 2006). The cytotoxic T cell response to LCMV is essential for the elimination of virus from infected mice and, in C57BL/6 mice, is shaped by $CD8^+$ T cells specific for the dominant GP-derived epitopes $GP_{33–41}/D^b$, $GP_{34–41}/K^b$, $GP_{276–286}/D^b$, and NP-derived $NP_{396–404}/D^b$, as well as the subdominant epitopes $GP_{92–101}/D^b$, $GP_{118–125}/K^b$, and $NP_{205–212}/K^b$ (van der Most et al., 1996; Gallimore et al., 1998; van der Most et al., 2003).

Results and Discussion

In order to uncover a potential role of FAT10 in the antiviral response, FAT10-deficient and wild-type C57BL/6 mice were infected with LCMV and the number of LCMV-specific cytotoxic T cells at seven, 14 and 20 days after infection was analyzed by intracellular cytokine staining. Spleen cells were separately stimu-

lated *ex vivo* with six different H-2^b-restricted epitopes and subsequently stained for expression of CD8 as well as for production of IFN-γ. The total number of LCMV-specific cytotoxic T cells was determined by combining the number of cells specific for each of the epitopes. As figure 30 demonstrates clearly, no difference in the number of LCMV-specific $CD8^+$ T cells could be observed on day seven post infection. However, at both 14 and 20 days after infection FAT10-deficient mice contained significantly more LCMV-specific $CD8^+$ T cells than C57BL/6 mice.

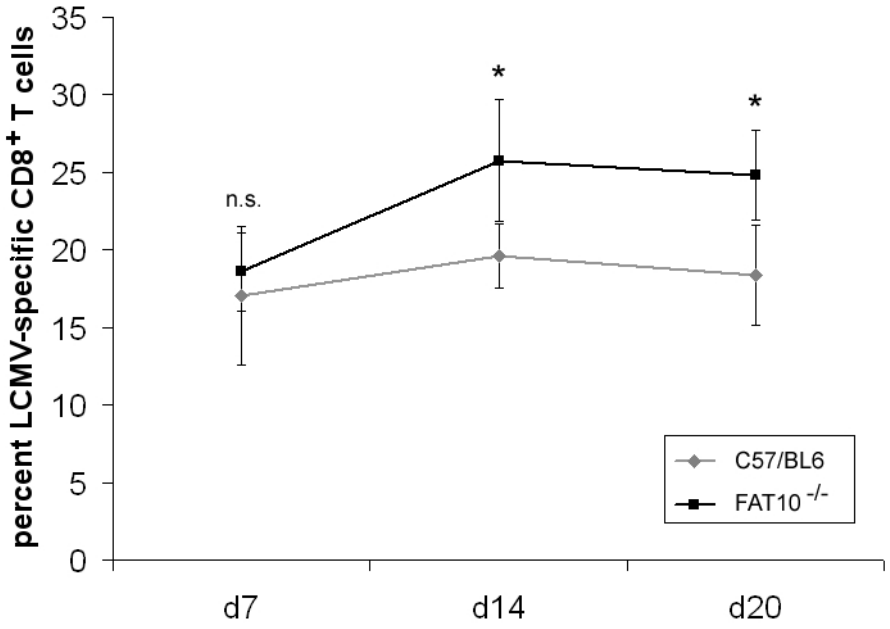

Figure 30: Figure 30. **FAT10-deficient mice retain more LCMV-specific $CD8^+$ T cells after infection than wild-type mice.** Mice were infected with 200 pfu of LCMV-WE and the frequency of specific IFN-γ producing $CD8^+$ T cells was analyzed by intracellular cytokine staining (ICS) 7, 14 and 20 days post infection. Statistical analysis was performed using Student's *t* test, error bars represent the standard deviation (SD). * = $p < 0.1$, n.s. = not significant, n = 5. One representative experiment out of two is shown.

It will now be important to determine whether this difference is due to the failure of FAT10-deficient mice to eliminate the pathogen or rather the result of defects in T cell homeostasis. In wild-type mice, LCMV infection is usually cleared after seven to nine days, therefore the determination of virus titers a week or longer after infection should clarify whether or not the observed increase in T cell numbers is a result of continued antigen supply due to persistent infection. Should this be the case, it would be highly interesting to see whether one of LCMV's proteins was perhaps a target of FAT10-conjugation – suggesting that FAT10 could be required for the efficient presentation of LCMV-derived epitopes and thus for the recognition and elimination of infected cells.

As both wild-type as well as FAT10-deficient mice display similar numbers of LCMV-specific T cells on day seven post infection, however, it seems more likely that the observed increase in specific T cell numbers at later time points is a result of defects in T cell homeostasis. In this case, it would be imporant to clarify whether this effect was due to a lack of T cell apoptosis or rather an increase in proliferation, which could for example be determined though BrdU incorporation or CFSE-labeling of T cells. Again, it seems more likely that the increased cell numbers are a result of impaired T cell death, since FAT10 could be shown to induce apoptosis in a number of different settings (Raasi et al., 2001; Ross et al., 2006).

The contraction phase of an immune response is characterized by massive cell death of antigen-specific T cells, which in most cases coincides with the clearance of infection (Sprent and Tough, 2001; Badovinac and Harty, 2002). As DCs are inherently short-lived cells (Kamath et al., 2000), removal of the pathogen from the host results in the immediate loss of T cell activation as pathogen-derived epitopes are no longer presented to circulating T cells in combination with co-stimulatory molecules. Interestingly, apoptosis of DCs after maturation is mostly regulated through the intrinsic pathway via the downregulation of BCL-2 (Nopora and Brocker, 2002) and BCL-X_L (Hon et al., 2004). Apoptosis of activated T cells, in turn, is regulated through a combination of both extrinsic as well as intrinsic pathways. T cell receptor restimulation of already activated and expanded T cells in the absence of appropriate co-stimulation can lead to the induction of activation-induced cell death (AICD) (Green et al., 2003). ACID is mediated mostly through the engagement of death receptors such as Fas (Dhein et al., 1995) or TNFR1 (Sytwu et al., 1996) and can be modulated both through the upregulation of these receptors (Li-Weber and Krammer, 2003) as well the inhibitory protein cFLIP (Refaeli et al., 1998; Schmitz et al., 2004). Activated cell-autonomous death (ACAD), on the other hand, is mostly mediated via the intrinsic pathway through the upregulation of the pro-apoptotic proteins BIM and PUMA (Hildeman et al., 2002; Erlacher et al., 2006) due to the absence of appropriate survival signals, such as cytokine deprivation. In addition, ACAD can be further promoted by the down-regulation of BCL-X_L and BCL-2 during T cell expansion (Sandalova et al., 2004; Schmitz et al., 2003).

Whether FAT10 primarily plays a role in the apoptosis of T cells themselves, or rather in the death of DCs and therefore the downregulation of T cell activation, could be determined by isolating either T cells or DCs and subjecting them to different apoptotic stimuli. Preliminary results from the study of bone marrow-

derived dendritic cells (BMDCs) argue against a role of FAT10 in the death of DCs, as BMDCs derived from FAT10-deficient as well as wild-type mice displayed no differences in the rate of maturation-induced apoptosis (data not shown). However, as BMDCs constitute a highly artificial system, these experiments will need to be repeated with spleenic DCs for a definite answer. In addition, spleenic T cells could be assayed for differences in apoptosis after bulk stimulation through receptor cross-linking with anti-CD3 and anti-CD28 antibodies and subsequent restimulation with either anti-CD3 antibodies alone, treatment with PMA/ionomycin or FasL to induce ACID; or they could be cultivated in cytokine-free medium to induce ACAD.

Materials and Methods

Mice. FAT10 gene-targeted mice were generated as previously described (Canaan et al., 2006) and were backcrossed on the C57BL/6 background until the 10^{th} generation was obtained. Genotyping of mice was performed as described previously, except for an alternative set of primers which was used to amplify the neomycin gene: NeoF2 (5'-TATCGCCTTCTTGACGAGTTC-3') and NeoR2 (5'-CATCAGGTG GAGTCTCTCTC-3'). C57BL/6 mice (H-2^b) mice were obtained originally from Charles River Laboratories. Mice were kept in a specific pathogen-free facility and used at 6 - 10 weeks of age. Animal experiments were approved by the Regierungspräsidium Freiburg.

Virus. LCMV-WE was obtained originally from F. Lehmann-Grube (Hamburg, Germany) and propagated in the fibroblast line L929. Mice were infected with a low dose of 200 pfu of LCMV-WE i.v., and the specific CTL response was analyzed at days 7, 14 and 20 post infection.

Intracellular staining (ICS) for IFN-γ. Splenocytes (2×10^6) were incubated in round-bottom 96-well plates with 10^{-7} M of the specific peptide in 100 μl medium containing 10 μg/ml brefeldin A for 5 h at 37°C. The staining, fixation, and permeabilization of the cells were performed exactly as previously described (Basler et al., 2004). Briefly, cells were first stained with an anti-CD8-Tri-color conjugate (Caltag) at 4°C followed by fixation in 4% paraformaldehyde. Cells were then permeabilized in 0.1% saponin, stained with an anti-IFN-γ-FITC conjugate (BD Biosciences) and analyzed in a FACScan flow cytometer.

Peptides. The synthetic peptides $GP_{33–41}$ (KAVYNFATC), $GP_{92–101}$ (CSANNSHHYI), $GP_{118–125}$ (ISHNFCNL), $GP_{276–286}$ (SGVENPGGYCL), $NP_{205–212}$ (YTVKYPNL), and $NP_{396–404}$ (FQPQNGQFI) were obtained from Echaz Microcollections.

BMDCs. Bone marrow-derived dendritic cells were generated as previously described (Schlosser et al., 2008). Briefly, bone marrow cells from $FAT10^{-/-}$ as well as C57BL/6 mice were cultured in the presence of GM-CSF for seven days. After differentiation, non- and semiadherent cells were harvested and treated wih 1μg/ml LPS to induce maturation. 24 and 48 hours later, cells were stained with FITC-coupled annexin-V and propidium iodide (both BD Biosciences) according to the manufacturer's instructions and analyzed for cell death in a FACScan flow cytometer.

Chapter 5

Generation of mouse monoclonal antibodies directed against human FAT10

Birte Kalveram, Gunter Schmidtke and Marcus Groettrup

Unpublished results.

Introduction

Antibodies are invaluable tools for the study of endogenous proteins and can be utilized for example for the determination of tissue specific expression patterns through western blot or histology or the analysis of intracellular localization by immunofluorescence. We have previously generated two polyclonal antibodies by immunizing rabbits with either recombinant GST-FAT10 or KLH-coupled synthetic peptides (Hipp et al., 2005; Raasi, 2001), which have been successfully used in a number of applications such as western blotting, immunoprecipitation and immunofluorescence. Unfortunately, use of the GST-FAT10 antiserum has been somewhat limited by its high level of cross-reactivity and we therefore decided to generate monoclonal antibodies directed against human FAT10 through the immunization of mice with recombinant GST-FAT10. Furthermore, the availability of two antibodies derived from different species will enable us to perform a number of additional applications, such as for example the detection of low levels of FAT10 protein in different tissues through the combination of immunoprecipitation and western blot.

Results and Discussion

Since a previous attempt to generate FAT10-specific monoclonal antibodies in BALB/c mice failed to yield any viable hybridomas, we decided to use FAT10-deficient mice for the immunization in the hope that these would carry a higher number of FAT10-specific precursor cells. Two mice were immunized with recombinant human GST-FAT10 and after three rounds of booster immunizations displayed a titer high enough to warrant performing the fusion. Unfortunately, immunizations had to be carried out with a GST-fusion protein as proteolytic removal of GST resulted in the immediate precipitation of untagged FAT10. Similarly, expression of FAT10 with a smaller tag (e.g. His_6) did not yield any soluble protein either. To exclude those hybridomas which produced antibodies directed against GST, hybridoma supernatants were screened by ELISA for reactivity against both GST-FAT10 as well as GST alone. The initial screening yielded five positive clones, two of which could be stabilized after two (in the case of 4F1) or three (in the case of 3A11) rounds of subcloning. Isotyping by ELISA revealed both antibodies to be of the IgG2a isotype.

The antibodies produced by both clones recognize transiently transfected and endogenous FAT10

To determine whether the antibodies were able to recognize FAT10 in a western blot, HEK293T cells were transiently transfected with FLAG-FAT10, treated with 500 U/ml hTNF-α and 200 U/ml hIFN-γ for 16 hours or left untreated. The cell lysates were subsequently analyzed by western blot with a 1:1000 dilution of the purified antibodies in 3% BSA, which resulted in a 6.8 μg/ml (3A11) or 4.4 μg/ml (4F1) working dilution, respectively. Both antibodies were able to recognize FAT10 equally well and the signal strength was comparable to that of an anti-FLAG western blot of the same lysates (Fig. 31). Interestingly, the antibodies from both hybridomas produce in the same background bands, are of the same isotype and recognize the N-terminal UBL domain of FAT10 (Fig. 36 and data now shown). This suggests that, even though both hybridomas are independent clones, they probably produce the same antibody.

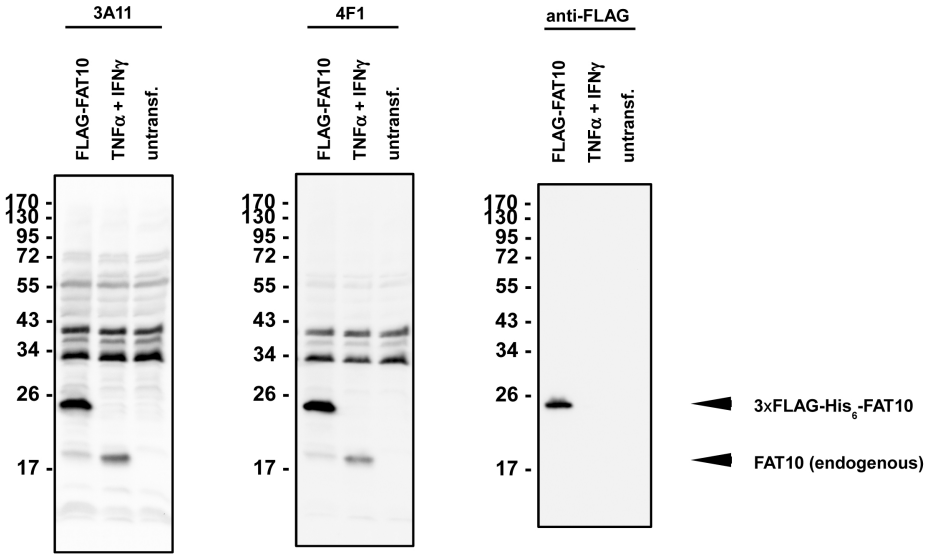

Figure 31: The antibodies produced by both hybridomas recognize ectopically expressed as well as endogenous FAT10 in a western blot. HEK293T cells were transiently transfected with human FLAG-FAT10, treated with IFN-γ and TNF-α or left untreated and cell lysates were analyzed by western blot with either anti-FLAG antibody (right panel) or clone 3A11 (left panel) or clone 4F1 (middle panel) at working dilutions of 4.4μg/ml and 6.8μg/ml, respectively.

Neither antibody is able to recognize murine FAT10

In order to determine whether the antibodies were perhaps also capable of recognizing murine FAT10 in addition to the human protein, equal amounts of recom-

binant human and mouse GST-FAT10 were loaded onto an SDS-PAGE and subsequently probed with a 1:1000 dilution of the purified antibodies in 3% BSA. Unfortunately, neither clone 3A11 nor clone 4F1 was capable of recognizing murine FAT10 in a western blot (Fig. 32).

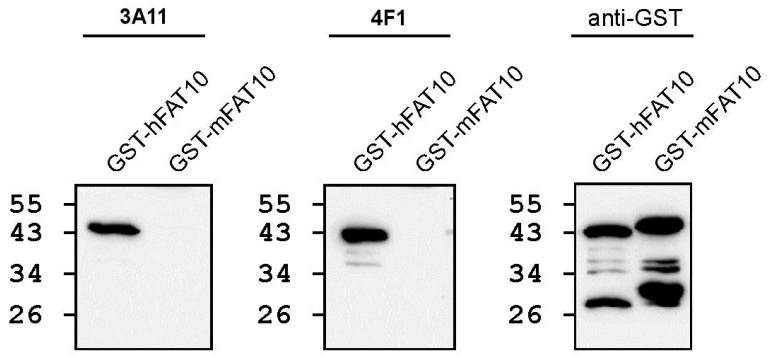

Figure 32: The antibodies produced by both hybridomas recognize only human and not murine FAT10. Clones 3A11 (left panel) and 4F1 (middle panel) at working dilutions of 4.4μg/ml and 6.8μg/ml, respectively, were tested for reactivity with recombinant human (GST-hFAT10) as well as mouse (GST-mFAT10) FAT10 by western blot. A blot probed with anti-GST antibody (Sigma) serves as the loading control (right panel).

The antibodies produced by both hybridomas recognize FAT10 in immunofluorescence

To determine whether the antibodies could be used to detect FAT10 in immunofluorescence stainings, HEK293T cells were grown on poly-L-lysine-coated cover slips, transiently transfected with HA-FAT10, fixed with 4% paraformaldehyde and stained with either anti-HA antibody or either 3A11 or 4F1 hybridoma supernatant which was first concentrated approximately 50-fold and subsequently diluted 1:5 in 1.5% normal goat serum. As can be seen in figure 33, the antibodies produced by both clones recognize FAT10 equally well and with little background in immunofluorescence.

The antibodies produced by both clones are able to immunoprecipitate FAT10

HEK293T cells were transiently transfected with HA-FAT10 or left untreated and their lysates were subjected to an immunoprecipitation with 5 μg of either anti-HA antibody or anti-FAT10 clone 3A11 or clone 4F1. The precipitates as well as the lysates before and after the IP were subsequently analyzed by western blot with an anti-HA antibody. As can be seen in figure 34, the antibodies produced by both clones are able to precipitate HA-FAT10 with the same efficiency as an anti-HA antibody.

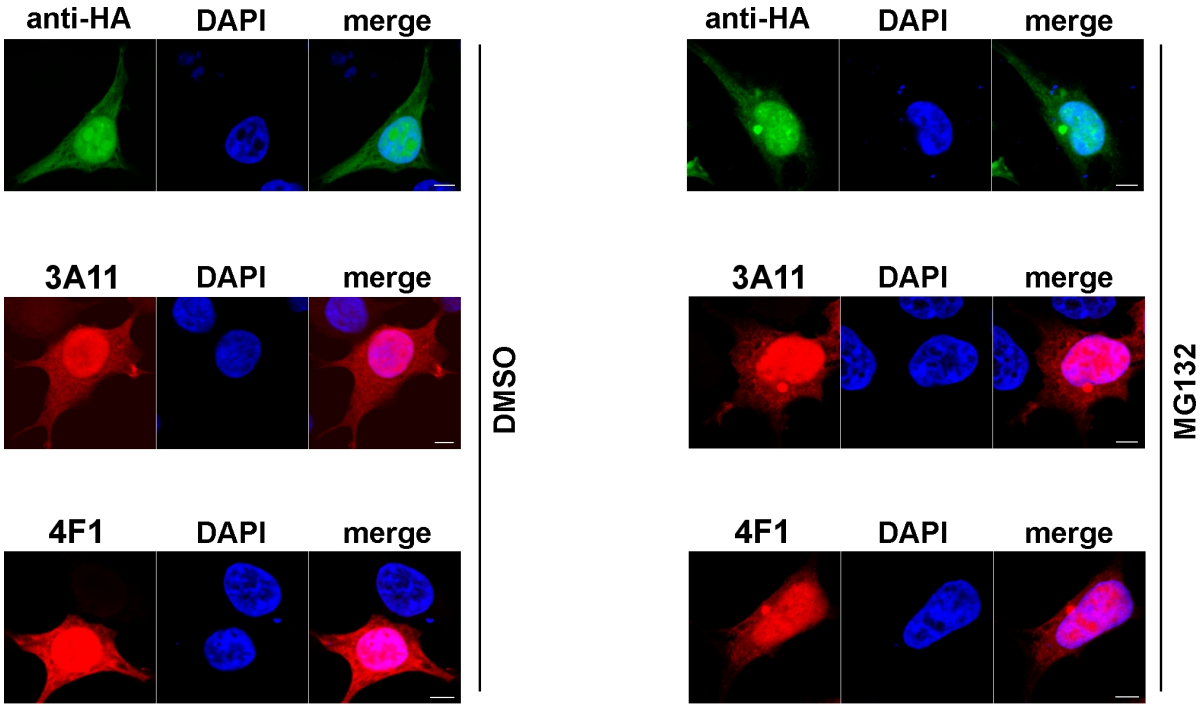

Figure 33: Immunofluorescence of hybridoma supernatants. HEK293T cells were grown on poly-L-lysine-coated coverslips, transiently transfected with human HA-FAT10 and treated with 5μM MG132 or solvent only for 6 hours. Cells were then fixed and stained with either an alexa-488-coupled anti-HA antibody (green) or 3A11 or 4F1 hybridoma supernatants followed by an alexa-546-coupled secondary anti-mouse antibody (red) as well as DAPI (blue). Untransfected cells serve as the negative control. Scale bar = 5μm.

The monoclonal anti-FAT10 antibody recognizes both monomeric FAT10 as well as FAT10-conjugates

As both hybridomas most likely produce the same antibody, the optimal working dilution was only titrated for one of the clones (4F1) and was determined to lie between 50 and 100 ng/ml. HEK293T cells were either left untreated or transiently transfected with HA-FAT10 and cell lysates as well as 1:2 and 1:10 dilutions of the HA-FAT10 lysates were analyzed by western blot with a 100 ng/ml dilution of anti-FAT10 (clone 4F1) antibody in 3% BSA. Both short and long exposures of the same blot are shown in figure 35 and the longer exposure reveals the presence of high molecular weight FAT10-conjugates in the cells transfected with HA-FAT10. A Ponceau staining of the membrane serves as a loading control.

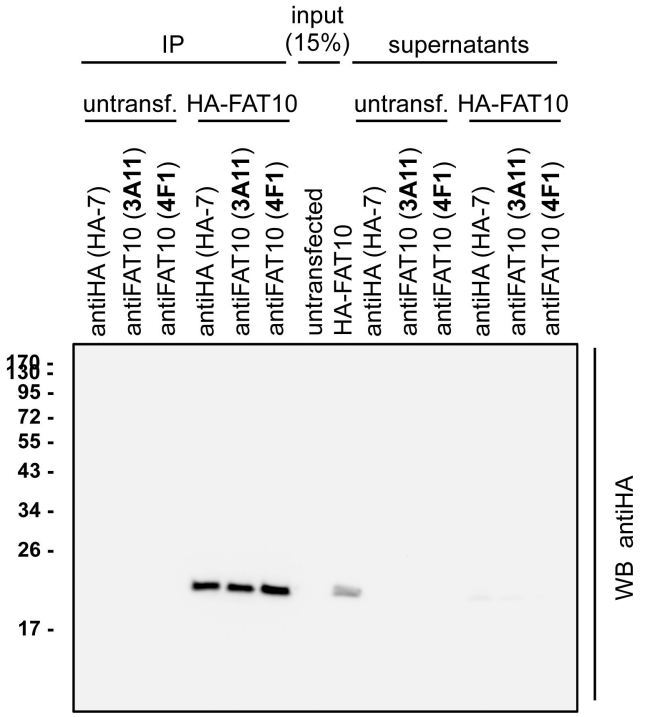

Figure 34: The antibodies produced by both hybridomas are able to immunoprecipitate FAT10. HEK293T cells were transiently transfected with HA-FAT10 or left untreated and the cell lysates were subjected to immunoprecipitation with 5 μg of either anti-HA antibody, clone 3A11 or clone 4F1. The precipitated proteins as well as the lysates before (input) as well as after (supernatants) the IP were analyzed by anti-HA western blot.

The monoclonal anti-FAT10 antibody specifically recognizes the N-terminal UBL domain of FAT10

To acquire information about the specificity of the antibody and the localization of the epitope recognized by it, HEK293T cells were transiently transfected with constructs containing N-terminal fusions of the isolated UBL domains or full-length FAT10 to GFP. Several other ubiquitin-like modifiers, namely ubiquitin-GFP, SUMO-GFP, LC3B-GFP and FLAG-NEDD8 were also transfected. In addition, expression of endogenous FAT10 was induced by treatment of cells with IFN-γ and TNF-α. Lysates of these cells were then analysed by western blot with either anti-GFP or anti-FLAG antibodies or a 50 ng/ml dilution of clone 4F1. Figure 36 reveals that the monoclonal anti-FAT10 antibody recognized both full-length FAT10 as well as its N-terminal UBL domain. In addition, it demonstrates that this antibody did not cross-react with any of the other ubiquitin-like modifiers investigated except for LC3 (ATG8). Interestingly, LC3 is the only one among the proteins assayed for cross-reactivity which shares no sequence homology with FAT10.

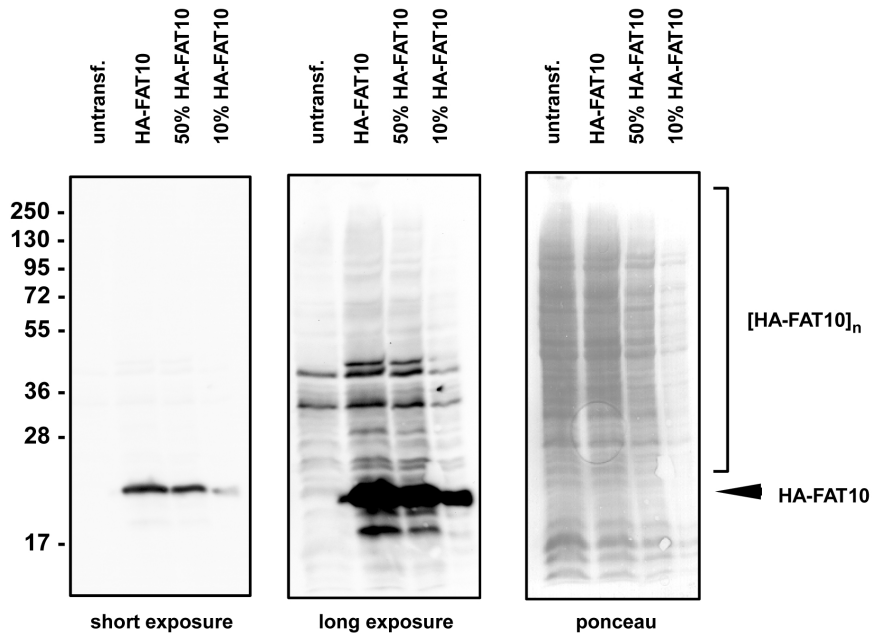

Figure 35: The antibody recognizes both monomeric FAT10 as well as FAT10 conjugates. HEK293T cells were transiently transfected with HA-FAT10 or left untreated and cell lysates were analyzed by western blot with a 100 ng/ml working dilution of clone 4F1. Both short as well as long exposures of the same blot are shown. A Ponceau staining of the membrane serves as a loading control.

Materials and Methods

Purification of recombinant proteins. The GST-FAT10 expression construct was generated as previously described by cloning the human FAT10 cDNA into pGEX-4T-3 (GE Healthcare) (Hipp et al., 2004). Recombinant proteins were purified in batch essentially according to the manufacturer's instructions. The proteins used for coating ELISA plates were purified in the absence of Triton X-100. After purification, the buffer was exchanged to either PBS (for use in ELISA) or 0.9% (w/v) NaCl (for use in immunization) using a HiTrap Desalting 5ml or NAP-5 column (both GE Healthcare).

Western blot, immunoprecipitation and immunofluorescence. Western blots, immunoprecipitations and immunofluorescences were performed as previously described (Kalveram et al., 2008).

Expression constructs. HA-FAT10, HA-FAT10-GFP, HA-Ubiquitin-GFP, HA-SUMO-GFP (Hipp et al., 2005), HA-FAT10-N-GFP, HA-FAT10-C-GFP (Schmidtke et al., 2006) as well as GST-FAT10, FLAG-NEDD8 (Hipp et al., 2004) and FLAG-

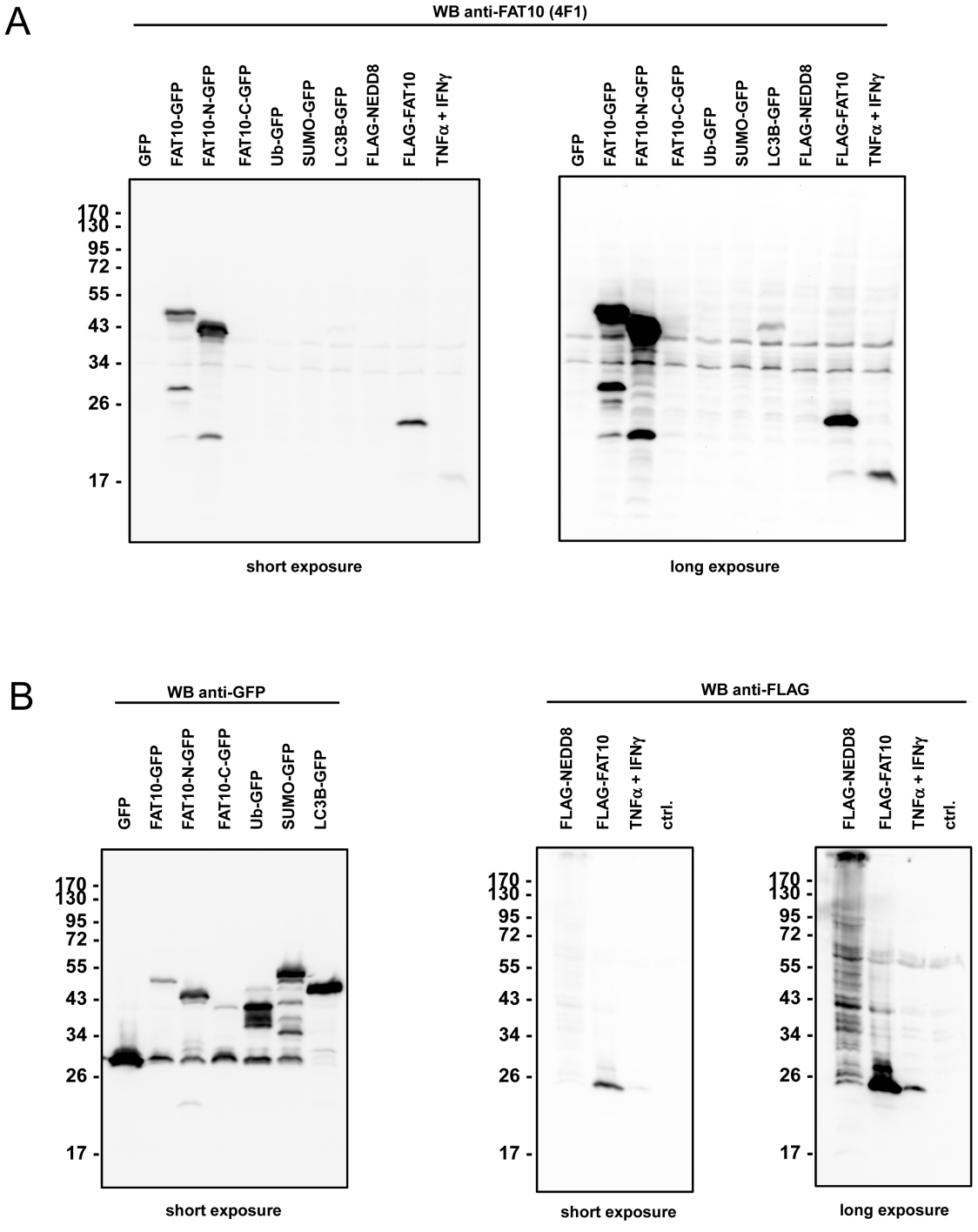

Figure 36: The antibody specifically recognizes the N-terminal UBL domain of FAT10. Lysates of HEK293T cells transiently transfected with the indicated constructs or treated with IFN-γ and TNF-α were analyzed by western blot with **(A)** either a 50 ng/ml working dilution of clone 4F1 or **(B)** anti-GFP or anti-FLAG antibodies as a loading control.

FAT10 (Chiu et al., 2007) have all been described previously. GFP-LC3B has been contributed by Trond Lamark (unpublished data). GST-mFAT10 was generated by amplifying the murine *fat10* cDNA by PCR and cloning it into the vector pGEX2-TK through its EcoRI and XbaI restriction sites (Neha Rani, unpublished results).

Generation of monoclonal antibodies. Monoclonal antibodies were generated in essence as previously described (Yokoyama et al., 2006). Briefly, two mice were each immunized with 100 μg of recombinant GST-FAT10 in lipopeptide. After three rounds of booster immunizations, the animals were sacrificed and their spleens were harvested and a single cell suspension was prepared. Spleen cells were then fused with SP2/0-Ag14 myeloma cells at a 1:1 ratio and plated into flat-bottom 96-well plates. After selection with HAT medium, the surviving cells were screened by ELISA for the production of GST-FAT10 specific antibodies. A GST ELISA was performed to exclude those hybridomas which produced antibodies with anti-GST reactivity. The resulting hybridomas were then subjected to three rounds of subcloning. After expansion, antibodies were purified from hybridoma supernatants using a protein G column (GE Healthcare).

ELISA. Antisera and hybridoma supernatants were screened by ELISA essentially as previously described (Hornbeck, 1992). Briefly, Microlon ELISA-plates (Greiner Bio-One) were coated with 20 μg/ml of recombinant protein. Antisera were diluted 1:25 or 1:50 in blocking buffer, hybridoma supernatants were diluted 1:2 in blocking buffer. Bound antibodies were detected with alkaline phosphatase-coupled protein G (Calbiochem) diluted 1:2500 in blocking buffer and developed with 3 mM *p*-nitrophenyl phosphate (Fluka). Substrate hydrolysis was measured at 405 nm wavelength in a Tecan microplate reader. Antibody isotypes were determined using the Mouse Immunoglobulin Isotyping ELISA kit from BD Biosciences according to the manufacturer's instructions.

Discussion

30 years ago, ubiquitin was first identified as a small protein capable of targeting cellular proteins for degradation through its covalent attachment (Ciechanover et al., 1978, 1980; Hershko et al., 1980). Later studies revealed it to be involved in the degradation of the majority of intracellular proteins in eukaryotes – and identified the 26S proteasome as the protease responsible for the proteolytic destruction of its target proteins (Hershko and Ciechanover, 1998). Polyubiquitylated proteins can either bind directly to the proteasome (Deveraux et al., 1994; Lam et al., 2002), or they can be indirectly delivered via linker proteins such as hHR23/Rad23 or hPLIC/Dsk2 (Chen and Madura, 2002; Funakoshi et al., 2002). In addition, evidence has accumulated during the past few years that, under conditions where the proteasome ceases to function, alternative adaptor proteins such as HDAC6 or p62 can instead target these substrates for lysosomal degradation via the autophagic pathway (Kawaguchi et al., 2003; Iwata et al., 2005; Shin, 1998; Bjørkøy et al., 2005).

Although ubiquitin was long thought to be the only protein capable of directly targeting others for destruction through its covalent attachment, the ubiquitin-like modifier FAT10 has recently emerged as cytokine-inducible alternative to ubiquitin-mediated proteasomal degradation. Interestingly, despite the fact that FAT10 can mediate the degradation of its substrates independently of ubiquitylation (Hipp et al., 2005 and chapter 2), its *modus operandi* is in many ways analogous to that of ubiquitin. Like ubiquitin, FAT10 can become covalently conjugated to its target proteins through its C-terminal glycine residue (Raasi et al., 2001) and can directly interact with the 26S proteasome. Alternatively, FAT10 can also be tethered to the proteasome through interaction with the UBL-UBA domain protein NUB1L, which – in addition to its role as an alternative proteasomal receptor for FAT10 – also functions as a facilitator of FAT10 degradation (chapter 1). As could be demonstrated for some polyubiquitylated substrates, mere physical attachment of a model FAT10-conjugate to the proteasome was insufficient to promote its degradation, which was instead dependent on the

presence of NUB1L (chapter 2). Interestingly, the facilitator-function of NUB1L relied solely on its ability to interact with the proteasome and not with FAT10 (chapter 1). Whether this requirement for facilitation only holds true for some FAT10-conjugates, however, or whether the degradation of all of its target proteins is dependent on NUB1L remains subject to investigation.

Strikingly, FAT10 not only promotes the proteasomal degradation of its target proteins in a manner analogous to that of ubiquitin, but also relies on the same fail-safe mechanism under conditions of proteasome impairment. When a cell suffers from misfolded protein stress, either due to direct inhibition of the proteasome or because it becomes overwhelmed by the accumulation of a large number of incorrectly folded proteins, the cytoplasmatic deacetylase HDAC6 associates with both polyubiquitin- as well as FAT10-conjugates and mediates their dynein-dependent transport to the aggresome – where they are first sequestered and subsequently cleared by autophagy (Kawaguchi et al., 2003; Iwata et al., 2005 and chapter 3). In both cases, the interaction with HDAC6 is strictly dependent on inhibition of the proteasome (Kawaguchi et al., 2003 and chapter 3), which raises the question of how the cell is able to recognize the accumulation of proteasomal substrates and how HDAC6 is prevented from interacting with them under conditions where the proteasome is functioning normally.

Two models have recently been proposed in which HDAC6 directly acts as a sensor of misfolded protein stress. The first model is based on the structures of the BUZ domains contained in the ubiquitin-specific proteases IsoT (Reyes-Turcu et al., 2006) and Ubp-M (Pai et al., 2007), which both bind ubiquitin through its free C-terminal diglycine motif. Pai et al. propose that HDAC6 acts as a sensor of the level of free ubiquitin in the cell by binding to monomeric ubiquitin through its BUZ domain as well as through a second, so far unidentified, domain. Owing to a much higher affinity of the BUZ domain for the C-terminus of ubiquitin rather than for polyubiquitin-conjugates, the majority of HDAC6 would normally be bound to free ubiquitin. Under conditions of proteasome impairment, however, the decline in the level of monomeric ubiquitin would release HDAC6, and possibly also induce a conformational change of HDAC6, thus enabling it to bind to polyubiquitin chains – and to FAT10.

Although this is certainly an elegant model which has the benefit of explaining the necessity of an additional binding domain for ubiquitin-like modifiers, there are several pieces of evidence which argue against it. First of all, several studies have shown the BUZ domain of HDAC6 to be capable of interacting with both

monomeric ubiquitin as well as polyubiquitin chains, and have also demonstrated the BUZ domain to be essential for the latter (Seigneurin-Berny et al., 2001; Hook et al., 2002; Kawaguchi et al., 2003). As the structure of this particular BUZ domain has yet to be solved, it is not entirely unlikely that it perhaps does not interact with ubiquitin through its C-terminal diglycine motif after all. Furthermore, even though the CAT1 domain of HDAC6 could be identified as a second FAT10-binding domain in addition to its BUZ domain (chapter 3), there is no evidence which suggests the CAT1 domain to be able to interact with ubiquitin as well.

Another group has subsequently suggested an alternative model in which HDAC6 senses an overload of polyubiquitylated proteins through the binding of polyubiquitin to its BUZ domain (Boyault et al., 2007). They were able to show that, under normal physiological conditions, HDAC6 forms a repressive complex together with heat-shock factor 1 (HSF1) as well as p97/VCP and HSP90. Based on this observation, they proposed that upon proteasome impairment the accumulating polyubiquitylated proteins would disrupt this complex, resulting in the release of both active HSF1 as well as HDAC6 – and this effect could indeed be mimicked by the addition of pentaubiquitin-chains, which did not contain a free C-terminal diglycine, to the purified complex.

Regardless of whichever mechanism regulates the association of FAT10 with HDAC6, the finding that it utilizes not only one, but both of the cell's major pathways for intracellular protein degradation suggests that the rapid removal of both monomeric FAT10 as well as its conjugates is essential for the cell. Several other findings further corroborate the notion that FAT10 functions as a quick and temporally restricted means to promote the specific degradation of a select group of proteins. First of all, it is not constitutively expressed in most cell types (Raasi et al., 1999; Liu et al., 1999; Canaan et al., 2006) and FAT10 gene-targeted mice kept under standard laboratory conditions display only minimal phenotypic abnormalities (Canaan et al., 2006). Both of these findings strongly suggest that FAT10 is not involved in the day-to-day turnover of cellular proteins. Secondly, FAT10-mediated degradation can be rapidly turned on by exposure of cells to proinflammatory cytokines (Raasi et al., 1999), but it can be just as quickly turned off again as, in addition to being degraded along with its conjugates, unused FAT10 is also rapidly removed from the cell (Hipp et al., 2004, 2005). Thirdly, even though both ectopic overexpression as well as physiological induction by cytokines – the latter of which would also serve to induce any potentially missing factors required for the conjugation of FAT10 to its target proteins – result in a

massive increase of cellular FAT10 levels, only very few FAT10-conjugates can be observed.

Now, why would an organism evolve such a specialized “rapid response” degradation system when it already has the fully functional, constitutive ubiquitin system at its disposal? Since FAT10 is only found in higher eukaryotes, it is in all likelihood not a remnant of the times prior to the invention of ubiquitin – which is probably the reason for the existence of another highly specialized system, namely the antizyme-mediated degradation of ODC.

Both the localization of the *fat10* gene in the MHC class I locus as well as its expression profile and cytokine inducibility strongly point toward a role of FAT10 in the immune response. A large number of studies has implicated both ubiquitin as well as autophagy in the recognition and removal of intracellular pathogens. The presence of a dedicated clearance system for these pathogens would present several advantages for the cell. Firstly, competition for its components by normal cellular constituents would be avoided, so that, once induced, it could concentrate all its efforts on the removal of the dangerous intruders. Secondly, many pathogens actively evade or even manipulate the host’s machinery for ubiquitylation and autophagic degradation (Loureiro and Ploegh, 2006; Munro et al., 2007; Schmid and Münz, 2007), so this relatively new system could have evolved as a response to the pathogens’ evasive strategies.

Up until now, no evidence for an involvement of FAT10 in MHC class I dependent antigen processing has been found. Experiments performed in a mouse fibroblast cell-line revealed the overexpression of FAT10 to have no influence on the level of overall MHC class I surface expression as well as on the presentation of two viral epitopes, the MCMV-derived epitope $pp89_{168\text{-}176}/L^d$ as well as the LCMV-derived epitope $NP_{118\text{-}126}/L^d$ (Raasi et al., 2001). However, a function of FAT10 in antigen processing might rely on the action of additional cytokine-inducible proteins, which would be missing in this model of ectopic overexpression. Furthermore, the two viral proteins investigated may not be among the few which are targeted for proteasomal degradation by FAT10. Then again, FAT10 might not only be involved in the targeting of single proteins to the proteasome but also in the transport of entire viral particles to the aggresome in an attempt to facilitate their removal via autophagy. Indeed, many viral core particles share characteristics with protein aggregates and are actively transported to the microtubule-organizing center, although the precise details of this targeting mechanism remain unknown (Wileman, 2006).

Alternatively, FAT10 could be responsible for the degradation of host factors involved in viral or bacterial replication. Depending on the nature of those proteins, their prolonged removal after clearance of the pathogen could very well have deleterious effects on the cell, which would be an elegant explanation for both the ability of FAT10 to induce apoptosis upon 24 to 48 hours after expression (Raasi et al., 2001) as well as the requirement for the rapid removal of unconjugated FAT10 (Hipp et al., 2004).

Of course, rather than being a side-effect, the induction of apoptosis – for example through proteasomal degradation of IAPs or other anti-apoptotic proteins – could instead be the principal function of FAT10. Indeed, several findings obtained through the study of FAT10-deficient mice argue in favor of this hypothesis. In comparison to wild-type animals, these mice display minor differences in the apoptosis of lymphocytes as well as a pronounced hypersensitivity to endotoxin-mediated septic shock (Canaan et al., 2006), which could easily be explained by a failure to remove cytokine-producing cells by apoptosis. Furthermore, investigation of their antiviral response revealed these mice to exhibit a prolonged $CD8^+$ T-cell response after LCMV infection, which is probably due to defects in the removal of superfluous antigen-activated T-cells after clearance of the virus (chapter 4).

The findings that FAT10 is capable of targeting its substrates to the aggresome (chapter 3) and that it has been found to be a component of Mallory-Denk bodies (Oliva et al., 2008), which are a specialized type of aggresome found in chronic liver disease (Zatloukal et al., 2007), raise the question whether FAT10 is perhaps involved in the pathogenesis of degenerative diseases. Alternatively, as the aggresome-like structures found in many neurodegenerative diseases have been found to exhibit cytoprotective functions by facilitating the removal of toxic protein aggregates from the cell (Taylor et al., 2003; Olanow et al., 2004), FAT10 could also be actively involved in the sequestration of these aggregates. However, a widespread role of FAT10 in the removal of misfolded proteins seems unlikely, as it is only induced in the course of an immune response and both the liver as well as the brain of healthy individuals display no signs of FAT10 expression (Canaan et al., 2006).

The results described in this thesis represent a great advancement in understanding the mechanistics of FAT10-mediated protein degradation. In the future, it will be imperative to shed some more light onto the physiological functions of FAT10-conjugation. To this aim, efforts are already well on the way to identify

the nature of FAT10's target proteins. In addition, post-mortem brains of patients with Huntington's or Alzheimer's disease are being investigated for signs of FAT10 enrichment and FAT10 gene-targeted mice will be utilized to examine the requirement for FAT10 in a drug-induced model of Mallory-Denk body formation. Furthermore, continuing studies investigating the role of FAT10 in lymphocyte homeostasis as well as in the response to a number of additional intracellular pathogens are also being conducted.

References

D. T. Akey, X. Zhu, M. Dyer, A. Li, A. Sorensen, S. Blackshaw, T. Fukuda-Kamitani, S. P. Daiger, C. M. Craft, T. Kamitani, and M. M. Sohocki. The inherited blindness associated protein AIPL1 interacts with the cell cycle regulator protein NUB1. *Hum Mol Genet*, 11(22):2723–2733, Oct 2002.

S. Alberti, J. Demand, C. Esser, N. Emmerich, H. Schild, and J. Hohfeld. Ubiquitylation of BAG-1 suggests a novel regulatory mechanism during the sorting of chaperone substrates to the proteasome. *J Biol Chem*, 277(48):45920–45927, Nov 2002.

B. Alvarez-Castelao and J. G. Castaño. Mechanism of direct degradation of IkappaBalpha by 20S proteasome. *FEBS Lett*, 579(21):4797–4802, Aug 2005.

A. Y. Amerik and M. Hochstrasser. Mechanism and function of deubiquitinating enzymes. *Biochim Biophys Acta*, 1695(1-3):189–207, Nov 2004.

A. N. Antoniou, S. J. Powis, and T. Elliott. Assembly and export of MHC class I peptide ligands. *Curr Opin Immunol*, 15(1):75–81, Feb 2003.

G. Asher, Z. Bercovich, P. Tsvetkov, Y. Shaul, and C. Kahana. 20S proteasomal degradation of ornithine decarboxylase is regulated by NQO1. *Mol Cell*, 17(5):645–655, Mar 2005.

G. Asher, N. Reuven, and Y. Shaul. 20S proteasomes and protein degradation "by default". *Bioessays*, 28(8):844–849, Aug 2006.

J. R. Babu, T. Geetha, and M. W. Wooten. Sequestosome 1/p62 shuttles polyubiquitinated tau for proteasomal degradation. *J Neurochem*, 94(1):192–203, Jul 2005.

V. P. Badovinac and J. T. Harty. CD8(+) T-cell homeostasis after infection: setting the 'curve'. *Microbes Infect*, 4(4):441–447, Apr 2002.

P. Bali, M. Pranpat, J. Bradner, M. Balasis, W. Fiskus, F. Guo, K. Rocha, S. Kumaraswamy, S. Boyapalle, P. Atadja, E. Seto, and K. Bhalla. Inhibition of histone deacetylase 6 acetylates and disrupts the chaperone function of heat shock protein 90: a novel basis for antileukemia activity of histone deacetylase inhibitors. *J Biol Chem.*, 280(29):26729–34. Epub 2005 Jun 2., 2005.

M. Basler, N. Youhnovski, M. V. D. Broek, M. Przybylski, and M. Groettrup. Immunoproteasomes down-regulate presentation of a subdominant T cell epitope from lymphocytic choriomeningitis virus. *J Immunol*, 173(6):3925–3934, Sep 2004.

E. E. Bates, O. Ravel, M. C. Dieu, S. Ho, C. Guret, J. M. Bridon, S. Ait-Yahia, F. Brière, C. Caux, J. Banchereau, and S. Lebecque. Identification and analysis of a novel member of the ubiquitin family expressed in dendritic cells and mature B cells. *Eur J Immunol*, 27(10):2471–2477, Oct 1997.

W. Baumeister, J. Walz, F. Zühl, and E. Seemüller. The proteasome: paradigm of a self-compartmentalizing protease. *Cell*, 92(3):367–380, Feb 1998.

R. Beal, Q. Deveraux, G. Xia, M. Rechsteiner, and C. Pickart. Surface hydrophobic residues of multiubiquitin chains essential for proteolytic targeting. *Proc Natl Acad Sci U S A*, 93(2):861–866, Jan 1996.

S. Ben-Shahar, A. Komlosh, E. Nadav, I. Shaked, T. Ziv, A. Admon, G. N. DeMartino, and Y. Reiss. 26 S proteasome-mediated production of an authentic major histocompatibility class I-restricted epitope from an intact protein substrate. *J Biol Chem*, 274(31):21963–21972, Jul 1999.

N. F. Bence, R. M. Sampat, and R. R. Kopito. Impairment of the ubiquitin-proteasome system by protein aggregation. *Science*, 292(5521):1552–1555, May 2001.

E. J. Bennett, N. F. Bence, R. Jayakumar, and R. R. Kopito. Global impairment of the ubiquitin-proteasome system by nuclear or cytoplasmic protein aggregates precedes inclusion body formation. *Mol Cell*, 17(3):351–365, Feb 2005.

B. L. Bertolaet, D. J. Clarke, M. Wolff, M. H. Watson, M. Henze, G. Divita, and S. I. Reed. UBA domains of DNA damage-inducible proteins interact with ubiquitin. *Nat Struct Biol*, 8(5):417–422, May 2001.

N. R. Bertos, B. Gilquin, G. K. Chan, T. J. Yen, S. Khochbin, and X. J. Yang. Role of the tetradecapeptide repeat domain of human histone deacetylase 6 in cytoplasmic retention. *J Biol Chem.*, 279(46):48246–54. Epub 2004 Sep 3., 2004.

S. Biggins, I. Ivanovska, and M. D. Rose. Yeast ubiquitin-like genes are involved in duplication of the microtubule organizing center. *J Cell Biol*, 133(6):1331–1346, Jun 1996.

G. Bjørkøy, T. Lamark, A. Brech, H. Outzen, M. Perander, A. Overvatn, H. Stenmark, and T. Johansen. p62/SQSTM1 forms protein aggregates degraded by autophagy and has a protective effect on huntingtin-induced cell death. *J Cell Biol*, 171(4):603–614, Nov 2005.

K. L. Borden and P. S. Freemont. The RING finger domain: a recent example of a sequence-structure family. *Curr Opin Struct Biol*, 6(3):395–401, Jun 1996.

C. Boyault, B. Gilquin, Y. Zhang, V. Rybin, E. Garman, W. Meyer-Klaucke, P. Matthias, C. W. Müller, and S. Khochbin. HDAC6-p97/VCP controlled polyubiquitin chain turnover. *EMBO J*, 25(14):3357–3366, Jul 2006.

C. Boyault, Y. Zhang, S. Fritah, C. Caron, B. Gilquin, S. H. Kwon, C. Garrido, T.-P. Yao, C. Vourc'h, P. Matthias, and S. Khochbin. HDAC6 controls major cell response pathways to cytotoxic accumulation of protein aggregates. *Genes Dev*, 21(17):2172–2181, Sep 2007.

M. H. Brush, A. Guardiola, J. H. Connor, T. P. Yao, and S. Shenolikar. Deactylase inhibitors disrupt cellular complexes containing protein phosphatases and deacetylases. *J Biol Chem.*, 279(9):7685–91. Epub 2003 Dec 10., 2004.

B. Bukau, J. Weissman, and A. Horwich. Molecular chaperones and protein quality control. *Cell*, 125(3):443–451, May 2006.

J. R. Cabrero, J. M. Serrador, O. Barreiro, M. Mittelbrunn, S. Naranjo-Suárez, N. Martín-Cófreces, M. Vicente-Manzanares, R. Mazitschek, J. E. Bradner, J. Avila, A. Valenzuela-Fernández, and F. Sánchez-Madrid. Lymphocyte chemotaxis is regulated by histone deacetylase 6, independently of its deacetylase activity. *Mol Biol Cell*, 17(8):3435–3445, Aug 2006.

A. Canaan, X. Yu, C. J. Booth, J. Lian, I. Lazar, S. L. Gamfi, K. Castille, N. Kohya, Y. Nakayama, Y. C. Liu, E. Eynon, R. Flavell, and S. M. Weissman. FAT10/Diubiquitin-Like Protein-Deficient Mice Exhibit Minimal Phenotypic Differences. *Mol Cell Biol.*, 26(13):5180–9., 2006.

C.-S. Chen, S.-C. Weng, P.-H. Tseng, H.-P. Lin, and C.-S. Chen. Histone acetylation-independent effect of histone deacetylase inhibitors on Akt through the reshuffling of protein phosphatase 1 complexes. *J Biol Chem*, 280(46):38879–38887, Nov 2005.

L. Chen and K. Madura. Rad23 promotes the targeting of proteolytic substrates to the proteasome. *Mol Cell Biol*, 22(13):4902–4913, Jul 2002.

L. Chen, U. Shinde, T. G. Ortolan, and K. Madura. Ubiquitin-associated (UBA) domains in Rad23 bind ubiquitin and promote inhibition of multi-ubiquitin chain assembly. *EMBO Rep*, 2(10): 933–938, Oct 2001.

X. Chen, Y. Chi, A. Bloecher, R. Aebersold, B. E. Clurman, and J. M. Roberts. N-acetylation and ubiquitin-independent proteasomal degradation of p21(Cip1). *Mol Cell*, 16(5):839–847, Dec 2004.

X. Chen, L. F. Barton, Y. Chi, B. E. Clurman, and J. M. Roberts. Ubiquitin-independent degradation of cell-cycle inhibitors by the REGgamma proteasome. *Mol Cell*, 26(6):843–852, Jun 2007.

Y.-H. Chiu, Q. Sun, and Z. J. Chen. E1-L2 Activates Both Ubiquitin and FAT10. *Mol Cell*, 27(6): 1014–1023, Sep 2007.

A. Ciechanover. Proteolysis: from the lysosome to ubiquitin and the proteasome. *Nat Rev Mol Cell Biol*, 6(1):79–87, Jan 2005.

A. Ciechanover, Y. Hod, and A. Hershko. A heat-stable polypeptide component of an ATP-dependent proteolytic system from reticulocytes. *Biochem Biophys Res Commun*, 81:1100–1105, 1978.

A. Ciechanover, H. Heller, S. Elias, A. L. Haas, and A. Hershko. ATP-dependent conjugation of reticulocyte proteins with the polypeptide required for protein degradation. *Proc Natl Acad Sci U S A*, 77(3):1365–1368, Mar 1980.

L. Coscoy and D. Ganem. PHD domains and E3 ubiquitin ligases: viruses make the connection. *Trends Cell Biol*, 13(1):7–12, Jan 2003.

O. Coux, K. Tanaka, and A. L. Goldberg. Structure and functions of the 20S and 26S proteasomes. *Annu Rev Biochem*, 65:801–847, 1996.

J. D'Cunha, S. Ramanujam, R. J. Wagner, P. L. Witt, E. Knight, and E. C. Borden. In vitro and in vivo secretion of human ISG15, an IFN-induced immunomodulatory cytokine. *J Immunol*, 157 (9):4100–4108, Nov 1996.

J. H. de Quintana, R. J. Evans, M. E. Cheetham, and J. van der Spuy. The Leber congenital amaurosis protein AIPL1 functions as part of a chaperone heterocomplex. *Invest Ophthalmol Vis Sci*, 49(7):2878–2887, Jul 2008.

O. Destaing, F. Saltel, B. Gilquin, A. Chabadel, S. Khochbin, S. Ory, and P. Jurdic. A novel Rho-mDia2-HDAC6 pathway controls podosome patterning through microtubule acetylation in osteoclasts. *J Cell Sci.*, 118(Pt 13):2901–11., 2005.

Q. Deveraux, V. Ustrell, C. Pickart, and M. Rechsteiner. A 26 S protease subunit that binds ubiquitin conjugates. *J Biol Chem*, 269(10):7059–7061, Mar 1994.

J. Dhein, H. Walczak, C. Bäumler, K. M. Debatin, and P. H. Krammer. Autocrine T-cell suicide mediated by APO-1/(Fas/CD95). *Nature*, 373(6513):438–441, Feb 1995.

P. P. Di Fiore, S. Polo, and K. Hofmann. When ubiquitin meets ubiquitin receptors: a signalling connection. *Nat Rev Mol Cell Biol*, 4(6):491–497, Jun 2003.

S. Elsasser, R. R. Gali, M. Schwickart, C. N. Larsen, D. S. Leggett, B. Müller, M. T. Feng, F. Tübing, G. A. G. Dittmar, and D. Finley. Proteasome subunit Rpn1 binds ubiquitin-like protein domains. *Nat Cell Biol*, 4(9):725–730, Sep 2002.

S. Elsasser, D. Chandler-Militello, B. Müller, J. Hanna, and D. Finley. Rad23 and Rpn10 serve as alternative ubiquitin receptors for the proteasome. *J Biol Chem*, 279(26):26817–26822, Jun 2004.

M. Erlacher, V. Labi, C. Manzl, G. Böck, A. Tzankov, G. Häcker, E. Michalak, A. Strasser, and A. Villunger. Puma cooperates with Bim, the rate-limiting BH3-only protein in cell death during lymphocyte development, in apoptosis induction. *J Exp Med*, 203(13):2939–2951, Dec 2006.

W. Fan, W. Cai, S. Parimoo, D. C. Schwarz, G. G. Lennon, and S. M. Weissman. Identification of seven new human MHC class I region genes around the HLA-F locus. *Immunogenetics*, 44(2): 97–103, 1996.

S. Fang and A. M. Weissman. A field guide to ubiquitylation. *Cell Mol Life Sci.*, 61(13):1546–61., 2004.

W. Fiskus, Y. Ren, A. Mohapatra, P. Bali, A. Mandawat, R. Rao, B. Herger, Y. Yang, P. Atadja, J. Wu, and K. Bhalla. Hydroxamic acid analogue histone deacetylase inhibitors attenuate estrogen receptor-alpha levels and transcriptional activity: a result of hyperacetylation and inhibition of chaperone function of heat shock protein 90. *Clin Cancer Res*, 13(16):4882–4890, Aug 2007.

A. M. Forsthoefel, M. M. O. Peña, Y. Y. Xing, Z. Rafique, and F. G. Berger. Structural determinants for the intracellular degradation of human thymidylate synthase. *Biochemistry*, 43(7):1972–1979, Feb 2004.

B. A. French, F. van Leeuwen, N. E. Riley, Q. X. Yuan, F. Bardag-Gorce, K. Gaal, Y. H. Lue, N. Marceau, and S. W. French. Aggresome formation in liver cells in response to different toxic mechanisms: role of the ubiquitin-proteasome pathway and the frameshift mutant of ubiquitin. *Exp Mol Pathol*, 71(3):241–246, Dec 2001.

E. C. Friedberg, A. R. Lehmann, and R. P. P. Fuchs. Trading places: how do DNA polymerases switch during translesion DNA synthesis? *Mol Cell*, 18(5):499–505, May 2005.

M. Funakoshi, T. Sasaki, T. Nishimoto, and H. Kobayashi. Budding yeast Dsk2p is a polyubiquitin-binding protein that can interact with the proteasome. *Proc Natl Acad Sci U S A*, 99(2):745–750, Jan 2002.

A. Gallimore, T. Dumrese, H. Hengartner, R. M. Zinkernagel, and H. G. Rammensee. Protective immunity does not correlate with the hierarchy of virus-specific cytotoxic T cell responses to naturally processed peptides. *J Exp Med*, 187(10):1647–1657, May 1998.

Y.-S. Gao, C. C. Hubbert, J. Lu, Y.-S. Lee, J.-Y. Lee, and T.-P. Yao. Histone deacetylase 6 regulates growth factor-induced actin remodeling and endocytosis. *Mol Cell Biol*, 27(24):8637–8647, Dec 2007.

R. Garcia-Mata, Z. Bebok, E. J. Sorscher, and E. S. Sztul. Characterization and dynamics of aggresome formation by a cytosolic GFP-chimera. *J Cell Biol.*, 146(6):1239–54., 1999.

R. Garcia-Mata, Y.-S. Gao, and E. Sztul. Hassles with taking out the garbage: aggravating aggresomes. *Traffic*, 3(6):388–396, Jun 2002.

R. N. Germain. MHC-dependent antigen processing and peptide presentation: providing ligands for T lymphocyte activation. *Cell*, 76(2):287–299, Jan 1994.

M. H. Glickman, D. M. Rubin, H. Fu, C. N. Larsen, O. Coux, I. Wefes, G. Pfeifer, Z. Cjeka, R. Vierstra, W. Baumeister, V. Fried, and D. Finley. Functional analysis of the proteasome regulatory particle. *Mol Biol Rep*, 26(1-2):21–28, Apr 1999.

A. L. Goldberg. Protein degradation and protection against misfolded or damaged proteins. *Nature*, 426(6968):895–899, Dec 2003.

A. L. Goldberg, P. Cascio, T. Saric, and K. L. Rock. The importance of the proteasome and subsequent proteolytic steps in the generation of antigenic peptides. *Mol Immunol*, 39(3-4):147–164, Oct 2002.

D. R. Green, N. Droin, and M. Pinkoski. Activation-induced cell death in T cells. *Immunol Rev*, 193:70–81, Jun 2003.

N. Gregersen, P. Bross, S. Vang, and J. H. Christensen. Protein Misfolding and Human Disease. *Annu Rev Genomics Hum Genet*, 7:103–124, Sep 2006.

M. Groettrup, S. Khan, K. Schwarz, and G. Schmidtke. Interferon-gamma inducible exchanges of 20S proteasome active site subunits: why? *Biochimie*, 83(3-4):367–372, 2001a.

M. Groettrup, M. van den Broek, K. Schwarz, A. Macagno, S. Khan, R. de Giuli, and G. Schmidtke. Structural plasticity of the proteasome and its function in antigen processing. *Crit Rev Immunol*, 21(4):339–358, 2001b.

M. Groettrup, C. Pelzer, G. Schmidtke, and K. Hofmann. Activating the ubiquitin family: UBA6 challenges the field. *Trends Biochem Sci*, 33(5):230–237, May 2008.

M. Groll and T. Clausen. Molecular shredders: how proteasomes fulfill their role. *Curr Opin Struct Biol*, 13(6):665–673, Dec 2003.

M. Groll, M. Bajorek, A. Köhler, L. Moroder, D. M. Rubin, R. Huber, M. H. Glickman, and D. Finley. A gated channel into the proteasome core particle. *Nat Struct Biol*, 7(11):1062–1067, Nov 2000.

T. Grune, T. Reinheckel, and K. J. Davies. Degradation of oxidized proteins in mammalian cells. *FASEB J*, 11(7):526–534, Jun 1997.

P. Guermonprez, J. Valladeau, L. Zitvogel, C. Théry, and S. Amigorena. Antigen presentation and T cell stimulation by dendritic cells. *Annu Rev Immunol*, 20:621–667, 2002.

S. Guerra, A. Cáceres, K.-P. Knobeloch, I. Horak, and M. Esteban. Vaccinia virus E3 protein prevents the antiviral action of ISG15. *PLoS Pathog*, 4(7):e1000096, Jul 2008.

S. Gunawardena, L.-S. Her, R. G. Brusch, R. A. Laymon, I. R. Niesman, B. Gordesky-Gold, L. Sintasath, N. M. Bonini, and L. S. B. Goldstein. Disruption of axonal transport by loss of huntingtin or expression of pathogenic polyQ proteins in Drosophila. *Neuron*, 40(1):25–40, Sep 2003.

S. J. Haggarty, K. M. Koeller, J. C. Wong, C. M. Grozinger, and S. L. Schreiber. Domain-selective small-molecule inhibitor of histone deacetylase 6 (HDAC6)-mediated tubulin deacetylation. *Proc Natl Acad Sci U S A.*, 100(8):4389–94. Epub 2003 Apr 3., 2003.

K. Haglund and I. Dikic. Ubiquitylation and cell signaling. *EMBO J*, 24(19):3353–3359, Oct 2005.

J. Hanna and D. Finley. A proteasome for all occasions. *FEBS Lett*, 581(15):2854–2861, Jun 2007.

J. Hanna, N. A. Hathaway, Y. Tone, B. Crosas, S. Elsasser, D. S. Kirkpatrick, D. S. Leggett, S. P. Gygi, R. W. King, and D. Finley. Deubiquitinating enzyme Ubp6 functions noncatalytically to delay proteasomal degradation. *Cell*, 127(1):99–111, Oct 2006.

R. Hartmann-Petersen, K. B. Hendil, and C. Gordon. Ubiquitin binding proteins protect ubiquitin conjugates from disassembly. *FEBS Lett*, 535(1-3):77–81, Jan 2003.

H. P. Hauser, M. Bardroff, G. Pyrowolakis, and S. Jentsch. A giant ubiquitin-conjugating enzyme related to IAP apoptosis inhibitors. *J Cell Biol*, 141(6):1415–1422, Jun 1998.

K. B. Hendil, P. Kristensen, and W. Uerkvitz. Human proteasomes analysed with monoclonal antibodies. *Biochem J*, 305 (Pt 1):245–252, Jan 1995.

J. P. Hendrick and F. U. Hartl. The role of molecular chaperones in protein folding. *FASEB J*, 9 (15):1559–1569, Dec 1995.

A. Hershko and A. Ciechanover. The ubiquitin system. *Annu Rev Biochem*, 67:425–479, 1998.

A. Hershko, A. Ciechanover, H. Heller, A. L. Haas, and I. A. Rose. Proposed role of ATP in protein breakdown: conjugation of protein with multiple chains of the polypeptide of ATP-dependent proteolysis. *Proc Natl Acad Sci U S A*, 77(4):1783–1786, Apr 1980.

L. Hicke. A new ticket for entry into budding vesicles-ubiquitin. *Cell*, 106(5):527–530, Sep 2001.

T. Hideshima, J. E. Bradner, J. Wong, D. Chauhan, P. Richardson, S. L. Schreiber, and K. C. Anderson. Small-molecule inhibition of proteasome and aggresome function induces synergistic antitumor activity in multiple myeloma. *Proc Natl Acad Sci U S A.*, 102(24):8567–72. Epub 2005 Jun 3., 2005.

D. A. Hildeman, Y. Zhu, T. C. Mitchell, P. Bouillet, A. Strasser, J. Kappler, and P. Marrack. Activated T cell death in vivo mediated by proapoptotic bcl-2 family member bim. *Immunity*, 16(6): 759–767, Jun 2002.

M. S. Hipp. *NUB1L and FAT10, two ubiquitin-like proteins involved in protein degradation.* PhD thesis, Universität Konstanz, 2004.

M. S. Hipp, S. Raasi, M. Groettrup, and G. Schmidtke. NEDD8 ultimate buster-1L interacts with the ubiquitin-like protein FAT10 and accelerates its degradation. *J Biol Chem.*, 279(16): 16503–10. Epub 2004 Feb 2., 2004.

M. S. Hipp, B. Kalveram, S. Raasi, M. Groettrup, and G. Schmidtke. FAT10, a ubiquitin-independent signal for proteasomal degradation. *Mol Cell Biol.*, 25(9):3483–91., 2005.

H. Hiyama, M. Yokoi, C. Masutani, K. Sugasawa, T. Maekawa, K. Tanaka, J. H. Hoeijmakers, and F. Hanaoka. Interaction of hHR23 with S5a. The ubiquitin-like domain of hHR23 mediates interaction with S5a subunit of 26 S proteasome. *J Biol Chem*, 274(39):28019–28025, Sep 1999.

C. Hoege, B. Pfander, G.-L. Moldovan, G. Pyrowolakis, and S. Jentsch. RAD6-dependent DNA repair is linked to modification of PCNA by ubiquitin and SUMO. *Nature*, 419(6903):135–141, Sep 2002.

K. Hofmann and P. Bucher. The UBA domain: a sequence motif present in multiple enzyme classes of the ubiquitination pathway. *Trends Biochem Sci*, 21(5):172–173, May 1996.

H. Hon, E. B. Rucker, L. Hennighausen, and J. Jacob. bcl-xL is critical for dendritic cell survival in vivo. *J Immunol*, 173(7):4425–4432, Oct 2004.

S. S. Hook, A. Orian, S. M. Cowley, and R. N. Eisenman. Histone deacetylase 6 binds polyubiquitin through its zinc finger (PAZ domain) and copurifies with deubiquitinating enzymes. *Proc Natl Acad Sci U S A*, 99(21):13425–13430, Oct 2002.

T. Hoppe. Multiubiquitylation by E4 enzymes: 'one size' doesn't fit all. *Trends Biochem Sci*, 30(4): 183–187, Apr 2005.

P. Hornbeck. *Current Protocols in Immunology: Unit 2.1 Enzyme-Linked Immunosorbent Assays*. John Wiley & Sons, 1992.

M. A. Hoyt, J. Zich, J. Takeuchi, M. Zhang, C. Govaerts, and P. Coffino. Glycine-alanine repeats impair proper substrate unfolding by the proteasome. *EMBO J*, 25(8):1720–1729, Apr 2006.

C. Hubbert, A. Guardiola, R. Shao, Y. Kawaguchi, A. Ito, A. Nixon, M. Yoshida, X. F. Wang, and T. P. Yao. HDAC6 is a microtubule-associated deacetylase. *Nature.*, 417(6887):455–8., 2002.

J. H. Hurley, S. Lee, and G. Prag. Ubiquitin-binding domains. *Biochem J*, 399(3):361–372, Nov 2006.

D. R. Hurst, A. Mehta, B. P. Moore, P. A. Phadke, W. J. Meehan, M. A. Accavitti, L. A. Shevde, J. E. Hopper, Y. Xie, D. R. Welch, and R. S. Samant. Breast cancer metastasis suppressor 1 (BRMS1) is stabilized by the Hsp90 chaperone. *Biochem Biophys Res Commun*, 348(4):1429–1435, Oct 2006.

K. Husnjak, S. Elsasser, N. Zhang, X. Chen, L. Randles, Y. Shi, K. Hofmann, K. J. Walters, D. Finley, and I. Dikic. Proteasome subunit Rpn13 is a novel ubiquitin receptor. *Nature*, 453(7194): 481–488, May 2008.

A. Iwata, B. E. Riley, J. A. Johnston, and R. R. Kopito. HDAC6 and microtubules are required for autophagic degradation of aggregated huntingtin. *J Biol Chem*, 280(48):40282–40292, Dec 2005.

D. M. Janse, B. Crosas, D. Finley, and G. M. Church. Localization to the proteasome is sufficient for degradation. *J Biol Chem*, 279(20):21415–21420, May 2004.

S. Jentsch and G. Pyrowolakis. Ubiquitin and its kin: how close are the family ties? *Trends Cell Biol*, 10(8):335–342, Aug 2000.

S. Jentsch, W. Seufert, T. Sommer, and H. A. Reins. Ubiquitin-conjugating enzymes: novel regulators of eukaryotic cells. *Trends Biochem Sci*, 15(5):195–198, May 1990.

S. Jentsch, W. Seufert, and H. P. Hauser. Genetic analysis of the ubiquitin system. *Biochim Biophys Acta*, 1089(2):127–139, Jun 1991.

V. Jesenberger and S. Jentsch. Deadly encounter: ubiquitin meets apoptosis. *Nat Rev Mol Cell Biol*, 3(2):112–121, Feb 2002.

J. Jiang, C. A. Ballinger, Y. Wu, Q. Dai, D. M. Cyr, J. Höhfeld, and C. Patterson. CHIP is a U-box-dependent E3 ubiquitin ligase: identification of Hsc70 as a target for ubiquitylation. *J Biol Chem*, 276(46):42938–42944, Nov 2001.

J. Jin, X. Li, S. P. Gygi, and J. W. Harper. Dual E1 activation systems for ubiquitin differentially regulate E2 enzyme charging. *Nature*, 447(7148):1135–1138, Jun 2007.

C. A. Joazeiro and A. M. Weissman. RING finger proteins: mediators of ubiquitin ligase activity. *Cell*, 102(5):549–552, Sep 2000.

E. S. Johnson. Protein modification by SUMO. *Annu Rev Biochem*, 73:355–382, 2004.

E. S. Johnson, B. Bartel, W. Seufert, and A. Varshavsky. Ubiquitin as a degradation signal. *EMBO J*, 11(2):497–505, Feb 1992.

E. S. Johnson, P. C. Ma, I. M. Ota, and A. Varshavsky. A proteolytic pathway that recognizes ubiquitin as a degradation signal. *J Biol Chem*, 270(29):17442–17456, Jul 1995.

J. A. Johnston, C. L. Ward, and R. R. Kopito. Aggresomes: a cellular response to misfolded proteins. *J Cell Biol*, 143(7):1883–1898, Dec 1998.

J. A. Johnston, M. J. Dalton, M. E. Gurney, and R. R. Kopito. Formation of high molecular weight complexes of mutant Cu, Zn-superoxide dismutase in a mouse model for familial amyotrophic lateral sclerosis. *Proc Natl Acad Sci U S A*, 97(23):12571–12576, Nov 2000.

J. A. Johnston, M. E. Illing, and R. R. Kopito. Cytoplasmic dynein/dynactin mediates the assembly of aggresomes. *Cell Motil Cytoskeleton*, 53(1):26–38, Sep 2002.

C. Kahana, G. Asher, and Y. Shaul. Mechanisms of protein degradation: an odyssey with ODC. *Cell Cycle*, 4(11):1461–1464, Nov 2005.

B. Kalveram, G. Schmidtke, and M. Groettrup. The ubiquitin-like modifier FAT10 interacts with HDAC6 and localizes to aggresomes under proteasome inhibition. *J. Cell Sci.*, in press, 2008.

A. T. Kamath, J. Pooley, M. A. O'Keeffe, D. Vremec, Y. Zhan, A. M. Lew, A. D'Amico, L. Wu, D. F. Tough, and K. Shortman. The development, maturation, and turnover rate of mouse spleen dendritic cell populations. *J Immunol*, 165(12):6762–6770, Dec 2000.

T. Kamitani, K. Kito, T. Fukuda-Kamitani, and E. T. Yeh. Targeting of NEDD8 and its conjugates for proteasomal degradation by NUB1. *J Biol Chem*, 276(49):46655–46660, Dec 2001.

K. Kanaya, M. M. Sohocki, and T. Kamitani. Abolished interaction of NUB1 with mutant AIPL1 involved in Leber congenital amaurosis. *Biochem Biophys Res Commun*, 317(3):768–773, May 2004.

Y. Kawaguchi, J. J. Kovacs, A. McLaurin, J. M. Vance, A. Ito, and T. P. Yao. The deacetylase HDAC6 regulates aggresome formation and cell viability in response to misfolded protein stress. *Cell.*, 115(6):727–38., 2003.

O. Kerscher, R. Felberbaum, and M. Hochstrasser. Modification of proteins by ubiquitin and ubiquitin-like proteins. *Annu Rev Cell Dev Biol*, 22:159–180, 2006.

S. Khan, A. Zimmermann, M. Basler, M. Groettrup, and H. Hengel. A cytomegalovirus inhibitor of gamma interferon signaling controls immunoproteasome induction. *J Virol*, 78(4):1831–1842, Feb 2004.

K. I. Kim, N. V. Giannakopoulos, H. W. Virgin, and D. E. Zhang. Interferon-inducible ubiquitin E2, Ubc8, is a conjugating enzyme for protein ISGylation. *Mol Cell Biol.*, 24(21):9592–600., 2004.

K. I. Kim, O. A. Malakhova, K. Hoebe, M. Yan, B. Beutler, and D.-E. Zhang. Enhanced antibacterial potential in UBP43-deficient mice against Salmonella typhimurium infection by up-regulating type I IFN signaling. *J Immunol*, 175(2):847–854, Jul 2005.

K. Kito, E. T. Yeh, and T. Kamitani. NUB1, a NEDD8-interacting protein, is induced by interferon and down-regulates the NEDD8 expression. *J Biol Chem*, 276(23):20603–20609, Jun 2001.

M. F. Kleijnen, A. H. Shih, P. Zhou, S. Kumar, R. E. Soccio, N. L. Kedersha, G. Gill, and P. M. Howley. The hPLIC proteins may provide a link between the ubiquitination machinery and the proteasome. *Mol Cell*, 6(2):409–419, Aug 2000.

P.-M. Kloetzel. The proteasome and MHC class I antigen processing. *Biochim Biophys Acta*, 1695 (1-3):225–233, Nov 2004.

P. M. Kloetzel and F. Ossendorp. Proteasome and peptidase function in MHC-class-I-mediated antigen presentation. *Curr Opin Immunol*, 16(1):76–81, Feb 2004.

E. Knight and B. Cordova. IFN-induced 15-kDa protein is released from human lymphocytes and monocytes. *J Immunol*, 146(7):2280–2284, Apr 1991.

D. M. Koepp, J. W. Harper, and S. J. Elledge. How the cyclin became a cyclin: regulated proteolysis in the cell cycle. *Cell*, 97(4):431–434, May 1999.

R. R. Kopito. Aggresomes, inclusion bodies and protein aggregation. *Trends Cell Biol.*, 10(12): 524–30., 2000.

J. J. Kovacs, P. J. M. Murphy, S. Gaillard, X. Zhao, J.-T. Wu, C. V. Nicchitta, M. Yoshida, D. O. Toft, W. B. Pratt, and T.-P. Yao. HDAC6 regulates Hsp90 acetylation and chaperone-dependent activation of glucocorticoid receptor. *Mol Cell*, 18(5):601–607, May 2005.

P. H. Krammer, R. Arnold, and I. N. Lavrik. Life and death in peripheral T cells. *Nat Rev Immunol*, 7(7):532–542, Jul 2007.

D. Krappmann and C. Scheidereit. A pervasive role of ubiquitin conjugation in activation and termination of IkappaB kinase pathways. *EMBO Rep*, 6(4):321–326, Apr 2005.

E. Kuusisto, A. Salminen, and I. Alafuzoff. Ubiquitin-binding protein p62 is present in neuronal and glial inclusions in human tauopathies and synucleinopathies. *Neuroreport*, 12(10):2085–2090, Jul 2001.

S. Kwon, Y. Zhang, and P. Matthias. The deacetylase HDAC6 is a novel critical component of stress granules involved in the stress response. *Genes Dev*, 21(24):3381–3394, Dec 2007.

E. C. Lai. Protein degradation: four E3s for the notch pathway. *Curr Biol*, 12(2):R74–R78, Jan 2002.

V. Lallemand-Breitenbach, M. Jeanne, S. Benhenda, R. Nasr, M. Lei, L. Peres, J. Zhou, J. Zhu, B. Raught, and H. de Thé. Arsenic degrades PML or PML-RARalpha through a SUMO-triggered RNF4/ubiquitin-mediated pathway. *Nat Cell Biol*, 10(5):547–555, May 2008.

Y. A. Lam, T. G. Lawson, M. Velayutham, J. L. Zweier, and C. M. Pickart. A proteasomal ATPase subunit recognizes the polyubiquitin degradation signal. *Nature*, 416(6882):763–767, Apr 2002.

D. Lambertson, L. Chen, and K. Madura. Pleiotropic defects caused by loss of the proteasome-interacting factors Rad23 and Rpn10 of Saccharomyces cerevisiae. *Genetics*, 153(1):69–79, Sep 1999.

M. F. Lavin and N. Gueven. The complexity of p53 stabilization and activation. *Cell Death Differ*, 13(6):941–950, Jun 2006.

C. G. L. Lee, J. Ren, I. S. Y. Cheong, K. H. K. Ban, L. L. P. J. Ooi, S. Y. Tan, A. Kan, I. Nuchprayoon, R. Jin, K.-H. Lee, M. Choti, and L. A. Lee. Expression of the FAT10 gene is highly upregulated in hepatocellular carcinoma and other gastrointestinal and gynecological cancers. *Oncogene*, 22(17):2592–2603, May 2003.

D. S. Leggett, J. Hanna, A. Borodovsky, B. Crosas, M. Schmidt, R. T. Baker, T. Walz, H. Ploegh, and D. Finley. Multiple associated proteins regulate proteasome structure and function. *Mol Cell*, 10(3):495–507, Sep 2002.

H. Lelouard, E. Gatti, F. Cappello, O. Gresser, V. Camosseto, and P. Pierre. Transient aggregation of ubiquitinated proteins during dendritic cell maturation. *Nature*, 417(6885):177–182, May 2002.

X. Li, D. M. Lonard, S. Y. Jung, A. Malovannaya, Q. Feng, J. Qin, S. Y. Tsai, M.-J. Tsai, and B. W. O'Malley. The SRC-3/AIB1 coactivator is degraded in a ubiquitin- and ATP-independent manner by the REGgamma proteasome. *Cell*, 124(2):381–392, Jan 2006.

X. Li, L. Amazit, W. Long, D. M. Lonard, J. J. Monaco, and B. W. O'Malley. Ubiquitin- and ATP-independent proteolytic turnover of p21 by the REGgamma-proteasome pathway. *Mol Cell*, 26 (6):831–842, Jun 2007.

M. Li-Weber and P. H. Krammer. Function and regulation of the CD95 (APO-1/Fas) ligand in the immune system. *Semin Immunol*, 15(3):145–157, Jun 2003.

C.-B. Lim, D. Zhang, and C. G. Lee. FAT10, a gene up-regulated in various cancers, is cell-cycle regulated. *Cell Div*, 1:20, 2006.

C.-W. Liu, L. Millen, T. B. Roman, H. Xiong, H. F. Gilbert, R. Noiva, G. N. DeMartino, and P. J. Thomas. Conformational remodeling of proteasomal substrates by PA700, the 19 S regulatory complex of the 26 S proteasome. *J Biol Chem*, 277(30):26815–26820, Jul 2002.

C.-W. Liu, M. J. Corboy, G. N. DeMartino, and P. J. Thomas. Endoproteolytic activity of the proteasome. *Science*, 299(5605):408–411, Jan 2003.

Y. C. Liu, J. Pan, C. Zhang, W. Fan, M. Collinge, J. R. Bender, and S. M. Weissman. A MHC-encoded ubiquitin-like protein (FAT10) binds noncovalently to the spindle assembly checkpoint protein MAD2. *Proc Natl Acad Sci U S A*, 96(8):4313–4318, Apr 1999.

J. Loureiro and H. L. Ploegh. Antigen presentation and the ubiquitin-proteasome system in host-pathogen interactions. *Adv Immunol*, 92:225–305, 2006.

S. Lukasiak, C. Schiller, P. Oehlschlaeger, G. Schmidtke, P. Krause, D. F. Legler, F. Autschbach, P. Schirmacher, K. Breuhahn, and M. Groettrup. Proinflammatory cytokines cause FAT10 up-regulation in cancers of liver and colon. *Oncogene*, Jun 2008.

F. Lévy, N. Johnsson, T. Rümenapf, and A. Varshavsky. Using ubiquitin to follow the metabolic fate of a protein. *Proc Natl Acad Sci U S A*, 93(10):4907–4912, May 1996.

J. Lüders, J. Demand, and J. Höhfeld. The ubiquitin-related BAG-1 provides a link between the molecular chaperones Hsc70/Hsp70 and the proteasome. *J Biol Chem*, 275(7):4613–4617, Feb 2000.

Y. Ma and L. M. Hendershot. The unfolding tale of the unfolded protein response. *Cell*, 107(7): 827–830, Dec 2001.

M. P. Malakhov, O. A. Malakhova, K. I. Kim, K. J. Ritchie, and D.-E. Zhang. UBP43 (USP18) specifically removes ISG15 from conjugated proteins. *J Biol Chem*, 277(12):9976–9981, Mar 2002.

M. P. Malakhov, K. I. Kim, O. A. Malakhova, B. S. Jacobs, E. C. Borden, and D.-E. Zhang. High-throughput immunoblotting. Ubiquitiin-like protein ISG15 modifies key regulators of signal transduction. *J Biol Chem*, 278(19):16608–16613, May 2003.

A. C. Massey, C. Zhang, and A. M. Cuervo. Chaperone-mediated autophagy in aging and disease. *Curr Top Dev Biol*, 73:205–235, 2006.

A. Matsuyama, T. Shimazu, Y. Sumida, A. Saito, Y. Yoshimatsu, D. Seigneurin-Berny, H. Osada, Y. Komatsu, N. Nishino, S. Khochbin, S. Horinouchi, and M. Yoshida. In vivo destabilization of dynamic microtubules by HDAC6-mediated deacetylation. *Embo J.*, 21(24):6820–31., 2002.

M. J. Matunis, E. Coutavas, and G. Blobel. A novel ubiquitin-like modification modulates the partitioning of the Ran-GTPase-activating protein RanGAP1 between the cytosol and the nuclear pore complex. *J Cell Biol*, 135(6 Pt 1):1457–1470, Dec 1996.

H. McDonough and C. Patterson. CHIP: a link between the chaperone and proteasome systems. *Cell Stress Chaperones*, 8(4):303–308, 2003.

B. Meusser, C. Hirsch, E. Jarosch, and T. Sommer. ERAD: the long road to destruction. *Nat Cell Biol*, 7(8):766–772, Aug 2005.

J. Miller and C. Gordon. The regulation of proteasome degradation by multi-ubiquitin chain binding proteins. *FEBS Lett*, 579(15):3224–3230, Jun 2005.

R. D. Miller, L. Prakash, and S. Prakash. Defective excision of pyrimidine dimers and interstrand DNA crosslinks in rad7 and rad23 mutants of Saccharomyces cerevisiae. *Mol Gen Genet*, 188 (2):235–239, 1982.

N. Mizushima. Autophagy: process and function. *Genes Dev*, 21(22):2861–2873, Nov 2007.

N. Mizushima and D. J. Klionsky. Protein turnover via autophagy: implications for metabolism. *Annu Rev Nutr*, 27:19–40, 2007.

D. Moradpour, B. Grabscheid, A. R. Kammer, G. Schmidtke, M. Groettrup, H. E. Blum, and A. Cerny. Expression of hepatitis C virus proteins does not interfere with major histocompatibility complex class I processing and presentation in vitro. *Hepatology*, 33(5):1282–1287, May 2001.

P. Munro, G. Flatau, and E. Lemichez. Bacteria and the ubiquitin pathway. *Curr Opin Microbiol*, 10(1):39–46, Feb 2007.

Y. Murakami, S. Matsufuji, T. Kameji, S. Hayashi, K. Igarashi, T. Tamura, K. Tanaka, and A. Ichihara. Ornithine decarboxylase is degraded by the 26S proteasome without ubiquitination. *Nature*, 360(6404):597–599, Dec 1992.

S. Murata, K. Sasaki, T. Kishimoto, S.-I. Niwa, H. Hayashi, Y. Takahama, and K. Tanaka. Regulation of CD8+ T cell development by thymus-specific proteasomes. *Science*, 316(5829):1349–1353, Jun 2007.

P. J. Murphy, Y. Morishima, J. J. Kovacs, T. P. Yao, and W. B. Pratt. Regulation of the dynamics of hsp90 action on the glucocorticoid receptor by acetylation/deacetylation of the chaperone. *J Biol Chem.*, 280(40):33792–9. Epub 2005 Aug 8., 2005.

S. Müller, C. Hoege, G. Pyrowolakis, and S. Jentsch. SUMO, ubiquitin's mysterious cousin. *Nat Rev Mol Cell Biol*, 2(3):202–210, Mar 2001.

U. Nagaoka, K. Kim, N. R. Jana, H. Doi, M. Maruyama, K. Mitsui, F. Oyama, and N. Nukina. Increased expression of p62 in expanded polyglutamine-expressing cells and its association with polyglutamine inclusions. *J Neurochem*, 91(1):57–68, Oct 2004.

J. Narasimhan, M. Wang, Z. Fu, J. M. Klein, A. L. Haas, and J.-J. P. Kim. Crystal structure of the interferon-induced ubiquitin-like protein ISG15. *J Biol Chem*, 280(29):27356–27365, Jul 2005.

E. A. Nigg. Cyclin-dependent protein kinases: key regulators of the eukaryotic cell cycle. *Bioessays*, 17(6):471–480, Jun 1995.

A. Nopora and T. Brocker. Bcl-2 controls dendritic cell longevity in vivo. *J Immunol*, 169(6): 3006–3014, Sep 2002.

A. J. Obaya and J. M. Sedivy. Regulation of cyclin-Cdk activity in mammalian cells. *Cell Mol Life Sci*, 59(1):126–142, Jan 2002.

Y. Ohsumi. Molecular dissection of autophagy: two ubiquitin-like systems. *Nat Rev Mol Cell Biol*, 2(3):211–216, Mar 2001.

C. W. Olanow, D. P. Perl, G. N. DeMartino, and K. S. P. McNaught. Lewy-body formation is an aggresome-related process: a hypothesis. *Lancet Neurol*, 3(8):496–503, Aug 2004.

J. Oliva, F. Bardag-Gorce, B. A. French, J. Li, L. McPhaul, F. Amidi, J. Dedes, A. Habibi, S. Nguyen, and S. W. French. Fat10 is an epigenetic marker for liver preneoplasia in a drug-primed mouse model of tumorigenesis. *Exp Mol Pathol*, 84(2):102–112, Apr 2008.

J. A. Olzmann and L.-S. Chin. Parkin-mediated K63-linked polyubiquitination: a signal for targeting misfolded proteins to the aggresome-autophagy pathway. *Autophagy*, 4(1):85–87, Jan 2008.

J. A. Olzmann, L. Li, M. V. Chudaev, J. Chen, F. A. Perez, R. D. Palmiter, and L.-S. Chin. Parkin-mediated K63-linked polyubiquitination targets misfolded DJ-1 to aggresomes via binding to HDAC6. *J Cell Biol*, 178(6):1025–1038, Sep 2007.

T. G. Ortolan, P. Tongaonkar, D. Lambertson, L. Chen, C. Schauber, and K. Madura. The DNA repair protein rad23 is a negative regulator of multi-ubiquitin chain assembly. *Nat Cell Biol*, 2 (9):601–608, Sep 2000.

F. Osaka, M. Saeki, S. Katayama, N. Aida, A. Toh-E, K. Kominami, T. Toda, T. Suzuki, T. Chiba, K. Tanaka, and S. Kato. Covalent modifier NEDD8 is essential for SCF ubiquitin-ligase in fission yeast. *EMBO J*, 19(13):3475–3484, Jul 2000.

M.-T. Pai, S.-R. Tzeng, J. J. Kovacs, M. A. Keaton, S. S.-C. Li, T.-P. Yao, and P. Zhou. Solution structure of the Ubp-M BUZ domain, a highly specific protein module that recognizes the C-terminal tail of free ubiquitin. *J Mol Biol*, 370(2):290–302, Jul 2007.

A. Palazzo, B. Ackerman, and G. G. Gundersen. Cell biology: Tubulin acetylation and cell motility. *Nature*, 421(6920):230, Jan 2003.

Z.-Q. Pan, A. Kentsis, D. C. Dias, K. Yamoah, and K. Wu. Nedd8 on cullin: building an expressway to protein destruction. *Oncogene*, 23(11):1985–1997, Mar 2004.

U. B. Pandey, Y. Batlevi, E. H. Baehrecke, and J. P. Taylor. HDAC6 at the intersection of autophagy, the ubiquitin-proteasome system and neurodegeneration. *Autophagy*, 3(6):643–645, 2007a.

U. B. Pandey, Z. Nie, Y. Batlevi, B. A. McCray, G. P. Ritson, N. B. Nedelsky, S. L. Schwartz, N. A. DiProspero, M. A. Knight, O. Schuldiner, R. Padmanabhan, M. Hild, D. L. Berry, D. Garza, C. C. Hubbert, T.-P. Yao, E. H. Baehrecke, and J. P. Taylor. HDAC6 rescues neurodegeneration and provides an essential link between autophagy and the UPS. *Nature*, 447(7146):859–863, Jun 2007b.

S. Pankiv, T. H. Clausen, T. Lamark, A. Brech, J.-A. Bruun, H. Outzen, A. Øvervatn, G. Bjørkøy, and T. Johansen. p62/SQSTM1 binds directly to Atg8/LC3 to facilitate degradation of ubiquitinated protein aggregates by autophagy. *J Biol Chem*, 282(33):24131–24145, Aug 2007.

F. R. Papa, A. Y. Amerik, and M. Hochstrasser. Interaction of the Doa4 deubiquitinating enzyme with the yeast 26S proteasome. *Mol Biol Cell*, 10(3):741–756, Mar 1999.

J.-H. Park, H.-S. Jong, S. G. Kim, Y. Jung, K.-W. Lee, J.-H. Lee, D.-K. Kim, Y.-J. Bang, and T.-Y. Kim. Inhibitors of histone deacetylases induce tumor-selective cytotoxicity through modulating Aurora-A kinase. *J Mol Med*, 86(1):117–128, Jan 2008.

C. Pelzer, I. Kassner, K. Matentzoglu, R. K. Singh, H.-P. Wollscheid, M. Scheffner, G. Schmidtke, and M. Groettrup. UBE1L2, a novel E1 enzyme specific for ubiquitin. *J Biol Chem*, 282(32): 23010–23014, Aug 2007.

C. M. Pickart. Mechanisms underlying ubiquitination. *Annu Rev Biochem*, 70:503–533, 2001.

C. M. Pickart and D. Fushman. Polyubiquitin chains: polymeric protein signals. *Curr Opin Chem Biol*, 8(6):610–616, Dec 2004.

P. Pierre. Dendritic cells, DRiPs, and DALIS in the control of antigen processing. *Immunol Rev*, 207:184–190, Oct 2005.

S. Raasi. *Functional analysis of FAT10, a cytokine-inducible ubiquitin-like protein.* PhD thesis, ETH Zürich, 2001.

S. Raasi and C. M. Pickart. Rad23 ubiquitin-associated domains (UBA) inhibit 26 S proteasome-catalyzed proteolysis by sequestering lysine 48-linked polyubiquitin chains. *J Biol Chem*, 278 (11):8951–8959, Mar 2003.

S. Raasi, G. Schmidtke, R. de Giuli, and M. Groettrup. A ubiquitin-like protein which is synergistically inducible by interferon-gamma and tumor necrosis factor-alpha. *Eur J Immunol.*, 29 (12):4030–6., 1999.

S. Raasi, G. Schmidtke, and M. Groettrup. The ubiquitin-like protein FAT10 forms covalent conjugates and induces apoptosis. *J Biol Chem.*, 276(38):35334–43. Epub 2001 Jul 9., 2001.

S. Raasi, I. Orlov, K. G. Fleming, and C. M. Pickart. Binding of polyubiquitin chains to ubiquitin-associated (UBA) domains of HHR23A. *J Mol Biol.*, 341(5):1367–79., 2004.

S. Raasi, R. Varadan, D. Fushman, and C. M. Pickart. Diverse polyubiquitin interaction properties of ubiquitin-associated domains. *Nat Struct Mol Biol*, 12(8):708–714, Aug 2005.

H. Rao and A. Sastry. Recognition of specific ubiquitin conjugates is important for the proteolytic functions of the ubiquitin-associated domain proteins Dsk2 and Rad23. *J Biol Chem*, 277(14): 11691–11695, Apr 2002.

W. S. Rasband. ImageJ. U. S. National Institutes of Health, Bethesda, Maryland, USA, http://rsb.info.nih.gov/ij/, 1997-2008.

M. Rechsteiner and C. P. Hill. Mobilizing the proteolytic machine: cell biological roles of proteasome activators and inhibitors. *Trends Cell Biol*, 15(1):27–33, Jan 2005.

M. Rechsteiner, C. Realini, and V. Ustrell. The proteasome activator 11 S REG (PA28) and class I antigen presentation. *Biochem J*, 345 Pt 1:1–15, Jan 2000.

M. Recht, E. C. Borden, and E. Knight. A human 15-kDa IFN-induced protein induces the secretion of IFN-gamma. *J Immunol*, 147(8):2617–2623, Oct 1991.

N. A. Reed, D. Cai, T. L. Blasius, G. T. Jih, E. Meyhofer, J. Gaertig, and K. J. Verhey. Microtubule acetylation promotes kinesin-1 binding and transport. *Curr Biol*, 16(21):2166–2172, Nov 2006.

Y. Refaeli, L. V. Parijs, C. A. London, J. Tschopp, and A. K. Abbas. Biochemical mechanisms of IL-2-regulated Fas-mediated T cell apoptosis. *Immunity*, 8(5):615–623, May 1998.

J. Ren, A. Kan, S. H. Leong, L. L. Ooi, K. T. Jeang, S. S. Chong, O. L. Kon, and C. G. Lee. Fat10 plays a role in the regulation of chromosomal stability. *J Biol Chem*, 22:22, 2006.

F. E. Reyes-Turcu, J. R. Horton, J. E. Mullally, A. Heroux, X. Cheng, and K. D. Wilkinson. The ubiquitin binding domain ZnF UBP recognizes the C-terminal diglycine motif of unanchored ubiquitin. *Cell*, 124(6):1197–1208, Mar 2006.

K. J. Ritchie, C. S. Hahn, K. I. Kim, M. Yan, D. Rosario, L. Li, J. C. de la Torre, and D. E. Zhang. Role of ISG15 protease UBP43 (USP18) in innate immunity to viral infection. *Nat Med.*, 10 (12):1374–8. Epub 2004 Nov 7., 2004.

M. S. Rodriguez, J. M. Desterro, S. Lain, C. A. Midgley, D. P. Lane, and R. T. Hay. SUMO-1 modification activates the transcriptional response of p53. *EMBO J*, 18(22):6455–6461, Nov 1999.

M. J. Ross, M. S. Wosnitzer, M. D. Ross, B. Granelli, G. L. Gusella, M. Husain, L. Kaufman, M. Vasievich, V. D. D'Agati, P. D. Wilson, M. E. Klotman, and P. E. Klotman. Role of Ubiquitin-Like Protein FAT10 in Epithelial Apoptosis in Renal Disease. *J Am Soc Nephrol*, 22:22, 2006.

S. Rumpf and S. Jentsch. Functional division of substrate processing cofactors of the ubiquitin-selective Cdc48 chaperone. *Mol Cell*, 21(2):261–269, Jan 2006.

K. Römisch. Cdc48p is UBX-linked to ER ubiquitin ligases. *Trends Biochem Sci*, 31(1):24–25, Jan 2006.

Y. Saeki, A. Saitoh, A. Toh-e, and H. Yokosawa. Ubiquitin-like proteins and Rpn10 play cooperative roles in ubiquitin-dependent proteolysis. *Biochem Biophys Res Commun*, 293(3):986–992, May 2002a.

Y. Saeki, T. Sone, A. Toh-e, and H. Yokosawa. Identification of ubiquitin-like protein-binding subunits of the 26S proteasome. *Biochem Biophys Res Commun*, 296(4):813–819, Aug 2002b.

E. Sakata, Y. Yamaguchi, E. Kurimoto, J. Kikuchi, S. Yokoyama, S. Yamada, H. Kawahara, H. Yokosawa, N. Hattori, Y. Mizuno, K. Tanaka, and K. Kato. Parkin binds the Rpn10 subunit of 26S proteasomes through its ubiquitin-like domain. *EMBO Rep*, 4(3):301–306, Mar 2003.

E. Sandalova, C.-H. Wei, M. G. Masucci, and V. Levitsky. Regulation of expression of Bcl-2 protein family member Bim by T cell receptor triggering. *Proc Natl Acad Sci U S A*, 101(9):3011–3016, Mar 2004.

C. Schauber, L. Chen, P. Tongaonkar, I. Vega, D. Lambertson, W. Potts, and K. Madura. Rad23 links DNA repair to the ubiquitin/proteasome pathway. *Nature*, 391(6668):715–718, Feb 1998.

M. Scheffner, J. M. Huibregtse, and P. M. Howley. Identification of a human ubiquitin-conjugating enzyme that mediates the E6-AP-dependent ubiquitination of p53. *Proc Natl Acad Sci U S A*, 91(19):8797–8801, Sep 1994.

E. Schlosser, M. Mueller, S. Fischer, S. Basta, D. H. Busch, B. Gander, and M. Groettrup. TLR ligands and antigen need to be coencapsulated into the same biodegradable microsphere for the generation of potent cytotoxic T lymphocyte responses. *Vaccine*, 26(13):1626–1637, Mar 2008.

D. Schmid and C. Münz. Innate and adaptive immunity through autophagy. *Immunity*, 27(1): 11–21, Jul 2007.

M. Schmidt, J. Hanna, S. Elsasser, and D. Finley. Proteasome-associated proteins: regulation of a proteolytic machine. *Biol Chem*, 386(8):725–737, Aug 2005.

G. Schmidtke, R. Kraft, S. Kostka, P. Henklein, C. Frömmel, J. Löwe, R. Huber, P. M. Kloetzel, and M. Schmidt. Analysis of mammalian 20S proteasome biogenesis: the maturation of beta-subunits is an ordered two-step mechanism involving autocatalysis. *EMBO J*, 15(24):6887–6898, Dec 1996.

G. Schmidtke, S. Emch, M. Groettrup, and H. G. Holzhutter. Evidence for the existence of a non-catalytic modifier site of peptide hydrolysis by the 20 S proteasome. *J Biol Chem*, 275(29): 22056–22063, Jul 2000.

G. Schmidtke, B. Kalveram, E. Weber, P. Bochtler, S. Lukasiak, M. S. Hipp, and M. Groettrup. The UBA domains of NUB1L are required for binding but not for accelerated degradation of the ubiquitin-like modifier FAT10. *J. Biol. Chem.*, 281(29):20045–20054, Jul 2006.

I. Schmitz, A. Krueger, S. Baumann, H. Schulze-Bergkamen, P. H. Krammer, and S. Kirchhoff. An IL-2-dependent switch between CD95 signaling pathways sensitizes primary human T cells toward CD95-mediated activation-induced cell death. *J Immunol*, 171(6):2930–2936, Sep 2003.

I. Schmitz, H. Weyd, A. Krueger, S. Baumann, S. C. Fas, P. H. Krammer, and S. Kirchhoff. Resistance of short term activated T cells to CD95-mediated apoptosis correlates with de novo protein synthesis of c-FLIPshort. *J Immunol*, 172(4):2194–2200, Feb 2004.

P. Schreiner, X. Chen, K. Husnjak, L. Randles, N. Zhang, S. Elsasser, D. Finley, I. Dikic, K. J. Walters, and M. Groll. Ubiquitin docking at the proteasome through a novel pleckstrin-homology domain interaction. *Nature*, 453(7194):548–552, May 2008.

U. Schubert, L. C. Antón, J. Gibbs, C. C. Norbury, J. W. Yewdell, and J. R. Bennink. Rapid degradation of a large fraction of newly synthesized proteins by proteasomes. *Nature*, 404(6779): 770–774, Apr 2000.

M. Seeger, R. Hartmann-Petersen, C. R. M. Wilkinson, M. Wallace, I. Samejima, M. S. Taylor, and C. Gordon. Interaction of the anaphase-promoting complex/cyclosome and proteasome protein complexes with multiubiquitin chain-binding proteins. *J Biol Chem*, 278(19):16791–16796, May 2003.

M. L. Seibenhener, J. R. Babu, T. Geetha, H. C. Wong, N. R. Krishna, and M. W. Wooten. Sequestosome 1/p62 is a polyubiquitin chain binding protein involved in ubiquitin proteasome degradation. *Mol Cell Biol*, 24(18):8055–8068, Sep 2004.

D. Seigneurin-Berny, A. Verdel, S. Curtet, C. Lemercier, J. Garin, S. Rousseaux, and S. Khochbin. Identification of components of the murine histone deacetylase 6 complex: link between acetylation and ubiquitination signaling pathways. *Mol Cell Biol.*, 21(23):8035–44., 2001.

J. M. Serrador, J. R. Cabrero, D. Sancho, M. Mittelbrunn, A. Urzainqui, and F. Sanchez-Madrid. HDAC6 deacetylase activity links the tubulin cytoskeleton with immune synapse organization. *Immunity.*, 20(4):417–28., 2004.

H. Shimura, N. Hattori, S. Kubo, Y. Mizuno, S. Asakawa, S. Minoshima, N. Shimizu, K. Iwai, T. Chiba, K. Tanaka, and T. Suzuki. Familial Parkinson disease gene product, parkin, is a ubiquitin-protein ligase. *Nat Genet*, 25(3):302–305, Jul 2000.

J. Shin. P62 and the sequestosome, a novel mechanism for protein metabolism. *Arch Pharm Res*, 21(6):629–633, Dec 1998.

E. Shvets, E. Fass, R. Scherz-Shouval, and Z. Elazar. The N-terminus and Phe52 residue of LC3 recruit p62/SQSTM1 into autophagosomes. *J Cell Sci*, 121(Pt 16):2685–2695, Aug 2008.

R. Sirkis, J. E. Gerst, and D. Fass. Ddi1, a eukaryotic protein with the retroviral protease fold. *J Mol Biol*, 364(3):376–387, Dec 2006.

K. E. Sloper-Mould, J. C. Jemc, C. M. Pickart, and L. Hicke. Distinct functional surface regions on ubiquitin. *J Biol Chem*, 276(32):30483–30489, Aug 2001.

D. M. Smith, N. Benaroudj, and A. Goldberg. Proteasomes and their associated ATPases: a destructive combination. *J Struct Biol*, 156(1):72–83, Oct 2006.

J. Sprent and D. F. Tough. T cell death and memory. *Science*, 293(5528):245–248, Jul 2001.

H. K. Sytwu, R. S. Liblau, and H. O. McDevitt. The roles of Fas/APO-1 (CD95) and TNF in antigen-induced programmed cell death in T cell receptor transgenic mice. *Immunity*, 5(1):17–30, Jul 1996.

T. Tanaka, H. Kawashima, E. T. H. Yeh, and T. Kamitani. Regulation of the NEDD8 conjugation system by a splicing variant, NUB1L. *J Biol Chem*, 278(35):32905–32913, Aug 2003.

T. Tanaka, E. T. H. Yeh, and T. Kamitani. NUB1-mediated targeting of the ubiquitin precursor UbC1 for its C-terminal hydrolysis. *Eur J Biochem*, 271(5):972–982, Mar 2004.

K. Tanji, T. Tanaka, and T. Kamitani. Interaction of NUB1 with the proteasome subunit S5a. *Biochem Biophys Res Commun*, 337(1):116–120, Nov 2005.

K. Tanji, T. Tanaka, F. Mori, K. Kito, H. Takahashi, K. Wakabayashi, and T. Kamitani. NUB1 suppresses the formation of Lewy body-like inclusions by proteasomal degradation of synphilin-1. *Am J Pathol*, 169(2):553–565, Aug 2006.

K. Tanji, F. Mori, A. Kakita, H. Zhang, K. Kito, T. Kamitani, H. Takahashi, and K. Wakabayashi. Immunohistochemical localization of NUB1, a synphilin-1-binding protein, in neurodegenerative disorders. *Acta Neuropathol (Berl)*, 4:365–371, Jun 2007.

M. H. Tatham, E. Jaffray, O. A. Vaughan, J. M. Desterro, C. H. Botting, J. H. Naismith, and R. T. Hay. Polymeric chains of SUMO-2 and SUMO-3 are conjugated to protein substrates by SAE1/SAE2 and Ubc9. *J Biol Chem*, 276(38):35368–35374, Sep 2001.

M. H. Tatham, M.-C. Geoffroy, L. Shen, A. Plechanovova, N. Hattersley, E. G. Jaffray, J. J. Palvimo, and R. T. Hay. RNF4 is a poly-SUMO-specific E3 ubiquitin ligase required for arsenic-induced PML degradation. *Nat Cell Biol*, 10(5):538–546, May 2008.

J. P. Taylor, F. Tanaka, J. Robitschek, C. M. Sandoval, A. Taye, S. Markovic-Plese, and K. H. Fischbeck. Aggresomes protect cells by enhancing the degradation of toxic polyglutamine-containing protein. *Hum Mol Genet*, 12(7):749–757, Apr 2003.

A. Thorburn. Apoptosis and autophagy: regulatory connections between two supposedly different processes. *Apoptosis*, 13(1):1–9, Jan 2008.

J. S. Thrower, L. Hoffman, M. Rechsteiner, and C. M. Pickart. Recognition of the polyubiquitin proteolytic signal. *EMBO J*, 19(1):94–102, Jan 2000.

G. K. Tofaris, R. Layfield, and M. G. Spillantini. alpha-synuclein metabolism and aggregation is linked to ubiquitin-independent degradation by the proteasome. *FEBS Lett*, 509(1):22–26, Nov 2001.

R. Touitou, J. Richardson, S. Bose, M. Nakanishi, J. Rivett, and M. J. Allday. A degradation signal located in the C-terminus of p21WAF1/CIP1 is a binding site for the C8 alpha-subunit of the 20S proteasome. *EMBO J*, 20(10):2367–2375, May 2001.

A. Townsend and J. Trowsdale. The transporters associated with antigen presentation. *Semin Cell Biol*, 4(1):53–61, Feb 1993.

A. D.-A. Tran, T. P. Marmo, A. A. Salam, S. Che, E. Finkelstein, R. Kabarriti, H. S. Xenias, R. Mazitschek, C. Hubbert, Y. Kawaguchi, M. P. Sheetz, T.-P. Yao, and J. C. Bulinski. HDAC6 deacetylation of tubulin modulates dynamics of cellular adhesions. *J Cell Sci*, ?(3):?, Mar 2007.

A. Valenzuela-Fernandez, S. Alvarez, M. Gordon-Alonso, M. Barrero, A. Ursa, J. R. Cabrero, G. Fernandez, S. Naranjo-Suarez, M. Yanez-Mo, J. M. Serrador, M. A. Munoz-Fernandez, and F. Sanchez-Madrid. Histone Deacetylase 6 Regulates Human Immunodeficiency Virus Type 1 Infection. *Mol Biol Cell*, 7:7, 2005.

R. G. van der Most, A. Sette, C. Oseroff, J. Alexander, K. Murali-Krishna, L. L. Lau, S. Southwood, J. Sidney, R. W. Chesnut, M. Matloubian, and R. Ahmed. Analysis of cytotoxic T cell responses to dominant and subdominant epitopes during acute and chronic lymphocytic choriomeningitis virus infection. *J Immunol*, 157(12):5543–5554, Dec 1996.

R. G. van der Most, K. Murali-Krishna, J. G. Lanier, E. J. Wherry, M. T. Puglielli, J. N. Blattman, A. Sette, and R. Ahmed. Changing immunodominance patterns in antiviral CD8 T-cell responses after loss of epitope presentation or chronic antigenic stimulation. *Virology*, 315(1): 93–102, Oct 2003.

J. van der Spuy and M. E. Cheetham. The Leber congenital amaurosis protein AIPL1 modulates the nuclear translocation of NUB1 and suppresses inclusion formation by NUB1 fragments. *J Biol Chem*, 279(46):48038–48047, Nov 2004.

J. van der Spuy, J. H. Kim, Y. S. Yu, A. Szel, P. J. Luthert, B. J. Clark, and M. E. Cheetham. The expression of the Leber congenital amaurosis protein AIPL1 coincides with rod and cone photoreceptor development. *Invest Ophthalmol Vis Sci*, 44(12):5396–5403, Dec 2003.

S. van Nocker, S. Sadis, D. M. Rubin, M. Glickman, H. Fu, O. Coux, I. Wefes, D. Finley, and R. D. Vierstra. The multiubiquitin-chain-binding protein Mcb1 is a component of the 26S proteasome in Saccharomyces cerevisiae and plays a nonessential, substrate-specific role in protein turnover. *Mol Cell Biol*, 16(11):6020–6028, Nov 1996.

A. Verdel and S. Khochbin. Identification of a new family of higher eukaryotic histone deacetylases. Coordinate expression of differentiation-dependent chromatin modifiers. *J Biol Chem*, 274(4):2440–2445, Jan 1999.

R. Verma, R. Oania, J. Graumann, and R. J. Deshaies. Multiubiquitin chain receptors define a layer of substrate selectivity in the ubiquitin-proteasome system. *Cell*, 118(1):99–110, Jul 2004a.

R. Verma, N. R. Peters, M. D'Onofrio, G. P. Tochtrop, K. M. Sakamoto, R. Varadan, M. Zhang, P. Coffino, D. Fushman, R. J. Deshaies, and R. W. King. Ubistatins inhibit proteasome-dependent degradation by binding the ubiquitin chain. *Science.*, 306(5693):117–20., 2004b.

S. Vijay-Kumar, C. E. Bugg, and W. J. Cook. Structure of ubiquitin refined at 1.8 A resolution. *J Mol Biol*, 194(3):531–544, Apr 1987.

A. G. von Arnim. A hitchhiker's guide to the proteasome. *Sci STKE*, 2001(97):PE2, Aug 2001.

K. J. Walters, M. F. Kleijnen, A. M. Goh, G. Wagner, and P. M. Howley. Structural studies of the interaction between ubiquitin family proteins and proteasome subunit S5a. *Biochemistry.*, 41 (6):1767–77., 2002.

R. L. Welchman, C. Gordon, and R. J. Mayer. Ubiquitin and ubiquitin-like proteins as multifunctional signals. *Nat Rev Mol Cell Biol*, 6(8):599–609, Aug 2005.

T. Wileman. Aggresomes and autophagy generate sites for virus replication. *Science*, 312(5775): 875–878, May 2006.

C. R. Wilkinson, M. Seeger, R. Hartmann-Petersen, M. Stone, M. Wallace, C. Semple, and C. Gordon. Proteins containing the UBA domain are able to bind to multi-ubiquitin chains. *Nat Cell Biol*, 3(10):939–943, Oct 2001.

M. I. Wilson, D. J. Gill, O. Perisic, M. T. Quinn, and R. L. Williams. PB1 domain-mediated heterodimerization in NADPH oxidase and signaling complexes of atypical protein kinase C with Par6 and p62. *Mol Cell*, 12(1):39–50, Jul 2003.

Z. Xie and D. J. Klionsky. Autophagosome formation: core machinery and adaptations. *Nat Cell Biol*, 9(10):1102–1109, Oct 2007.

W. Xiong, X. Wang, X.-Y. Liu, L. Xiang, L.-J. Zheng, J.-X. Liu, and Z.-H. Yuan. Analysis of gene expression in hepatitis B virus transfected cell line induced by interferon. *Sheng Wu Hua Xue Yu Sheng Wu Wu Li Xue Bao (Shanghai)*, 35(12):1053–1060, Dec 2003.

D. P. Xirodimas, M. K. Saville, J. C. Bourdon, R. T. Hay, and D. P. Lane. Mdm2-mediated NEDD8 conjugation of p53 inhibits its transcriptional activity. *Cell.*, 118(1):83–97., 2004.

S. D. Yan, H. Zhu, A. Zhu, A. Golabek, H. Du, A. Roher, J. Yu, C. Soto, A. M. Schmidt, D. Stern, and M. Kindy. Receptor-dependent cell stress and amyloid accumulation in systemic amyloidosis. *Nat Med*, 6(6):643–651, Jun 2000.

X.-J. Yang and S. Grégoire. Class II histone deacetylases: from sequence to function, regulation, and clinical implication. *Mol Cell Biol*, 25(8):2873–2884, Apr 2005.

T. Yao, L. Song, W. Xu, G. N. DeMartino, L. Florens, S. K. Swanson, M. P. Washburn, R. C. Conaway, J. W. Conaway, and R. E. Cohen. Proteasome recruitment and activation of the Uch37 deubiquitinating enzyme by Adrm1. *Nat Cell Biol*, 8(9):994–1002, Sep 2006.

E. T. Yeh, L. Gong, and T. Kamitani. Ubiquitin-like proteins: new wines in new bottles. *Gene*, 248 (1-2):1–14, May 2000.

J. W. Yewdell, L. C. Antón, and J. R. Bennink. Defective ribosomal products (DRiPs): a major source of antigenic peptides for MHC class I molecules? *J Immunol*, 157(5):1823–1826, Sep 1996.

J. W. Yewdell, U. Schubert, and J. R. Bennink. At the crossroads of cell biology and immunology: DRiPs and other sources of peptide ligands for MHC class I molecules. *J Cell Sci*, 114(Pt 5): 845–851, Mar 2001.

W. M. Yokoyama, M. Christensen, G. Dos Santos, and D. Miller. *Current Protocols in Immunology: Unit 2.5 Production of Monoclonal Antibodies*. John Wiley & Sons, 2006.

W. Yuan and R. M. Krug. Influenza B virus NS1 protein inhibits conjugation of the interferon (IFN)-induced ubiquitin-like ISG15 protein. *EMBO J*, 20(3):362–371, Feb 2001.

K. Zatloukal, C. Stumptner, A. Fuchsbichler, H. Heid, M. Schnoelzer, L. Kenner, R. Kleinert, M. Prinz, A. Aguzzi, and H. Denk. p62 Is a common component of cytoplasmic inclusions in protein aggregation diseases. *Am J Pathol*, 160(1):255–263, Jan 2002.

K. Zatloukal, S. W. French, C. Stumptner, P. Strnad, M. Harada, D. M. Toivola, M. Cadrin, and M. B. Omary. From Mallory to Mallory-Denk bodies: what, how and why? *Exp Cell Res*, 313 (10):2033–2049, Jun 2007.

D. Zhang, S. Raasi, and D. Fushman. Affinity makes the difference: nonselective interaction of the UBA domain of Ubiquilin-1 with monomeric ubiquitin and polyubiquitin chains. *J Mol Biol*, 377(1):162–180, Mar 2008a.

D. W. Zhang, K. T. Jeang, and C. G. Lee. p53 negatively regulates the expression of FAT10, a gene upregulated in various cancers. *Oncogene*, 27:27, 2006a.

M. Zhang, C. M. Pickart, and P. Coffino. Determinants of proteasome recognition of ornithine decarboxylase, a ubiquitin-independent substrate. *EMBO J*, 22(7):1488–1496, Apr 2003a.

X. Zhang, Z. Yuan, Y. Zhang, S. Yong, A. Salas-Burgos, J. Koomen, N. Olashaw, J. T. Parsons, X.-J. Yang, S. R. Dent, T.-P. Yao, W. S. Lane, and E. Seto. HDAC6 modulates cell motility by altering the acetylation level of cortactin. *Mol Cell*, 27(2):197–213, Jul 2007.

Y. Zhang, N. Li, C. Caron, G. Matthias, D. Hess, S. Khochbin, and P. Matthias. HDAC-6 interacts with and deacetylates tubulin and microtubules in vivo. *Embo J.*, 22(5):1168–79., 2003b.

Y. Zhang, B. Gilquin, S. Khochbin, and P. Matthias. Two catalytic domains are required for protein deacetylation. *J Biol Chem.*, 281(5):2401–4. Epub 2005 Nov 6., 2006b.

Y. Zhang, S. Kwon, T. Yamaguchi, F. Cubizolles, S. Rousseaux, M. Kneissel, C. Cao, N. Li, H.-L. Cheng, K. Chua, D. Lombard, A. Mizeracki, G. Matthias, F. W. Alt, S. Khochbin, and P. Matthias. Mice lacking histone deacetylase 6 have hyperacetylated tubulin but are viable and develop normally. *Mol Cell Biol*, 28(5):1688–1701, Mar 2008b.

S. Zhong, S. Müller, S. Ronchetti, P. S. Freemont, A. Dejean, and P. P. Pandolfi. Role of SUMO-1-modified PML in nuclear body formation. *Blood*, 95(9):2748–2752, May 2000.

Abbreviations

aa	amino acid
AAA	ATPase associated with various cellular activities
Ab	antibody
ACAD	activated cell-autonomous death
AICD	activation-induced cell death
AIPL1	aryl hydrocarbon receptor-interacting protein-like 1
APC	anaphase promoting complex
ATG	autophagy related
ATP	adenosine-5'-triphosphate
AZ	antizyme
BAG	Bcl-2-associated athanogene
BMDCs	bone marrow-derived dendritic cells
BrdU	bromodeoxyuridine
BUZ	binder of ubiquitin zinc-finger
C-terminal	carboxy-terminal
CAT	catalytic (domain)
cDNA	complementary DNA
CHIP	carboxyl-terminus of HSC70 interacting protein
cpm	counts per minute
DALIS	dendritic cell aggresome-like induced structures
DC	dendritic cell
DHFR	dihydrofolate reductase
DLB	dementia with Lewy bodies
DNA	deoxyribonucleic acid
DUB	de-ubiquitinating enzyme
E6-AP	E6-associated protein
ER	endoplasmatic reticulum
ERAD	endoplasmatic reticulum-associated degradation
FAT10	HLA-F locus associated transcript
GAPDH	glyceraldehyde 3-phosphate dehydrogenase
GFP	green fluorescent protein
GSH	glutathione
GST	glutathione-S-transferase
HA	hemagglutinin
HDAC	histone deacetylase
HECT	homologous to E6-AP carboxyl-terminus
HIV	human immunodeficiency virus
HSC	heat-shock cognate
HSF1	heat-shock factor 1
HSP	heat-shock protein

IAP	inhibitor of apoptosis
IF	immunofluorescence
IFN	interferon
IκBα	NF-κB inhibitory protein α
IL	interleukin
IP	immunoprecipitation
IPTG	isopropylβ-D-1-thiogalactopyranoside
ISG15	interferon-stimulated gene 15
LB	Lewy body
LCA	Leber congenital amaurosis
LCMV	lymphocytic choriomeningitis virus
LMP	low molecular-weight protein
LPS	lipopolysaccharide
MCMV	mouse cytomegalovirus
MHC	major histocompatibility locus
mRNA	messenger ribonucleic acid
MTOC	microtubule organizing center
N-terminal	amino-terminal
NEDD8	neuronal precursor cell-expressed developmentally down-regulated 8
NF-κB	nuclear factor-κB
NLS	nuclear localization signal
NUB1	NEDD8 ultimate buster 1
NUB1L	NEDD8 ultimate buster 1-Long
ODC	ornithine decarboxylase
PCR	polymerase chain reaction
PD	Parkinson's disease
Pi	orthophosphate ion
PML	promyelotic leukemia
qRT	quantitative real-time
RING	really interesting new gene
RT	room temperature
SCF	Skp1-Cullin-F-box protein
shRNA	short hairpin RNA
siRNA	small interfering RNA
SUMO	small ubiquitin-like modifier
TLR	Toll-like receptor
TNF	tumor necrosis factor
TNFR	tumor necrosis factor receptor
TSA	trichostatin A
Ub	ubiquitin
UBA	ubiquitin associated
UBD	ubiquitin domain protein
UbL	ubiquitin-like modifier
UBL	ubiquitin-like
ULP	UbL-specific protease
UPS	ubiquitin proteasome system
VCP	valoisin containing protein
WB	Western blot
wt	wild-type

Amino Acids

Alanine	Ala	A
Arginine	Arg	R
Asparagine	Asn	N
Aspartic acid	Asp	D
Cysteine	Cys	C
Glutamine	Gln	Q
Glutamic acid	Glu	E
Glycine	Gly	G
Histidine	His	H
Isoleucine	Ile	I
Leucine	Leu	L
Lysine	Lys	K
Methionine	Met	K
Phenylalanine	Phe	F
Proline	Pro	P
Serine	Ser	S
Threonine	Thr	T
Tryptophane	Trp	W
Tyrosine	Tyr	Y
Valine	Val	V

Record of Contributions

Chapter 1: The UBA domains of NUB1L are required for binding but not for accelerated degradation of the ubiquitin-like modifier FAT10

I performed the experiments depicted in figures 6, 13G and 13H and helped write the paper. This chapter was published in *J. Biol. Chem.* 281(29): 20045-54. 2006.

Chapter 2: Degradation of FAT10 by the 26S proteasome *in vitro* is independent of ubiquitylation but relies on NUB1L

I established the *in vitro* degradation assay and wrote the paper. This chapter was submitted for publication.

Chapter 3: The ubiquitin-like modifier FAT10 interacts with HDAC6 and localizes to aggresomes under proteasome inhibition

I designed and performed all of the experiments in this chapter and wrote the paper. This chapter was published in *J. Cell Sci.* 121(24): 4079-4088. 2008.

Chapter 4: FAT10-deficient mice display a prolonged $CD8^+$ T-cell response after LCMV infection

I performed the genotyping and supervised the breeding of $FAT10^{-/-}$ mice. In addition, I performed the experiments investigating the maturation-induced apoptosis of BMDCs as well as preliminary experiments investigating the $CD8^+$ T cell response to LCMV.

Chapter 5: Generation of mouse monoclonal antibodies directed against human FAT10

I generated the antibodies and performed the experiments depicted in all figures except for figure 32.